



Szmaja, Tomasz (2018) *Transport of glutathione across the endoplasmic reticulum membrane*. PhD thesis.

<https://theses.gla.ac.uk/9112/>

Copyright and moral rights for this work are retained by the author

A copy can be downloaded for personal non-commercial research or study, without prior permission or charge

This work cannot be reproduced or quoted extensively from without first obtaining permission in writing from the author

The content must not be changed in any way or sold commercially in any format or medium without the formal permission of the author

When referring to this work, full bibliographic details including the author, title, awarding institution and date of the thesis must be given

Enlighten: Theses

<https://theses.gla.ac.uk/>
research-enlighten@glasgow.ac.uk



University of Glasgow

Transport of glutathione across the endoplasmic reticulum membrane

Tomasz Szmaja (BSc Hons, MRes)

Supervisors: Professor Neil Bulleid and Professor Richard Hartley

Submitted in fulfilment of the requirements for the Degree of Doctor of Philosophy

Institute of Molecular, Cell and Systems Biology College of Medical, Veterinary and

Life Sciences

University of Glasgow

February 2018

Abstract

γ -L-glutamyl-L-cysteinylglycine known as glutathione is tripeptide synthesised in the cytoplasm. Glutathione plays important role in several cellular processes and has many functions, for example detoxification of xenobiotics, oxidative protein folding, protection against reactive oxygen species, modulation of cell proliferation and apoptosis. Glutathione is present in almost all organelles within the cell, however, it is still not known how glutathione is transported from the cytoplasm to other cellular compartments. Here we investigated the transport of glutathione into the ER where glutathione plays an important role in oxidative protein folding. Two assays to monitor glutathione transport across the ER membrane were developed and an attempt to identify the putative glutathione transporter was made. Both assays rely on selective permeability of biological membranes and use microsomes to mimic the ER environment. Microsomes were prepared from HT1080 cells expressing either redox sensitive green fluorescent protein (roGFP-iE) or glutathione S-transferase P1 (GSTP1-1A) inside the ER. By measuring the change in fluorescence of roGFP-iE it was possible to measure the rate at which glutathione is transported inside microsomes. GSTP1-1A is able to conjugate glutathione to various substrates and form a stable product, by measuring the increase in glutathione conjugates it was possible to estimate the transport of glutathione inside microsomes. Using both roGFP-iE and GSTP1-1A based assays we were able to measure glutathione transport into microsomes, both assays provide slightly different information about glutathione transport and both have different limitations. In order to identify the glutathione transporter, we used GSH as an affinity ligand and isolated all ER membrane proteins interacting with glutathione. The first approach using glutathione Sepharose beads allowed to isolate several proteins, however, all of them belonged to GST family. A second approach relied on isolating the transporter using glutathione attached to Mts-Aft-Biotin a photo activated crosslinker. Mts-Aft-Biotin approach did not result in isolation of any proteins binding specifically to GSH, this approach requires more work and needs to be improved. We showed that it is possible to isolate GSH binding proteins using GSH as affinity ligand, using this strategy it might be possible to isolate GSH transporter in the future. Both assays presented in this work are the first assays specific for the transport of glutathione across the ER membrane. In the future these assays can be used to investigate the transport of glutathione even further and contribute to the understanding of redox homeostasis in the ER.

Table of contents

Abstract	i
Table of contents	ii
List of figures	vi
List of tables	viii
Acknowledgements	ix
Author's declaration	x
Definitions/Abbreviations	xi
IPTG Isopropyl- β -D-thiogalactoside	xii
Chapter 1 Introduction	1
1.1 Introduction to glutathione	2
1.1.1 <i>History of glutathione</i>	2
1.2 Synthesis and functions of glutathione	3
1.2.1 <i>Synthesis of glutathione</i>	3
1.2.2 <i>Overview of glutathione functions</i>	4
1.2.3 <i>Cellular functions of glutathione</i>	5
1.3 Glutathione and the redox status of cytosol	8
1.3.1 <i>GSH / GSSG balance in the cytosol</i>	8
1.3.2 <i>Glutathione as an indicator of the cytosolic redox environment</i>	10
1.4 New role for GSH in the cytosol	11
1.4.1 <i>GSH in iron metabolism</i>	11
1.4.2 <i>GSH as an ancillary system for the thioredoxin pathway</i>	11
1.4.3 <i>Split role between iron metabolism and thiol-redox maintenance</i>	12
1.4 The ER and the redox status of the ER	14
1.4.1 <i>Overview of redox reactions in the ER</i>	14
1.6 Protein folding and the disulfide exchange reactions in the ER	16
1.7.1 <i>Principles of protein folding</i>	16
1.7.1 <i>Protein Disulfide Isomerase</i>	17
1.7.2 <i>Ero1 Pathway</i>	19
1.7.3 <i>PRX4 pathway</i>	21
1.7.4 <i>VKOR pathway</i>	22
1.7.5 <i>GPX7 and GPX8 pathway</i>	23
1.7.6 <i>QSOX pathway</i>	23
1.8 Glutathione in the ER	25
1.8.1 <i>Role of glutathione in the ER</i>	25
1.8.2 <i>Maintenance of GSH:GSSG ratio inside the ER</i>	26

1.9 Glutathione transporters	28
1.9.1 <i>Glutathione efflux</i>	29
1.9.2 <i>Glutathione uptake from the extracellular environment</i>	31
1.9.3 <i>Glutathione transport in organelles</i>	32
1.10 Summary	34
1.10.1 <i>Aims of the project</i>	34
1.10.2 <i>Impact of the project</i>	35
Chapter 2 Materials and methods	36
2.1 Cell culture	37
2.2 Protein methods	37
2.2.1 SDS-PAGE.....	37
2.2.2 Silver staining.....	37
2.2.3 Western blot.....	38
2.3 GSH transport assay (roGFP)	38
2.3.1 Preparation of microsomes.....	38
2.3.2 Optimising the concentration of reducing agents	38
2.3.3 roGFP transport assay of reducing agents across the ER membrane	39
2.3.4 Serine protease digestion of microsomes	39
2.3.5 Alkylation of glutathione	39
2.3.6 Inhibition of transport by N-ethylsuccinimido-S-glutathione (ESG)	40
2.3.7 GOH synthesis.....	40
2.3.8 GOH inhibition of GSH transport.....	41
2.4 Generation of stable cell line expressing GSTP1-1A in the ER	42
2.4.1 GSTP1-1A plasmid construct designing.....	42
2.4.2 Transformation.....	42
2.4.3 Plasmid purification.....	42
2.4.4 Restriction digest.....	43
2.4.5 Agarose gel electrophoresis	43
2.4.6 DNA gel extraction/purification.....	43
2.4.7 Ligation.....	43
2.4.8 Plasmid purification and sequencing.....	44
2.4.9 Transfections into HT1080.....	44
2.4.10 Selection.....	44
2.4.11 Cultivation.....	44
2.5 Cloning and purification of GSTP1-1A	45
2.5.1 Polymerase chain reaction (PCR)	45
2.5.2 PCR product analysis and purification	45

2.5.3 Cloning into pET28 expression vector	45
2.5.4 Transformation.....	45
2.5.5 GSTP1-1A Expression	46
2.5.6 Purification of GSTP1-1A.....	46
2.5.7 Purified GSTP1-1A activity	46
2.6 GSH transport assay (GST)	47
2.6.1 Estimate concentration of GSTP1-1A inside microsomes.....	47
2.6.2 <i>In vivo</i> activity of GST	47
2.6.3 GST based transport assay using Cl-BODIPY as substrate (fluorescence spectra).....	47
2.6.4 Mass spectrometry identification of conjugates	47
2.6.5 GST based transport assay endpoint and time course (CDNB and BODIPY) ...	48
2.6.6 Inhibition of GSTP1-1A activity using GOH.....	48
2.7 Isolating a GSH transporter	49
2.7.1 Preparation of rat liver microsomes (RLM).....	49
2.7.2 Isolation of proteins using glutathione Sepharose beads.	49
2.7.3 Mass spectrometry identification	49
2.7.4 Conjugation of GSH to Mts-Aft-Biotin.....	50
2.7.5 Photocrosslinker isolation of GSH binding proteins.....	50
Chapter 3 roGFP assay for GSH transport	52
3.1 Introduction	53
3.2 roGFP transport assay	56
3.2.1 <i>Optimising the concentration of reducing agents</i>	58
3.2.2 <i>Kinetics</i>	62
3.3 Inhibition of GSH transport	65
3.3.1 <i>Broad range proteases inhibition</i>	65
3.3.2 <i>Alkylation of GSH</i>	69
3.3.3 <i>Glutathione analogue synthesis</i>	74
3.3.4 <i>GOH effect on GSH transport</i>	77
3.4 Glutaredoxin roGFP fusion	80
3.4.1 <i>Glutaredoxin roGFP fusion – GOH inhibition</i>	84
3.5 Discussion	85
Chapter 4 GST assay for GSH transport	88
4.1 Introduction	89
4.2 GSTP1-A-KDEL cell line	93
4.3 GST based transport assay	94
4.3.1 <i>Purified GSTP1-1A activity</i>	98

4.3.2 Estimate the concentration of GSTP1-1A inside microsomes	102
4.3.3 In vivo activity of GSTP1-1A.....	103
4.3.4 Mass spectrometry and HPLC identification of conjugated product.....	105
4.3.5 Transport assay – endpoint.....	111
4.3.6 Transport assay – time course.....	115
4.3.7 Inhibition of GSH transport.....	117
4.4 Discussion.....	119
Chapter 5 Isolating putative GSH transporters.....	121
5.1 Introduction.....	122
5.2 Glutathione Sepharose beads approach.....	124
5.2.1 Isolating GSH interacting proteins using glutathione Sepharose beads.....	126
5.2.2 Protein identification by mass spectrometry.....	130
5.3 Mts-Aft-Biotin photocrosslinking.....	134
5.4 Discussion.....	146
Chapter 6 Discussion.....	148
6.1 Discussion.....	149
References.....	154
Appendix	167

List of figures

Figure 1.1 Structure of glutathione	2
Figure 1.2 Synthesis of glutathione	3
Figure 1.3 Structure of oxidised glutathione	5
Figure 1.4 Cellular functions of glutathione	7
Figure 1.5 Reactions leading to oxidation and reduction of glutathione	9
Figure 1.6 Glutathione split role between iron metabolism and thiol-redox maintenance ..	13
Figure 1.7 Overview of redox reactions in the ER	15
Figure 1.8 Schematic representation of disulphide formation and isomerisation by PDI....	18
Figure 1.9 Oxidative folding in the ER	20
Figure 1.10 PRDX4 mechanism of action	21
Figure 1.11 Proposed VKOR role in disulphide bond formation	22
Figure 1.12 Schematic representation of QSOX.....	24
Figure 1.13 Diagrammatic representation of <i>Saccharomyces cerevisiae</i> with indicated GSH transporters	28
Figure 2.1 ¹ H NMR spectrum of GOH.....	41
Figure 3.1. GSH transport in microsomes	57
Figure 3.2. Optimising the concentration of TCEP	58
Figure 3.3. Selecting an optimum concentration of GSH.....	60
Figure 3.4. Optimising the concentration of DTT	61
Figure 3.5a. roGFP-iE based GSH transport assay in intact microsomes	63
Figure 3.5b. roGFP-iE based GSH transport assay in permeabilised microsomes.....	64
Figure 3.6. Proteinase K treatment.....	66
Figure 3.7. Trypsin and chymotrypsin treatment.....	68
Figure 3.8. Reaction of GSH with NEM	69
Figure 3.9. RP-HPLC chromatogram of ESG , GSH and NEM	71
Figure 3.10. ESG inhibition of GSH transport.....	73
Figure 3.11 GOH synthesis	75
Figure 3.12. GOH effect on GSH transport in intact microsomes.....	77
Figure 3.13. GOH effect on GSH transport in permeabilised microsomes	79
Figure 3.14 Grx1-roGFP – mechanism of action and diagrammatic representation	81
Figure 3.15a. Kinetics of GRx_roGFP-iL reduction in intact microsomes	82
Figure 3.15b. Kinetics of GRx_roGFP-iL reduction in permeabilized microsomes.....	83
Figure 3.16. GOH effect on GSH transport in GRx_roGFP-iL intact microsomes	84
Figure 4.1. Principles of GSH transport based on conjugation of GSH to CDNB by GST .	92
Figure 4.2. Immunofluorescence Western blot analysis of FLAG tagged GSTP1-1A.....	93

Figure 4.3. Fluorescence spectra of CI-BODIPY.	95
Figure 4.4 GST based assay of GSH transport across microsomal membranes	97
Figure 4.5. Purified GSTP1-1A activity	99
Figure 4.6. Purified GSTP1-1A activity towards CI-BODIPY.....	101
Figure 4.7 Western blot analysis of FLAG tagged GSTP1-1A.....	102
Figure 4.8 <i>In vivo</i> binding of GSTP1-1A to GSH-Sepharose	104
Figure 4.9 HPLC and mass spectrometry analysis of GS-DNB conjugate.....	110
Figure 4.10 Endpoint measurement of GS-DNB conjugate.....	112
Figure 4.11 Endpoint measurement of GS-BODIPY conjugate.....	114
Figure 4.12 GST based assay of GSH transport across microsomal membranes.....	116
Figure 4.13. GOH inhibition of GSTP1-1A.	118
Figure 5.1 Isolation of putative glutathione transporter	125
Figure 5.2 RLM proteins bound to glutathione Sepharose beads	127
Figure 5.3 RLM proteins bound to glutathione Sepharose beads with controls.....	129
Figure 5.4 Chemical structure of Mts-Aft-Biotin.....	134
Figure 5.5a. Attachment of GSH to Mts-Aft-Biotin crosslinker	135
Figure 5.5b. The mechanism of action of GS-Mts-Aft-Biotin	136
Figure 5.6 HPLC chromatogram of GSH conjugation to Mts-Aft-Biotin.....	137
Figure 5.7 Mass spectrometry analysis of HPLC peaks from GSH to Mts-Aft-Biotin conjugation	140
Figure 5.8 Silver stain analysis of proteins crosslinked and biotinylated by GS-Mts-Aft- Biotin	142
Figure 5.9 Silver stain analysis of proteins crosslinked and biotinylated by GS-Mts-Aft- Biotin (more washes).....	143
Figure 5.10 Western blot analysis of biotinylated protein.	145

List of tables

Table 5.1 Mass spectrometry identification of proteins in gel fragment around 25 kDa.....	131
Table 5.2 Mass spectrometry identification of proteins in gel fragment around 46 kDa.....	132
Table 5.3 Mass spectrometry identification of eluted proteins.	133

Acknowledgements

First and foremost, I would like to thank my supervisor Professor Neil Bulleid for giving me the opportunity to do this PhD, his guidance, encouragement, and for believing in me even when I didn't.

I would like to thank all the members of Bulleid Lab, including Dr Fiona Chalmers, Dr Philip Robinson, Dr Greg Poet, Dr Rachel Martin, Esraa Haji, Dr Chloe Stoye, Marie Anne Pringle, Lorna Mitchell, Dr Zhenbo Cao and Xiaofei Cao. It was a great pleasure to work with them and learn from them. Special thanks to Dr Marcel Van Lith for guiding me at the beginning of my PhD and helping me a lot with roGFP assay and Dr Ojore Oka for helping and guiding me at many occasions.

Also, big thanks to Professor Robert Liskamp and his research group really helped me with the chemistry part of my project, especially Dr Helmus Van De Langemheen who was supervising me.

Finally, I would like to thank my family and friends for constant support, especially Korbkarn Limsombatanan for helping me with diagrams.

Author's declaration

I declare that, except where explicit reference is made to the contribution of others, this thesis is the result of my own work and has not been submitted for any other degree at the University of Glasgow or any other institution.

Tomasz Szmaja

February 2018

Definitions/Abbreviations

2-5-DHC	2-5-dihydroxychalcone
ABC	ATP-Binding Cassette
ABCG2	ATP-binding cassette sub-family G member 2
BODIPY	4,4-difluoro-4-bora-3a,4a-diaza-s-indacene
BSA	Bovine serum albumins
CAT	Cationic amino acid transporter
CDNB	1-chloro-2,4-dinitrobenzene
DCC/DIC	Dicarboxylate carriers
DCM	Dichloromethane
DIPEA	N,N-Diisopropylethylamine
DTNB	5,5-dithio-bis-(2-nitrobenzoic acid
DTT	Dithiothreitol
ER	Endoplasmic reticulum
Ero1	ER oxireductin
ESG	N-ethylsuccinimido-S-glutathione
GCL	Glutamate cysteine ligase
GCLC	Glutamate cysteine ligase catalytic subunit
GCLM	Glutamate cysteine ligase modifier subunit
GPX	Glutathione peroxidase

GR	Glutathione reductase
GS	Glutathione synthase
GSH	Glutathione
GSH1	γ -glutamyl cysteine synthetase
GSSG	Oxidised glutathione
GST	Glutathione S-Transferase
GSX	Glutathione/proteins mix disulfide
HPLC	High-performance liquid chromatography
ICS	Iron–sulfur cluster
IPTG	Isopropyl- β -D-thiogalactoside
LCMS	Liquid chromatography mass spectrometry
MAPEG	Membrane-associated proteins in eicosanoid and glutathione metabolism
MRP	Multidrug resistance-associated protein
NEM	N-Ethylmaleimide
NMR	Nuclear magnetic resonance
OGC	Oxoglutarate carriers
OTA	Organic anion transport
OTP	Oligopeptide transporter family
PBS	Phosphate buffered saline
PCR	Polymerase chain reaction

PDI	Protein disulfide isomerase
PNS	Postnuclear supernatant
PRDX	Peroxiredoxin
PTR	Peptide transporter
QSOX	Quiescin sulfhydryl oxidase
RLM	Rat liver microsomes
roGFP	redox sensitive Green Fluorescent Protein
ROS	Reactive nitrogen species
ROS	Reactive oxygen species
RP-HPLC	Reverse phase high-performance liquid chromatography
RT	Room temperature
RT	Retention time
RyR1	Ryanodine receptor calcium channel type 1
SDS	Sodium dodecyl sulfate
SLCO1A2	Solute carrier organic anion transporter family, member 1A2
SOH	Sulfenylated cysteine
SPPS	Solid Phase Peptide Synthesis
SR	Sarcoplasmic reticulum
TCA	Trichloroacetic acid
TCEP	tris(2-carboxyethyl)phosphine
TFA	Trifluoroacetic acid

TRAM	Trans-locating chain-associated membrane protein
UPR	Unfolded protein response
UV	Ultra violet
v/v	Volume/volume
VKOR	Vitamin K epoxide reductase
w/v	Weight/volume
Ycf1p	Yeast cadmium factor-1
γ -GT/GGT	γ -glutamyl transpeptidase

Chapter 1

Introduction

1.1 Introduction to glutathione

1.1.1 History of glutathione

It has been over 125 years since the tripeptide (γ -L-glutamyl-L-cysteinylglycine) glutathione (GSH) (Figure 1.1), the most abundant non-protein thiol compound, was discovered (Lillig and Berndt, 2013). Joseph de Rey-Pailhade was the man who isolated GSH from various sources in 1888 and described it as sulfur-loving compound named “philothion” (Lillig and Berndt, 2013). The name glutathione was coined by Frederick Gowland Hopkins who “re-discovered” the compound in 1921 describing it as a dipeptide, and noticing its oxidation – reduction properties (Lillig and Berndt, 2013, Hopkins, 1929). Six years later in 1927 George Hunter and Blythe Alfred Eagles presented a vast array of evidence suggesting the presence of an additional amino acid in GSH, thereby questioning the dipeptide nature of GSH described by Hopkins (Lillig and Berndt, 2013). After 2 years of intensive research, Hopkins confirmed the tripeptide nature of GSH and admitted his previous work on GSH was erroneous (Hopkins, 1929). Years later in 1950/51 Robert B. Johnston and Konrad Bloch described the synthesis of GSH (Johnston and Bloch, 1951). Two years later Bloch was able to characterise γ -glutamyl-cysteine synthetase and glutathione synthetase (Snock and Bloch, 1952, Snock et al., 1953). In 1980’s and 1990’s Alton Meister conducted several pioneering experiments leading to discovering of biochemistry of GSH metabolism (Lillig and Berndt, 2013). Meister’s research greatly contributed to our understanding of GSH and opened ways for new scientists to study it even more (Lillig and Berndt, 2013).

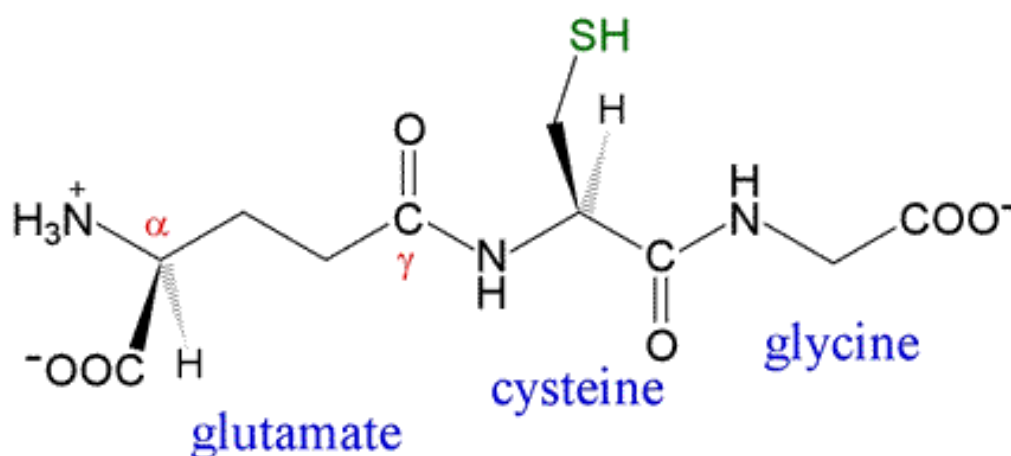


Figure 1.1 Structure of glutathione. Adapted from (Valsta et al., 1988)

1.2 Synthesis and functions of glutathione

1.2.1 Synthesis of glutathione

GSH synthesis takes place in the cytoplasm which has the biggest reservoir of GSH within the cell, accounting for 80-85% of total GSH with the concentration of GSH ranging from 1 mM to 10 mM (Lu, 2013). The amount of oxidised glutathione (GSSG) in the cytosol is very low and the GSH:GSSG is estimated to be even as high as 3000:1 (Ostergaard et al., 2004). GSH is synthesised from its precursor amino acids, glutamate, cysteine and glycine in a two step reaction catalysed by glutamate cysteine ligase (GCL, E.C. 6.3.2.2) and glutathione synthase (GS, E.C. 6.3.2.3), both reactions are ATP-dependent (Figure 1.2) (Lu, 2013).

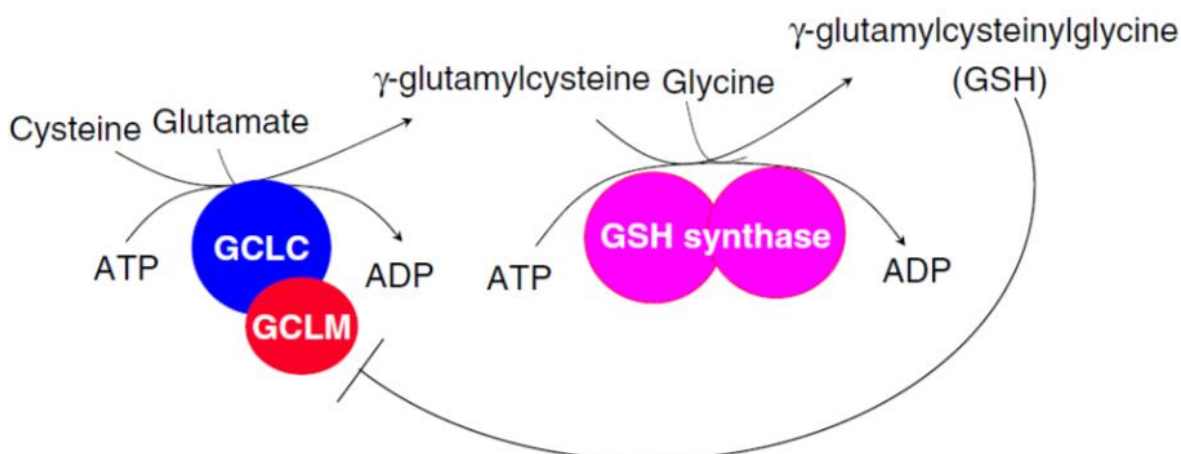


Figure 1.2 Synthesis of glutathione. GSH is synthesised in two ATP dependent steps. First step, conjugation of cysteine to glutamate, results in formation of γ -glutamylcysteine. This conjugation is catalysed by glutamate cysteine ligase (GCL), an enzyme composed of 2 subunits, catalytic subunit (GCLC) and modifier subunit (GCLM). Second step, the addition of glycine is catalysed by glutathione synthase (GS) and results in the formation of γ -glutamylcysteinylglycine known as glutathione. Adapted from Lu, 2013

GCL is composed of 2 subunits, the heavier catalytic subunit (GCLC, Mr 73 kDa) and lighter modifier subunit (GCLM, Mr 31 kDa) (Lu, 2013). GCLC displays all the catalytic properties of the enzyme while GCLM does not have any enzymatic properties but is important in regulation of the GCLC subunit (Seelig et al., 1984). GCL catalyses the first step in GSH synthesis and the reaction results in the formation of γ -glutamylcysteine from glutamate and cysteine; this is also the rate limiting step (Lu, 2013). Glutathione synthase (GS) is a homodimer (Mr 118 kDa) that catalyses the second step of GSH synthesis (Oppenheimer et al., 1979). The reaction catalysed by GS results in formation of GSH from γ -glutamylcysteine and glycine (Lu, 2013). Dysregulation of GSH synthesis can occur at many stages and is associated with many human diseases, including haemolytic anemia, aminoaciduria, spinocerebellar degeneration, schizophrenia, cardiovascular diseases, stroke, asthma, diabetes mellitus, cystic fibrosis and pulmonary fibrosis (Ballatori et al., 2009).

1.2.2 Overview of glutathione functions

Glutathione protects against oxidative stress by scavenging reactive oxygen species (ROS) and free radicals (Wu et al., 2004). GSH is capable of scavenging lipid peroxy radical, H_2O_2 , hydroxyl radical, and peroxy nitrite directly, and indirectly through enzymatic reactions (Fang et al., 2002). GSH is important in detoxification of xenobiotics, it can react with acetaminophen and bromobenzene to form mercapturates (Fang et al., 2002, Wu et al., 2004). Glutathione plays an important role in disulfide bond formation, immune function, apoptosis, modulates cell proliferation, and is also a key determinant of redox signalling (Wu et al., 2004, Chakravarthi et al., 2006).

GSH is often described as a cellular thiol "redox buffer" as it is used to maintain a required level of thiol/disulfide redox potential (Sies, 1999). The presence of peptidic γ -linkage, that protects GSH from degradation by aminopeptidases, and the lack of the toxicity associated with cysteine make GSH suitable to perform its role as redox buffer (Sies, 1999). In cells glutathione is present in two forms, reduced glutathione (GSH) and oxidized glutathione (GSSG), also known as glutathione disulfide (Figure 1.3). However >98% of total glutathione exists as GSH (Lu, 2013).

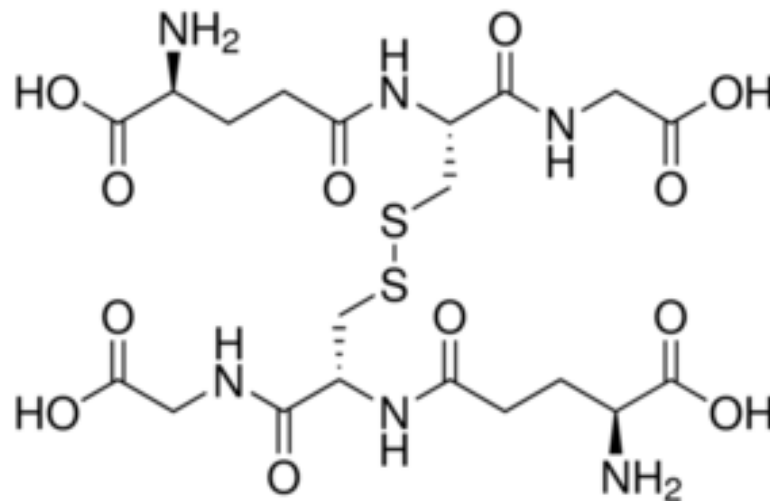


Figure 1.3 Structure of oxidised glutathione

1.2.3 Cellular functions of glutathione

After successful synthesis GSH can be used for various purposes (Figure 1.4). GSH can function as an antioxidant; this function is largely accomplished by reactions catalysed by GSH peroxidase (GPx) (Lu, 2013). As a substrate for GPx, GSH helps reduce H_2O_2 to water and lipid hydroperoxides to the corresponding alcohols, this reaction also results in the oxidation of GSH and the formation of GSSG (Dickinson and Forman, 2002). At the expense of NADPH newly formed GSSG can be reduced to GSH by glutathione reductase (GR), alternatively GSH/protein mix disulfides (GSX) transport protein can export GSSG outside the cell (Lu, 2009). These properties makes GSH particularly important in defending against both physiologically and pathologically generated oxidative stress (Garcia-Ruiz and Fernandez-Checa, 2006).

By modifying the oxidation state of critical cysteine residues in proteins, GSH plays a major role in regulation of redox-dependent cell signalling (Dalle-Donne et al., 2009, Forman et al., 2009). Proteins can be either activated or inactivated by adding GSH to the -SH of protein cysteine residues, a process called glutathionylation. (Dalle-Donne et al., 2009). This serves to prevent loss of GSH under oxidative conditions but more important it is a protective mechanism to prevent protein thiols

from irreversible oxidation (Lu, 2013). Glutaredoxins and sulfiredoxins can deglutathionylate proteins using GSH as a reductant (Liu and Pravia, 2010). Many critical cysteine residues present in transcription factors and signalling molecules can be oxidised and regulated thus way, therefore this mechanism allows reactive oxygen and nitrogen species (ROS and RNS) to regulate some protein function and cell signalling through glutathionylation (Liu and Pravia, 2010, Lu, 2009).

The availability of free cysteine within the cell is low, moreover this amino acid is very unstable and easily auto-oxidized extracellularly. Glutathione plays an important role as a source of cysteine through a process called the γ -glutamyl cycle (Lu, 2013). The γ -glutamyl cycle begins when GSH is transported outside of the cell. γ -Glutamyl transpeptidase (GGT) can degrade GSH to form γ -glu-amino acid and cys-gly dipeptide (Lu, 2013). The γ -glu-amino acid can be taken up by the cell and broken down to the amino acid 5-oxoproline, which is later converted to glutamate, at the expense of ATP, and can be used for GSH synthesis (Lu, 2013). Extracellular dipeptidase breaks down cysteinylglycine to generate cysteine and glycine, which are transported back in to the cell. Once inside the cell cysteine is mostly incorporated into GSH, proteins and degraded into sulfate and taurine (Lu, 2009)

GSH levels increase during cell cycle progression when the cell leaves G₀ phase of the cell cycle and enters G₁ phase. When this increase was blocked DNA synthesis during S phase was reduced by 33% (Lu and Ge, 1992, Huang et al., 2001). Therefore GSH is required for normal cell cycle progression (Lu, 2013). The main role of GSH in DNA synthesis is through the maintenance of glutaredoxin or thioredoxin (not directly) in reduced state, these two enzymes are needed for the activity of the rate-limiting enzyme in DNA synthesis - ribonucleotide reductase (Sengupta and Holmgren, 2014). Moreover, as mentioned before, GSH can affect the activity of transcription factors and signalling molecules, many of which are important for cell cycle progression and cell death (Lemasters, 2005, Lu, 2013).

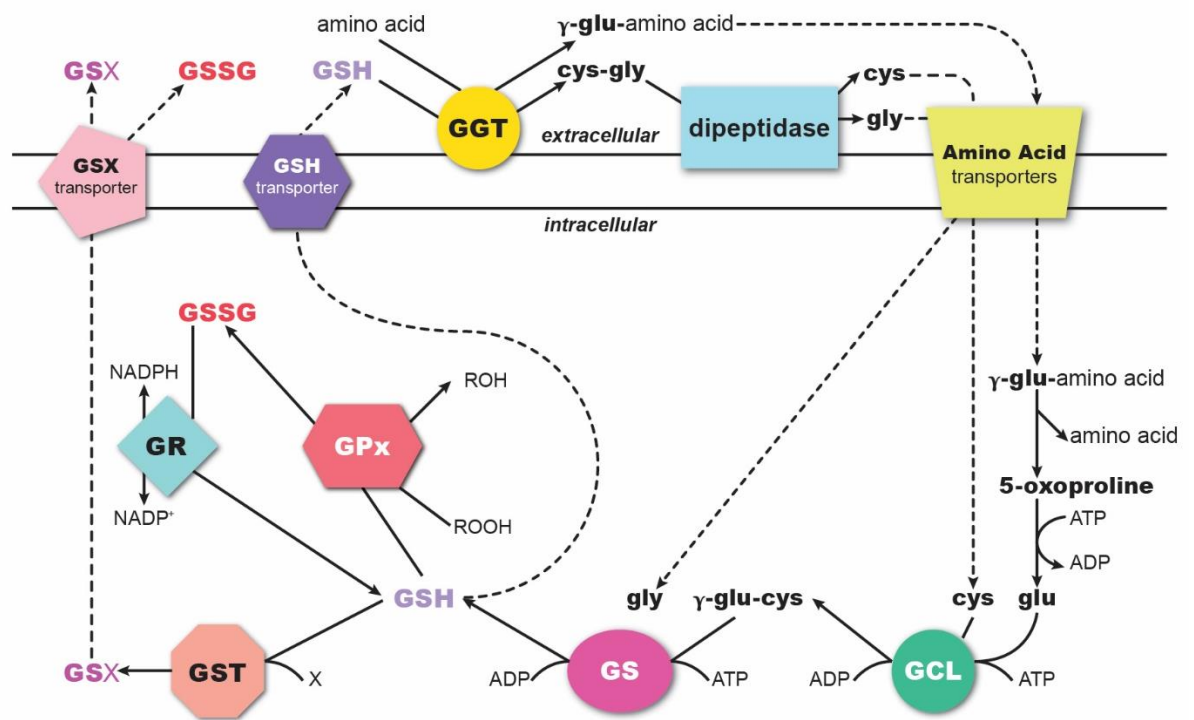


Figure 1.4 Cellular functions of glutathione. GSH is synthesised in two ATP dependant steps by glutamate cysteine ligase (GCL), which conjugate cys and glu, resulting in γ -glu-cys. Gly is added to γ -glu-cys by glutathione synthase (GS), resulting in the formation of GSH. GSH can form mix disulfides with proteins (GSX) in a reaction catalysed by glutathione S-transferase (GST). GSX can be exported outside cell by a GSX transporter. GSH can help remove ROS and become oxidised in this process, a reaction catalysed by glutathione peroxidase (GPx). GSSG can be reduced back to GSH by glutathione reductase (GG). Both GSSG and GSH can be transported outside the cell where they can be break down to their amino acids precursors and imported back to cell. Adapted from Dickson and Forman, 2002

1.3 Glutathione and the redox status of cytosol

Among many of GSH's functions there is one often described as the main function of GSH, to maintain a given thiol/disulfide redox potential as cellular thiol "redox buffer" (Sies, 1999). The integrity of cellular components and the maintenance of the metabolic competence of the cell are dependent on maintaining a proper redox balance in the cytosol (Lopez-Mirabal and Winther, 2008).

1.3.1 GSH / GSSG balance in the cytosol

To keep reactive oxygen species (ROS) and glutathionylated proteins at very low levels the cytosol redox status is highly reduced by maintaining a high GSH to GSSG ratio (even as high as 3000:1) (Ostergaard et al., 2004). There are several enzymes in the cytosol that specialise in reactions involving GSH and GSSG, making sure the right balance between GSH and GSSG is maintained (Lopez-Mirabal and Winther, 2008). GSSG can be generated during the reduction of H₂O₂ a reaction catalysed by GPx (Figure 1.5) (Dickinson and Forman, 2002). Glutathione reductase (GR) is a FAD-bound homodimer responsible for reduction of GSSG to GSH in a NADPH-dependent manner, thus keeping GSSG at very low concentration (Figure 1.5) (Massey and Williams, 1965). In *in vitro* experiments the thioredoxin/thioredoxin-reductase systems from some organisms, including humans, can also reduce GSSG (Kanzok et al., 2000). In some organisms like *Schizosaccharomyces pombe* deficiency in GR is lethal, while in humans it is a cause of congenital diseases (Roos et al., 1979). These findings highlight the importance of GR to maintain low level of GSSG (Lopez-Mirabal and Winther, 2008).

A study by Morgan et al. (2013) showed that in *S. cerevisiae* the cytosolic GSH/GSSG homeostasis is independent on subcellular GSSG, levels and that GSSG which is not immediately reduced in the cytosol, is transported to vacuoles by ABC transporter Ycf1 (Morgan et al., 2013). The concentration of GSSG present in the cytosol is tightly regulated by Ycf1 even during severe oxidative stress (Morgan et al., 2013). Upon deletion of Ycf1, the cytosolic glutathione pool is resistant to chemical and genetic oxidative stress-induced perturbation (Morgan et al., 2013).



Figure 1.5 Reactions leading to oxidation and reduction of glutathione. By reduction of H_2O_2 glutathione peroxidase (GPx) can generate oxidised glutathione (GSSG). Glutathione reductase (GR) is responsible for reduction of GSSG to GSH in a NADPH-dependent manner.

1.3.2 Glutathione as an indicator of the cytosolic redox environment

GSH is the main indicator of the cytosolic redox environment, mostly because of its abundance and the amount of enzymes catalysing redox reactions between glutathione and protein (Schafer and Buettner, 2001). The accurate measurement of the GSH redox potential, depending on GSH concentration and the ratio between GSH and GSSG, is often difficult, especially in different cellular compartments (Schafer and Buettner, 2001, Lopez-Mirabal and Winther, 2008). For many years the overall cytosolic GSH/GSSG ratio was seen as the overall cellular GSH/GSSG ratio measured after cell disruption. The invention of redox sensitive Green Fluorescent Protein (roGFP) contributed significantly to the redox biology field as a whole, but also improved our understanding of cytosolic GSH redox potential (Dooley et al., 2004). The fluorescence properties of roGFP depend on the formation of disulfide bond between two genetically engineered cysteines, present on the surface of roGFP (Meyer and Dick, 2010b). roGFP equilibrates with the redox potential of the intracellular GSH/GSSG when is targeted to different cellular compartments, (Ostergaard et al., 2004, Van Lith et al., 2011, Hanson et al., 2004). The estimation of GSH redox potential using roGFP has been very efficient in many cell types and proved that cytosolic GSH redox potential is much lower than previous research suggested (Lopez-Mirabal and Winther, 2008). Because GSH can regulate cell growth and death, the GSH redox potential changes during these events (Lopez-Mirabal and Winther, 2008)

1.4 New role for GSH in the cytosol

1.4.1 GSH in iron metabolism

A genome-wide study of GSH presence at toxic levels as well as GSH depletion studies have been questioned the role of GSH as the major cytosolic buffer and pointed a new role for GSH related to iron metabolism (Kumar et al., 2011). By using yeast strain overexpressing HGT1, a high affinity GSH transporter present in yeast needed for GSH uptake from the extracellular medium, or a strain lacking γ -glutamyl cysteine synthetase (GSH1), a rate limiting enzyme needed for GSH synthesis, Kumar et al. (2011) showed that both, GSH depletion and toxic levels of GSH, resulted in extra-mitochondrial Fe-S enzyme inactivation and an intense iron starvation-like response without affecting thiol-redox metabolism (except high level of GSH that caused UPR in the ER) (Bourbouloux et al., 2000, Kumar et al., 2011). The importance of GSH in iron metabolism has been hinted at several times in the past (Kispal et al., 1997, Auchere et al., 2008, Sipos et al., 2002). Yeast response to GSH depletion had a genome-wide consequence and resulted not only in a major iron starvation-like response but also remodelled of most of the mitochondrial iron-dependent pathways (Kumar et al., 2011). The effect of GSH depletion on iron-sulfur cluster (ISC) was not improved by the addition of DTT, however, the addition of iron was able to partially correct the ISC defect (Sipos et al., 2002, Kumar et al., 2011). This suggested that the conventional thiol-disulfide reductase activity of GSH may not be playing a role in iron metabolism (Kumar et al., 2011). The fact that the addition of iron improved the ISC defect, caused by GSH depletion, may imply that GSH plays a role in cytosolic iron delivery (Kumar et al., 2011). However, the iron phenotype of GSH depletion was recapitulated by toxic levels of GSH (Kumar et al., 2011).

1.4.2 GSH as an ancillary system for the thioredoxin pathway

These results also questioned the role of GSH as the major cytosolic buffer and even suggested that GSH may not be needed for cytosolic thiol-redox maintenance (Kumar et al., 2011). GSH depletion does not cause proteome-wide thiol oxidation, furthermore, the genome-wide study of mRNA profiles revealed that GSH depletion does not cause redox imbalance (Kumar et al., 2011, Le Moan et al., 2006). These two results indicate that the cell is able to maintain thiol-redox balance regardless

of GSH levels (Kumar et al., 2011). This theory was further confirmed by the data showing that high levels of GSH only have an effect on the ER, causing reduction of protein disulfide isomerase (PDI) and Ero1 and leading to the UPR, but had no effect of redox status of the cytosol (Kumar et al., 2011). Addition of GSH did not help maintain a proper redox balance in cells with an inactivate thioredoxin pathway (Kumar et al., 2011). Even when GSH levels were increased 3-fold, it was not able to sustain a proper redox balance in cells lacking thioredoxin reductase and cell growth was still limited. These results were thought to be associated with aerobic metabolism, however, it was observed under both anaerobic and aerobic growth conditions (Kumar et al., 2011). When cells with an active thioredoxin pathway were depleted of GSH they were able to maintain redox balance without any protein compensatory increase. This means that GSH is not needed to maintain a proper redox balance and the thioredoxin pathway can maintain the redox balance of the cytosol on its own (Kumar et al., 2011). These results suggest that GSH may only be an ancillary system for the thioredoxin pathway (Kumar et al., 2011).

1.4.3 Split role between iron metabolism and thiol-redox maintenance

Both iron-metabolism and maintenance of thiol-redox balance are essential for the cell, therefore the fact that GSH is required for cell viability, could be connected to these functions (Kumar et al., 2011). However, proving that GSH does not play a major role in thiol-redox maintenance and serves only as backup of thioredoxin excludes this function of GSH as essential requirement for cell viability (Kumar et al., 2011). The results support the fact that the essential function of GSH may be related to iron-metabolism, as shown that GSH depletion causes intense iron starvation-like response leading to cell death (Kumar et al., 2011). Therefore, a new model of GSH role within the cell has emerged. GSH function is split between thiol-redox control and iron metabolism, however only small amounts of GSH are required for proper function of iron metabolism while large amounts of GSH are needed as a backup for the role in thiol-redox maintenance (Figure 1.6).

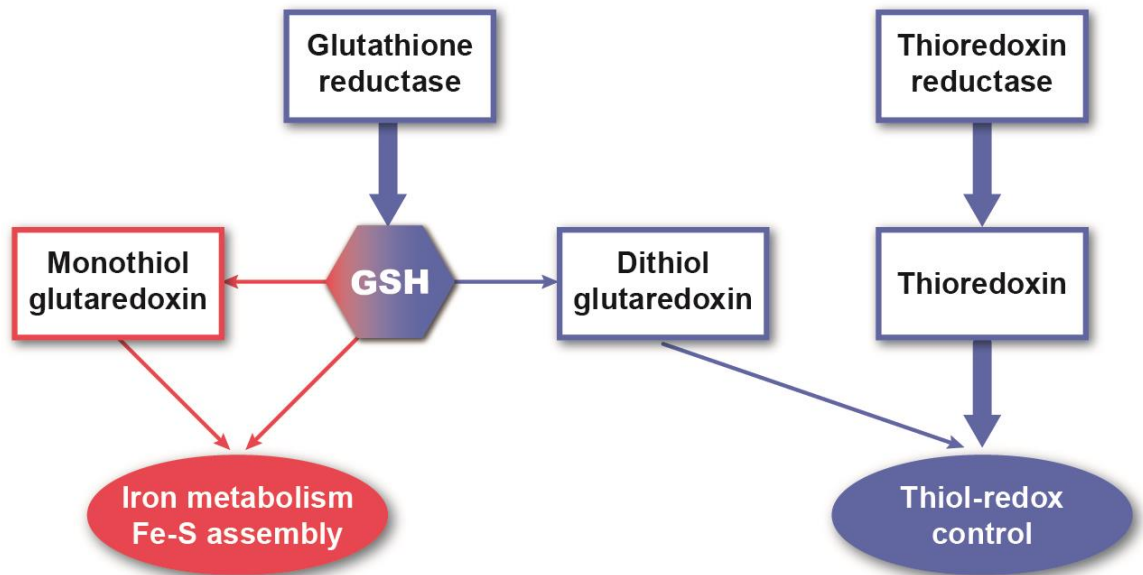


Figure 1.6 GSH split role between iron metabolism and thiol-redox maintenance. Diagrammatic representation of GSH split role between iron metabolism (red) and thiol-redox maintenance (blue). Only small amount of GSH is needed for its function in iron metabolism, however this function is vital. GSH function as a backup for thioredoxin in thiol-redox control and much higher amounts of GSH are needed to fulfil this function. Adapted from Kumar et al., 2011.

1.4 The ER and the redox status of the ER

Besides being present in the cytosol GSH is also present in all organelles with GSH predominantly existing in its reduced form (Forman et al., 2009). However, in the endoplasmic reticulum (ER) the redox environment is more oxidising as the GSH/GSSG ratio is considered to be lower, around 3:1 (Hwang et al., 1992).

The ER is a membrane enclosed organelle specialised in folding of the proteins destined for the secretory pathway (Braakman and Bulleid, 2011). The ER membrane is an impermeable barrier for most proteins and ions, with the exception of small molecules that can diffuse across the lipid bilayer (Le Gall et al., 2004). The ER contains set of unique proteins specialised in disulfide exchange reactions (Bulleid and Ellgaard, 2011).

1.4.1 Overview of redox reactions in the ER

Redox reactions are important for maintaining the oxidising environment of the ER. In the ER, the formation of new disulfide bonds in nascent polypeptide is catalysed by members of protein disulfide isomerase (PDI), the same proteins are involved in isomerisation of non-native disulfides formed during protein folding (Bulleid and Ellgaard, 2011). ER oxidoreductin (Ero1) directly oxidises PDIs after they become reduced in the process of introducing disulfides to newly formed proteins (Sevier and Kaiser, 2006). Oxygen is the final electron acceptor in these electron transfer reactions (Tu and Weissman, 2002). GSH makes sure that members of PDI family are maintained in their reduced states, ready for another cycle of disulfide exchange, and becomes oxidised in the process (Figure 1.7) (Chakravarthi et al., 2006). Because the ER lacks the enzymes specialising in reduction of GSSG (namely the glutathione reductase system), it is unclear how GSSG is recycled back to GSH (Appenzeller-Herzog, 2011). GSSG could be secreted from the ER through the secretory pathway, transported to cytosol where it can be reduced by GR or simply reduced within the ER (Appenzeller-Herzog, 2011). The inability to reduce GSSG to GSH could explain the high concentration of GSSG in the ER. However, it is still unknown if this is the only mechanism maintaining the oxidising environment of the ER.

The low GSH/GSSG ratio in the ER may function to facilitate disulfide bond formation in newly synthesised proteins thus playing an important role in protein folding. However, before discussing oxidative protein folding and the disulfide exchange reactions taking place in the ER in detail, it is important to introduce the general principles governing protein folding.

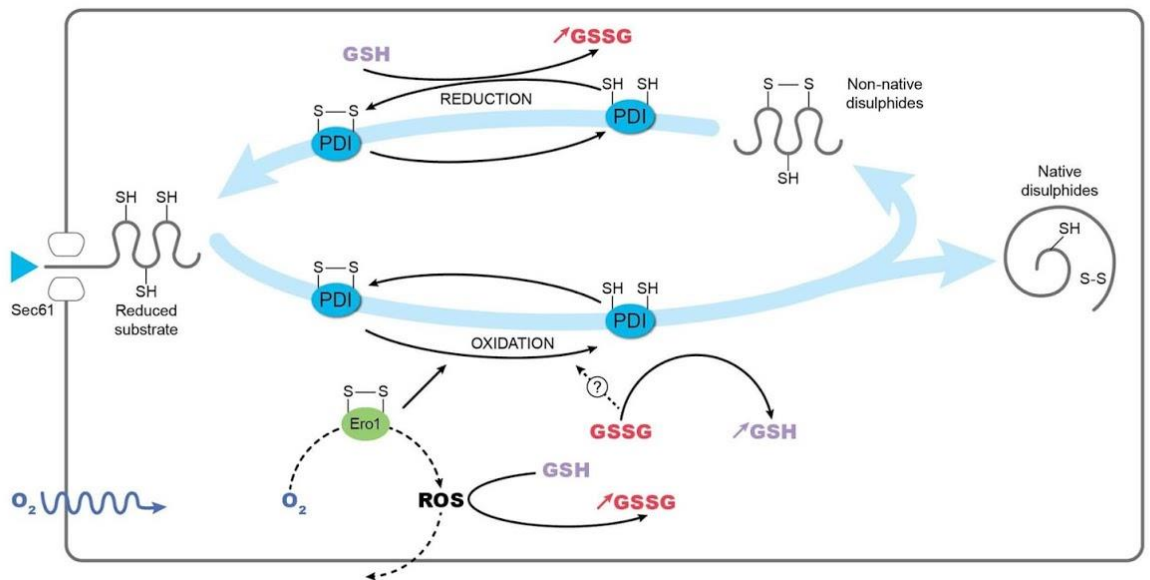


Figure 1.7 Overview of redox reactions in the ER. Nascent polypeptide chain enters the ER through Sec61. Protein disulfide isomerase (PDI) can introduce disulfide bonds into nascent polypeptide chains and becomes reduced in the process. PDI can be oxidised by Ero1 or possibly directly by GSSG. Reduced PDI can help isomerize non-native disulfide bonds. GSH keeps PDI reduced, becoming oxidised in the process. Adapted from Chakravarthi et al., 2006

1.6 Protein folding and the disulfide exchange reactions in the ER

1.7.1 Principles of protein folding

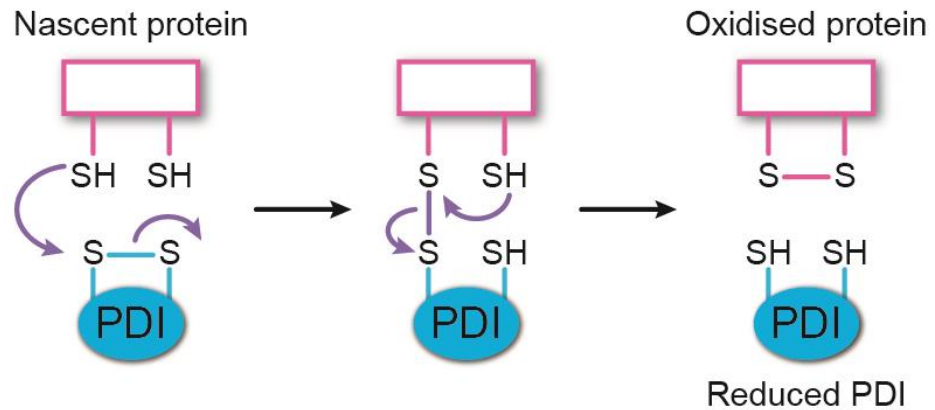
“The folding of proteins into their native three-dimensional structures is the most fundamental and universal example of biological self-assembly” (Dobson, 2003). Only the correctly folded proteins are able to fulfil their biological functions, are able to interact selectively with their natural partners and have long-term stability in crowded biological environments (Dobson, 2003). Achieving native structure allows proteins to enter the most energy favourable state, under these conditions proteins are thermodynamically stable under physiological conditions (Dobson, 2003). To fold correctly the polypeptide chain tries to find native interactions between amino acids residues by a process of trial and error, native interactions are more persistent and stable than non-native interactions, this allows the polypeptide chain to enter its lowest-energy state step by step (Dobson, 2003). *In vivo* experiments and computer simulations revealed that this process is very fast and some of proteins structures can be folded very rapidly, 1 ms for individual β -turns and less than 100 ns in the case of α -helices (Eaton et al., 1998). *In vitro* folding of simple small helical proteins is achieved in less than 50 ms (Mayor et al., 2003). However, there are some examples of proteins whose most stable conformation is different from the native fold, for instance prions (Si, 2015). Folding of proteins in cells differs greatly from protein folding *in vitro*. Experiments on *in vitro* protein folding take places in highly regulated, diluted, cold environments using small and simple proteins (Braakman and Balleid, 2011). On the other hands proteins folded in cells are exposed to crowded and warm environment, these proteins are usually large and contain multiple domains (Braakman and Balleid, 2011). In the test tube folding of proteins starts with the complete protein, while in cell proteins are synthesised on ribosomes and folding is often co-translational (Braakman and Balleid, 2011, Hardesty and Kramer, 2001). Nascent polypeptide chains are exposed to solvents and are prone to interactions with other molecules present inside the crowded environment of the cell (Ellis, 2001). Proteins within the cell often fold in different cellular compartments, for example the endoplasmic reticulum (ER) or mitochondria, depending on their role (Dobson, 2003).

1.7.1 Protein Disulfide Isomerase

The ER is an organelle in which the folding of many secreted proteins takes place. The stability of proteins entering the secretory pathway often depends on the formation of disulfide bonds which affect protein folding and function (Tu and Weissman, 2004). Disulfide bonds stabilise protein structure by decreasing the conformational energy of the denatured state of nascent polypeptide chain (Collet and Bardwell, 2005). In his famous experiment on refolding of ribonuclease A, Anfinsen provided evidence that in favourable conditions disulfide bond formation is a spontaneous process (Anfinsen et al., 1961). However, this process required an electron acceptor and was very slow when compared to high rate of protein folding and secretion *in vivo*. These results suggested that the process of disulfide bond formation might be catalysed by a specialised set of proteins. A few years later this theory was confirmed by the discovery of PDI by Goldberger (Goldberger et al., 1963).

PDI family members are involved in both formation of new disulfide bonds as well as isomerisation of non-native disulfide bonds (Figure 1.8) (Hatahet and Ruddock, 2009). Each member of PDI family contains at least one thioredoxin domain and a CXXC motif at the active sites that shuttles between the dithiol and disulfide states (Hatahet and Ruddock, 2009).

Disulphide Formation



Disulphide Isomerisation

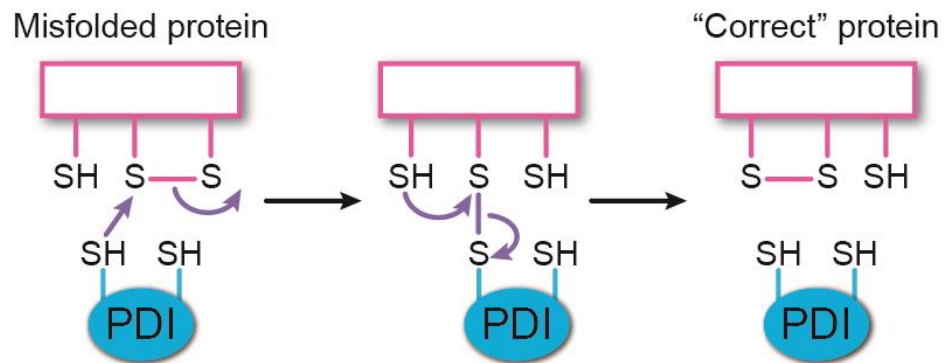


Figure 1.8 Schematic representation of disulfide formation and isomerisation by PDI. Oxidised PDI can transfer disulfides into nascent proteins, becoming reduced in the process. Reduced PDI is able to isomerase non-native disulfides present in misfolded proteins, thus helping proteins achieve their native conformation. Adapted from Perri et al., 2016

1.7.2 Ero1 Pathway

Ero1 is key player in the ER involved in disulfide exchange reactions. Ero1 oxidises PDIs family members directly, rather than through small molecules such as GSH, making sure they are ready for another round of disulfide formation (Figure 1.9) (Sevier and Kaiser, 2006). As a consequences of oxidation of PDI by Ero1, H₂O₂ is created, which is later used in the peroxiredoxin-dependent pathway (Gross et al., 2006). Ero1 is essential for disulfide bond formation in yeast but not in higher eukaryotes (Frand and Kaiser, 1998, Bulleid and Ellgaard, 2011). Mice and humans have two Ero1 paralogs, Ero1 α and Ero1 β (Pagani et al., 2000, Cabibbo et al., 2000). Ero1 β is expressed in insulin producing cells located in the pancreas, therefore it was not surprising that the knockout of Ero1 β in mice resulted in a defect in the folding of proinsulin (Zito et al., 2010). However, the double knockout of both Ero1 α and Ero1 β did not result in a more severe phenotype (Zito et al., 2010). These results suggested that there must be an Ero1 independent pathway involved in disulfide bond formation in mammals (Bulleid and Ellgaard, 2011). To date four Ero1 independent pathways have been identified, each is named after the key enzyme: peroxiredoxin 4 (PRX4), glutathione peroxidase (GPX7 and GPX8), quiescin sulfhydryl oxidase (QSOX) and vitamin K epoxide reductase (VKOR) (Bulleid and Ellgaard, 2011).

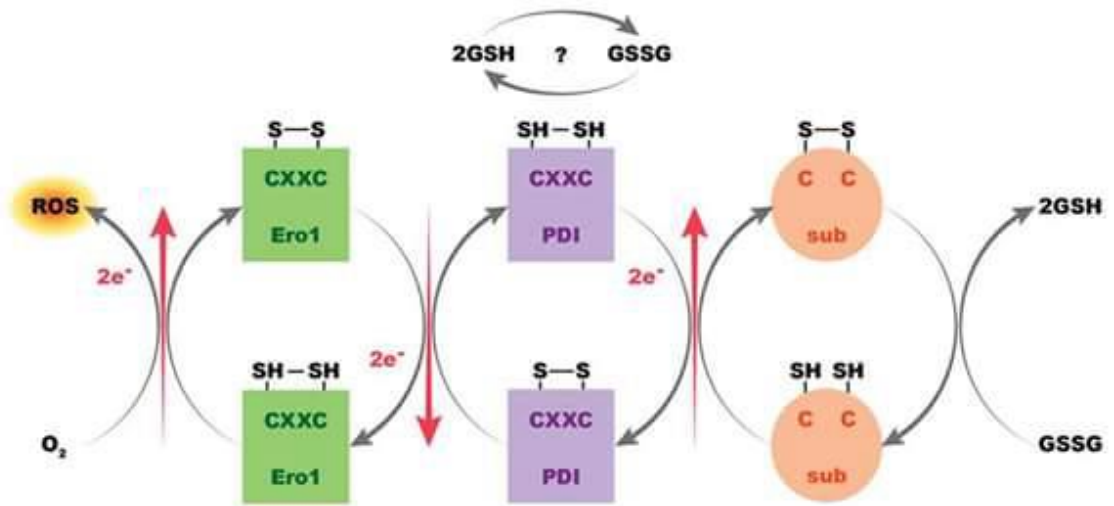


Figure 1.9 Oxidative folding in the ER. Oxidised PDI can transfer disulfides into substrate proteins, becoming reduced in the process. Ero1 can transfer disulfide into reduced PDI and become oxidised again generating ROS in the process. Adapted from Pandol et al., 2011

1.7.3 PRX4 pathway

As a consequence of oxidising PDI by Ero1 H_2O_2 is created. The removal of this ROS by PRX4 resulted in the formation of disulfide bonds (Bulleid and Ellgaard, 2011). PRX4 belongs to peroxiredoxin family, a group anti-oxidising enzymes metabolising H_2O_2 . The role of PRX4 in disulfide bond formation was confirmed by *in vivo* and *in vitro* studies (Tavender et al., 2010, Zito et al., 2010b). PRX4 disulfide bond formation starts with the active-site cysteine, which becomes oxidised to sulfenic acid; after that the sulfenylated cysteine reacts with a second cysteine, present in an adjacent polypeptide, as a result an interchain disulfide bond is formed (Figure 1.10) (Bulleid and Ellgaard, 2011). Any protein with a thioredoxin-domain can now exchange a disulfide with PRX4. In the ER PRX4 exists as a decamer and is active in both disulfide bond formation and H_2O_2 removal (Tavender et al., 2010).

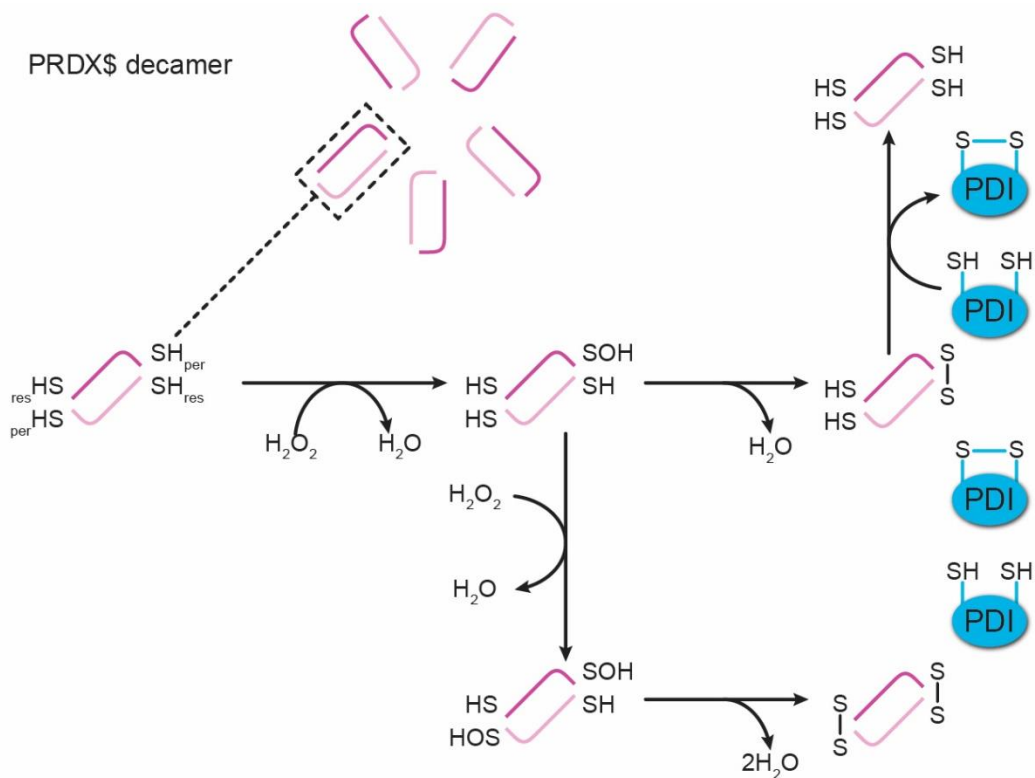


Figure 1.10 PRX4 mechanism of action. Peroxidatic cysteine (per) which becomes oxidised to sulfenic acid, after that the sulfenylated cysteine (SOH) reacts with a resolving cysteine (res), present in an adjacent polypeptide, as a result an interchain disulfide bond is formed. PRX4 can then oxidise PDI. Adapted from Bulleid and Ellgaard, 2011.

1.7.4 VKOR pathway

Vitamin K 2,3-epoxide reductase (VKOR) is a warfarin-sensitive transmembrane enzyme involved in the vitamin K cycle. VKOR contains a thioredoxin-like CXXC domain that can reduce vitamin K1 2,3-epoxide to generate vitamin K hydroquinone (Wajih et al., 2007). Once vitamin K1 2,3-epoxide is reduced, a disulfide bond is formed within the CXXC motif of VKOR (Wajih et al., 2007). Therefore, VKOR is another potential enzyme for Ero1-independent pathway involved in disulfide formation. The role of disulfide bonds formation by VKOR is still unclear, however, VKOR has been trapped in a mixed-disulfide complex with some PDI family members (Schulman et al., 2010). Moreover inhibition of VKOR activity in Ero1 and PRX4 double knockout hepatoma cells was lethal (Rutkevich and Williams, 2012). This result suggests that in hepatoma cells there is no other ER oxidative pathway sufficient to support essential cell functions (Rutkevich and Williams, 2012). The role of VKOR in disulfide bonds formation is shown in figure 1.11.

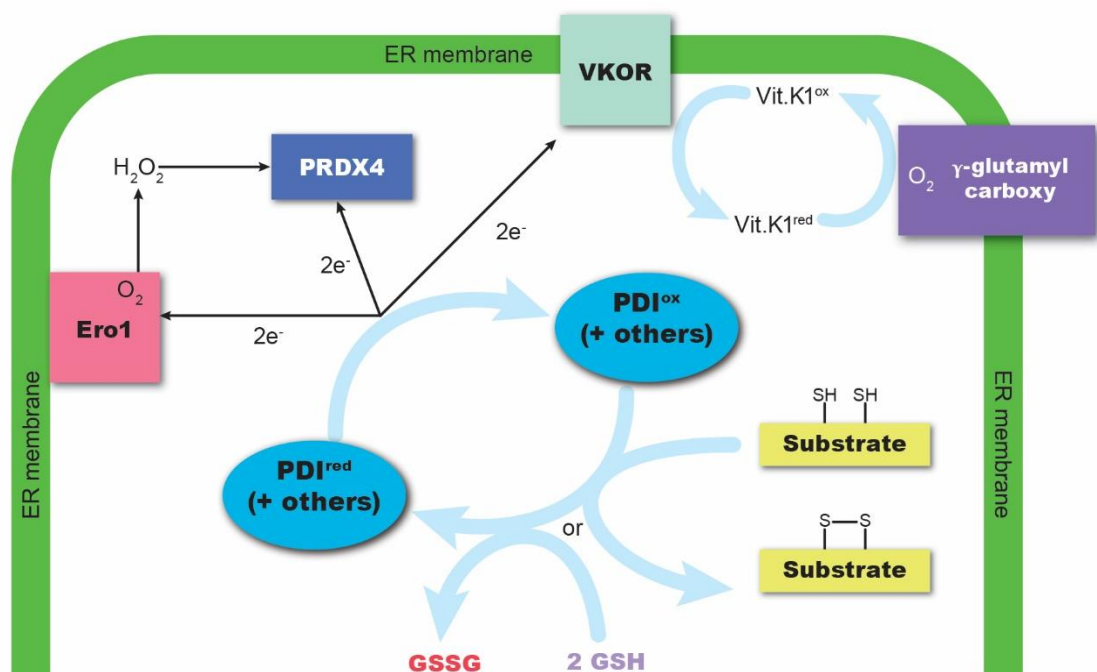


Figure 1.11 Proposed VKOR role in disulfide bond formation. VKOR similar to Ero1 and PRX4 can oxidise PDI family members. The disulfide comes from the reduction of vitamin K. Adapted from Rutkevich and Williams 2012.

1.7.5 GPX7 and GPX8 pathway

GPX7 and GPX8 are enzymes capable of reducing H_2O_2 in the ER. These homologous enzymes belong to the family of thioredoxin GPX like peroxidases (Toppo et al., 2008). GPX7 and GPX8 are PDI peroxidases, by reducing H_2O_2 they are able to oxidise some of PDI family members (Nguyen et al., 2011). Apparently GSH is rather a poor substrate for peroxide-mediated oxidation by GPX7 and GPX8, however, in the presence of GPXs some PDI family members are easily oxidised (Nguyen et al., 2011). The importance of GPX7 and GPX8 in redox reactions was confirmed by bimolecular fluorescence complementation, in which a physical association between Ero1 α and both GPX7 and GPX8 was observed in cells (Nguyen et al., 2011). Other evidence for GPX7 and GPX8 involvement in disulfide formation comes from measuring the *in vitro* rate of oxygen consumption by Ero1 α . After the addition of GPX7 the rate of oxygen consumption by Ero1 α (as a measure of PDI oxidation) increased. This indicates that oxygen consumption by Ero1 α is more efficient in the presence of GPX7 (Nguyen et al., 2011).

1.7.6 QSOX pathway

While searching for other alternative pathways that could compensate for the lack of Ero1 in yeast, Erv2p a sulfhydryl oxidase was discovered (Sevier et al., 2001). Erv2p is related to mammalian QSOX whose physiological role is still not clear, however, it is known that QSOX can transfer disulfides into proteins *in vitro* (Kodali and Thorpe, 2010). QSOX shares some similarities with Ero1, both are flavoproteins able to catalyse *de novo* disulfide formation producing H_2O_2 (Kodali and Thorpe, 2010b). In contrast to Ero1, QSOX can introduce disulfides to a broad range of substrates other than PDI, however, the formation of native disulfide bonds in proteins is greatly improved in the presence of PDI (Rancy and Thorpe, 2008). This might be due the fact that QSOX is not able to isomerise non-native disulfides (Rancy and Thorpe, 2008). Mammalian QSOX has a sulfhydryl oxidase module composed of Erv domain harbouring the oxidase activity and oxidoreductase module composed of two thioredoxin domains (Figure 1.12) (Limor-Waisberg et al., 2013).

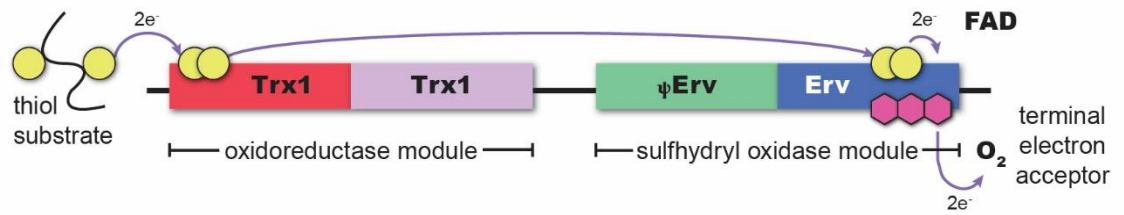


Figure 1.12 Schematic representation of QSOX. QSOX contains a sulfhydryl oxidase module composed of Erv domain harbouring the oxidase activity and oxidoreductase module composed of two thioredoxin domains. Trx1 domain accepts electrons from thiol substrate and transfer it to Erv domain of the sulfhydryl oxidase module and then to FAD cofactor. Electrons can be then transferred to oxygen or passed to PDI. Adapted from Limor-Waisberg et al., 2013

1.8 Glutathione in the ER

It has been proven that in the ER the ratio of GSH:GSSG is lower than elsewhere in the cell, around 3:1 (Hwang et al., 1992). The fact that this GSH:GSSG ratio in the ER is optimal for disulfide-bond formation indicates the importance of GSH for this process (Lyles and Gilbert, 1991). However, for a long time the exact role of GSH in the disulfide bond formation was unclear. Until the discovery of Ero1 it was believed that the primary role of GSSG was to oxidise PDI. It was found that the production of GSSG is an indirect consequence of Ero1 activity. Only recently have new roles for GSH in the ER emerged (Cuozzo and Kaiser, 1999, Molteni et al., 2004).

1.8.1 Role of glutathione in the ER

Although the GSH:GSSG ratio in the secretory pathway is low, the overall GSH buffer system is still reducing (Cuozzo and Kaiser, 1999). It was observed in yeast that if cellular levels of GSH are decreased, the growth of the *ero1* depleted strain can be restored (Cuozzo and Kaiser, 1999). The activity of Ero1 is also counterbalanced by GSH in mammalian cells clearly suggesting that the generation of GSSG is an indirect consequence of Ero1 activity (Cuozzo and Kaiser, 1999). The reducing environment provided by GSH is important in keeping PDI family members partially reduced (Chakravarthi et al., 2006, Jessop and Bulleid, 2004). This is important for preventing formation of non-native disulfide by facilitating substrate reduction (Chakravarthi et al., 2006, Jessop and Bulleid, 2004). Cells treated with the reducing agent dithiothreitol (DTT) rapidly re-established the normal cellular GSH:GSSG ratio (Appenzeller-Herzog et al., 2010). Moreover, after treating cells overexpressing Ero1 with DTT the six-fold excess of GSSG in the ER was quickly restored to normal cellular levels after the washout of the reducing agent (Appenzeller-Herzog et al., 2010). These data indicate that maintaining the cellular level of GSH is important, also the GSH:GSSG ratio in the ER must be tightly balanced.

The mentioned results highlight two central features of ER redox control. Because of the high total GSH concentration in the ER (in millimolar range) GSH is able to provide an excellent buffering capacity against reductive and oxidative stress

(Appenzeller-Herzog et al., 2010). In addition to free GSH, glutathionylated proteins in the ER also constitute a major cellular pool for buffering oxidative stress (Hansen et al., 2009). However, more research needs to be done in order to precisely quantify the amount of glutathionylated proteins in the ER as well as their role. It has been shown that feedback regulation of Ero1 activity is an important factor in ER redox control. In fact, the activity of all forms of Ero1 is shut down in response to hyperoxidation, this is due to the presence of regulatory disulfides (Bulleid and Ellgaard, 2011). In the case of Ero1 α the regulatory disulfide is formed depending on the redox state of PDI (Appenzeller-Herzog et al., 2008). When reduced PDI is abundant and Ero1 α is active, however, if the levels of oxidised PDI are high Ero1 α becomes inactivated (Appenzeller-Herzog et al., 2010). Using this mechanism PDI “informs” Ero1 about the redox status of the ER to ensure that Ero1 does not generate disulfides and H₂O₂ unless it is necessary (Appenzeller-Herzog et al., 2010). The reason why PDI can sense the ER redox state is most likely the fact that PDI reacts very rapidly with both GSH and GSSG, this feature is probably shared by most PDI family members (Lappi and Ruddock, 2011). Moreover, the reaction between PDI and GSSG is much faster than between GSSG and any other reduced substrate (Karala et al., 2009a). Interestingly GSH is not the first choice substrate for all the enzymes described in section 1.6, instead they prefer interaction with PDI family members (Karala et al., 2009b). The general conclusion is that all the enzymes described in section 1.6 are generating oxidizing equivalents which are passed on to PDI family members. The PDI then oxidise substrate proteins or – in a competing reaction – GSH (Bulleid and Ellgaard, 2011).

1.8.2 Maintenance of GSH:GSSG ratio inside the ER

There is one important question related to GSH in the ER. How is the GSH:GSSG ratio maintained and regulated inside the ER? It was shown that microsomes derived from the ER can import GSH, however, this is not the case for GSSG, suggesting that GSSG may not be transported to the cytosol at substantial levels (Banhegyi et al., 1999). GSSG was found to exit the ER through vesicular transport but this mechanism of efflux did not prove to be effective in restoring the ER GSH homeostasis when cells were treated with reducing agent (Appenzeller-Herzog et al., 2010). Adding the fact that microsomes lack reductase activity gives rise to the question of how GSSG generated in the ER is removed to prevent the ER from

hyperoxidation. (Bulleid and Ellgaard, 2011). Perhaps importing GSH together with other reducing equivalents, such as free sulfhydryl groups on newly synthesized proteins from the cytosol is the key factor preventing hyperoxidation of the ER. However, when this hypothesis was tested by inhibiting protein translation and decreasing cellular GSH levels, the distribution of oxidized and reduced PDI proteins did not change (Appenzeller-Herzog et al., 2010). Therefore, the most logical explanation of how the ER redox homeostasis is restored after oxidative stress and how GSSG is removed from the ER is that GSSG reacts with substrate proteins or PDI family members (Bulleid and Ellgaard, 2011). This clearly indicates the importance of GSSG in oxidative protein folding, as high reaction rate of GSSG with PDI shows that GSSG is not just a by-product of redox reactions that needs to be removed from the ER (Bulleid and Ellgaard, 2011).

1.9 Glutathione transporters

GSH is synthesised in the cytoplasm and functions as a cellular redox buffer. GSH is also present in most organelles within the cell, including mitochondria, nucleus, chloroplast (in plants), and the ER. GSH is also present in vacuoles and extracellular milieu. Cells have the ability to uptake GSH from extracellular environment as well as exporting GSH outside the cell (Bachhawat et al., 2013). The total GSH concentration and GSH:GSSG ratio is different in each organelle, suggesting that the transport and homeostasis inside each organelle must be regulated. Although we have been aware of the requirement for GSH transporters, to date very few have been identified, and these have been mostly found in yeasts (Figure 1.13).

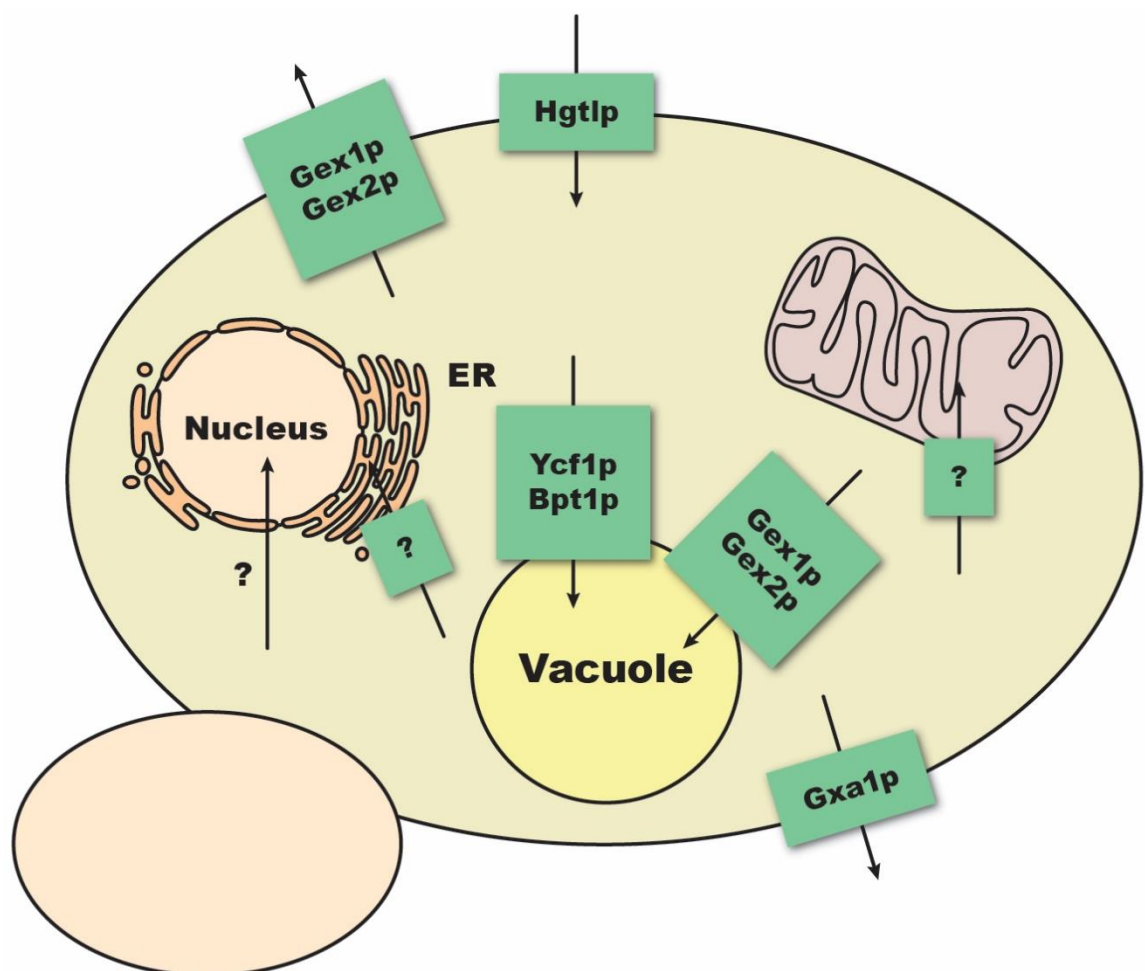


Figure 1.13 Diagrammatic representation of *Saccharomyces cerevisiae* with indicated GSH transporters. Adopted from Bachhawat et al. (2013)

1.9.1 Glutathione efflux

Multidrug resistance-associated protein (MRP), a member of a subclass of the ATP-Binding Cassette (ABC) transporter superfamily, was the first GSH transporter identified in the yeast *Saccharomyces cerevisiae*. MRP is involved in GSH efflux from the vacuole in yeast, however, MRP was also identified as being responsible for GSH efflux at the plasma membrane in mammalian cells (Rebbeor et al., 1998b). There are nine MRP family members in humans, MRP1 to MRP9, all of them are plasma membrane localised and use ATP hydrolysis for pumping substrates out of the cell (Bachhawat et al., 2013). MRP is a multi-specific organic anion transporter and as the name suggests, MRP's main role is in multidrug resistance. The progress in our understanding of the role of MRP in GSH efflux had been slow and has encountered many technical difficulties such as the presence of multiple transporters in the plasma membrane that interfere with the studies, the lack of suitable inhibitors and the inherent technical difficulties in studying efflux (Bachhawat et al., 2013). Despite the difficulties, over the years evidence had confirmed that MRP is indeed involved in GSH efflux, but has low affinity for GSH and primarily transport GSH conjugates rather than GSH itself (Bachhawat et al., 2013). The strongest evidence for a role of MRP family in GSH efflux in mammalian cells comes from the overexpression of MRP1, which correlates with an increased efflux of GSH (Zaman et al., 1995, Lautier et al., 1996). Overexpression of MRP2 lead to a similar effect but in addition to secreting more GSH, the level of intracellular GSH levels were lower when compared to cells which did not overexpress MRP2 (Rebbeor et al., 2002). The yeast cadmium factor 1 (Ycf1p), yeast orthologue of mammalian MRP1, confirmed the role of MRP in GSH transport in experiments measuring the uptake of radiolabelled GSH by vacuolar membrane vesicles expressing Ycf1p (Rebbeor et al., 1998b). Later these results were validated by MRP1 reconstitution in proteoliposomes, ultimately proving MRP's role in GSH transport (Mao et al., 2000). Unfortunately, the mechanism of GSH efflux by MRP is not well understood and there are at least four different suggested mechanisms of GSH transport by MRP. These mechanisms include GSH transport being enhanced by certain compounds that are not themselves substrates for MRP1, GSH being required for the cotransport of certain MRP1 substrates, GSH stimulating the transport of certain compounds by MRP1 but is not translocated across the membrane itself and GSH acting as a direct low-affinity substrate for MRP1 (Ballatori et al., 2005, Bachhawat et al., 2013).

There are other examples of mammalian transporters responsible for GSH efflux, however, they are less well characterised than MRP. These include ATP-binding cassette sub-family G member 2 (ABCG2) belonging to the ABCG subfamily of ATP-binding cassette (ABC) transporters. ABCG2 protects cells against chemical damage similar to MRP. First evidences of ABCG2 involvement in GSH transport came from the observation that extracellular levels of GSH increased in an ABCG2-dependent manner when treated with 2-5-dihydroxychalcone (2-5-DHC), the results were validated by inhibiting the transport of MTX, a known ABCG2 substrate (Bachhawat et al., 2013). These results suggest that there is a competition between MTX and GSH for export through ABCG2 (Bachhawat et al., 2013). A further confirmation of a role for ABCG2 in GSH efflux came from experiments in yeast. Overexpression of ABCG2 in *S. cerevisiae* lead to a 2.5-fold increase of extracellular GSH. Moreover, this effect was inhibited by MTX (Bachhawat et al., 2013). Decrease of extracellular levels of GSH was observed in mammalian cells after shRNA silencing of ABCG2 mRNA (Brechbuhl et al., 2010).

There has been evidence that gap junctions, channels between two adjacent cells, are able to release GSH from cultured rat astrocytes (Ranat and Dringen, 2007). Each gap junction channel is made up of hemi-channels, which are made up of 6 connexin proteins. The role of gap junctions is to control the passage of molecules smaller than 1 kDa in size (Stout et al., 2002). The role of gap junctions in GSH transport has been validated by inhibiting the transport either by specific hemi-channel blockers or by an increase of calcium concentration in the media (Bachhawat et al., 2013).

The OATP (SLCO1A2 — solute carrier organic anion transporter family, member 1A2) belongs to family of transporters functioning independently of ATP and sodium gradients (Hagenbuch and Meier, 2003). A role for OATP in GSH transport has been demonstrated in *X. laevis* oocytes, however, there are many independent studies questioning these results (Li et al., 1998, Mahagita et al., 2007).

Initial investigation of GSH uptake in *S. cerevisiae* implied there must be a mechanism responsible for transporting GSH into the cytoplasm (Miyake et al., 1998). The following studies identified Hgt1p as the first high affinity GSH transporter needed for GSH uptake from the extracellular medium (Bourbouloux et al., 2000). Knockout of the yeast gene encoding Hgt1p resulted in the inability to

uptake radiolabelled GSH from the medium (Bourbouloux et al., 2000) Hgt1p belongs to the oligopeptide transporter family (OPT), it was thought that OPT are only able to transport short oligopeptides, 4 to 8 amino acids in length (Bachhawat et al., 2013). The simultaneous discovery, by a different group, that Hgt1p also transports some oligopeptides, including leu-enkephalin (Tyr–Gly–Gly–Phe–Leu) and met-enkephalin (Tyr–Gly–Gly–Phe–Met), led to confusion and to question the true nature of Hgt1p as high affinity GSH transporter (Hauser et al., 2000). However further research confirmed that the main role of Hgt1p is in fact GSH transport (Srikanth et al., 2005, Osawa et al., 2006, Miyake et al., 2002). It was not possible to inhibit Hgt1p mediated transport of GSH by competition with amino acids or other tripeptides, however the uptake was sensitive to inhibition by GSSG and GSH conjugates, implying these are also substrates for Hgt1p (Bourbouloux et al., 2000). Unfortunately, there is no Hgt1p homologue in higher eukaryotes (Bachhawat et al., 2013).

1.9.2 Glutathione uptake from the extracellular environment

It has been established that in order to maintain intracellular and interorgan GSH homeostasis mammalian cells require GSH transport across the plasma membrane (Bachhawat et al., 2013). For many years the uptake of the GSH molecule into the cell had been debated, despite the fact that transport of GSH into the cytoplasm was proposed as early as 1979 (Griffith and Meister, 1979, Lash, 2005). Nowadays there are several pieces of evidence supporting two main mechanisms of glutathione uptake into the mammalian cells (Bachhawat et al., 2013).

There is evidence for both Na⁺ dependent and Na⁺ independent GSH transport in different tissues, including brain cells, small intestine, and renal basolateral membrane (Iantomasi et al., 1997, Lash and Jones, 1984, Kannan et al., 1999). Inhibition of γ -glutamyl transpeptidase (γ -GT) by the irreversible inhibitor acivicin did not block GSH uptake, suggesting there is a transporter able to take up intact GSH (Lash and Jones, 1983, Bachhawat et al., 2013). Studies on renal basolateral membrane using various substrates and inhibitors of known GSH transporters helped identify three putative GST transporters responsible for GSH uptake (Bachhawat et al., 2013). Two of these transporters are sodium independent renal organic anion transport (OAT) systems, OAT1 (Gene name SLC22A6 — solute carrier family 22 (organic anion transporter), member 6 and OAT3 (Gene name

SLC22A8 — solute carrier family 22 (organic anion transporter), member 8. In addition sodium-dependent dicarboxylate carriers (NaC3 or SDCT-2, Gene name SLC13A3 — solute carrier family 13 (sodium-dependent dicarboxylate transporter), member 3 has been implicated in GSH uptake across the renal basolateral (Lash, 2005, Lash and Putt, 1999). Reconstitution of OAT3 into proteoliposomes also showed GSH transport (Bachhawat et al., 2013).

By extracellular degradation and uptake of its constitutive amino acids (glutamate, cysteine and glycine), GSH can be transported indirectly into the cytoplasm (Bachhawat et al., 2013). Extracellular degradation of GSH is catalysed by γ -GT which breaks down GSH into cys-gly dipeptide and glutamate (Bachhawat et al., 2013). These GSH precursors are then transported back into the cell where GSH is resynthesised (Bachhawat et al., 2013). This model of indirect GSH transport is presumed to operate in all mammalian cells. The facts that inhibition of γ -GT activity, or its inactivation due to genetic disorder, resulted in glutathionuria, a high level of GSH in the urine, only confirms the role of γ -GT in indirect GSH transport (Griffith and Meister, 1979, Njalsson and Norgren, 2005)

1.9.3 Glutathione transport in organelles

GSH is present in the nucleus where it plays an important role in the cell cycle, in cell proliferation and redox signalling (Markovic et al., 2007). Small molecules and ions are allowed to diffuse through the nuclear pore complex, therefore it was assumed that GSH can also enter the nucleus by diffusion (Bachhawat et al., 2013). Some evidence suggests ATP dependent GSH transport into the nucleus by antiapoptotic factor Bcl-2, which forms a pore-like structure (Voehringer et al., 1998). However the role of Bcl-2 in GSH transport has not been clearly established (Voehringer et al., 1998).

GSH in the mitochondria constitutes around 10-15% of total cellular GSH. In the mitochondrial inner membrane several transporters had been characterised as capable of transporting GSH, dicarboxylate carriers (DCC or DIC, gene name SLC25A10 — solute carrier family 25 (mitochondrial carrier; dicarboxylate transporter), member 10) and 2-oxoglutarate carriers (OGC, gene name SLC25A11 — solute carrier family 25 (mitochondrial carrier; oxoglutarate carrier), member 11)

(Bachhawat et al., 2013). The role of these transporters in GSH transport has been established by reconstitution in proteoliposomes (Chen et al., 2000). It is assumed that the presence of porins in the outer mitochondrial membrane allows GSH to diffuse through the outer membrane (Bachhawat et al., 2013). The evidence supporting this theory comes from observations that the level of GSH in the mitochondrial matrix did not change after disruption of the integrity of the outer mitochondrial membrane, also implying that the influx into the mitochondrial matrix is not limited by the rate of GSH transport across the outer membrane (Bachhawat et al., 2013). However, no significant decrease of GSH transport was observed after disruption of pore forming proteins, suggesting there may be other GSH transporters present (Cummings et al., 2000).

Because of low GSH:GSSG ratio in the ER it was suggested that only GSSG is selectively transported across the ER membrane (Hwang et al., 1992). Although, later studies suggested that GSH is the preferred substrate for transport into the ER, GSSG is also transported into the ER at slower rate (Banhegyi et al., 1999). Some evidence suggests that the ryanodine receptor, RyR1 (ryanodine receptor calcium channel type 1) may play an important role in GSH transport into the ER or sarcoplasmic reticulum (SR) of skeletal muscles (Csala et al., 2001). Microsomes prepared from a HEK-293 cell line transfected with RyR1 showed an increase of GSH transport when compared to microsomes prepared from a non-transfected HEK-293 cell line, suggesting that RyR1 may have a role in GSH transport. RyR1 contains a high number of cysteine residues and some studies argue that the increase of GSH transport might be in fact a consequence of S-glutathionylation (Bachhawat et al., 2013). The fact that the kinetics of GSH transport across SR membrane is different than the transport across the ER membrane in liver cells is also controversial (Bachhawat et al., 2013).

1.10 Summary

Despite over 125 years since the initial discovery of GSH, there are still many things unknown related to this tripeptide, especially its transport. Some of GSH functions were only mentioned briefly in this introduction. The main function of GSH is however, considered to be a cellular thiol “redox buffer” used to maintain a required level of thiol/disulfide redox potential. In the ER GSH plays a central role in maintaining the ER redox homeostasis. GSH equilibrates with PDI to provide feedback and to regulate Ero1. This system prevents the generation of disulfide when unnecessary, therefore preventing hyper oxidation.

GSH is also essential for correct protein folding. Protein folding is a complicated process, therefore it is not surprising that it is prone to errors. Misfolded proteins result in a wide variety of pathological conditions. Some of diseases related to protein misfolding result from proteins not being able to fulfil their proper biological function, for example cystic fibrosis (Dobson, 2003). These diseases are often caused by genetic mutations and are referred to as familial disorders. Because proteins will always try to find their most energetically favourable state some proteins will achieve it by aggregation. These proteins usually escape all the quality control mechanisms ensuring correct folding. As more and more aggregates accumulate within the cell, or extracellular space, the disease progresses. Type II diabetes, Alzheimer’s disease, Parkinson’s disease and the spongiform encephalopathies are the most common disease caused by the aggregation of misfolded proteins. There are some known proteins able to transport GSH across the plasma membrane, but few known transporters are able to transport GSH to other organelles.

1.10.1 Aims of the project

In this project, we tried to develop an assay suitable for measuring the transport of GSH into the ER, using microsomes prepared from a cell line expressing the ER localised roGFP. roGFP is a powerful tool used in redox biology, by localising roGFP into a specific cellular compartments it is possible to understand the differences in redox potential in different parts of the cell. However, in our assay roGFP is used as an indirect indicator of GSH transport across the microsomal membrane. A more

quantitative assay relying on GSH conjugation to different substrates by glutathione S-transferase (GST) was also developed. These two assays complement each other and help understand GSH transport across the microsomal membrane in different ways. The ultimate aim of the project was to identify the ER glutathione transporter(s). Although this can potentially be achieved by several methods we presumed there must be a direct interaction between GSH and the transporter, thus by exploit this interaction we may be able to separate the transporter from other proteins present in the ER membrane.

1.10.2 Impact of the project

This project will contribute to expanding our knowledge in several fields, including protein folding. Secreted proteins contain disulfide bonds, which are essential for protein stability. However, the knowledge of how correct disulfides are formed, and incorrect disulfides are removed, is still limited. In the last decade, many proteins contributing to disulfide bond formation and non-native bond isomerisation were described. GSH plays an important role in disulfide bond formation, therefore by understanding how GSH is transported into the ER it might be possible to understand more about how disulfides are formed and proteins are folded.

The redox homeostasis within the cell and other organelles, including the ER is tightly regulated, however this process, especially in the ER, is still not clearly understood. When the redox homeostasis in the ER is disrupted it has strong impact for all the functions of the ER. Disruption of the transport of GSH into the ER maybe the main cause of redox imbalance in the ER. By knowing more about GSH transport it might be possible to understand more about how redox homeostasis is maintained within the ER.

The molecular identity of many GSH transporters is still not known. There are also many ambiguities related to the known GSH transporters. Therefore, identifying the first ER GSH transporters would have an enormous impact on the entire field. More over by knowing more about the ER GSH transporter it might be possible to stimulate it in a way that would accelerate GSH transport, possibly having a beneficial effect on disulfide bonds formation, possibly mitigating effects of some diseases related to misfolded protein.

Chapter 2

Materials and methods

2.1 Cell culture

All cells were propagated in Dulbecco's Modified Eagle Medium (ThermoFisher, cat. No. 21969035) supplemented with 10% (v/v) fetal bovine serum, 50 U/ml of penicillin, 50 µg/ml streptomycin and 2 mM L-glutamine until confluent at 37°C under 5% CO₂. Cells were cultured in 75 cm² flasks and split 1:10 when they became confluent. Before the passage cells were washed with 1X PBS (ThermoFisher, cat. No. 14190094) and then trypsinised with 0.05% Trypsin-EDTA (ThermoFisher, cat. No.25300054).

2.2 Protein methods

2.2.1 SDS-PAGE

All proteins were analysed by 12.5% SDS-PAGE under reducing conditions followed by Coomassie blue (10% (v/v) phosphoric acid, 10% (v/v) ammonium sulfate, 0.12% (w/v) Coomassie G250, and 20% (v/v) methanol) staining or silver staining. 4X sample buffer (200 mM TrisHCl pH 6.8, 8% (w/v) SDS, 0.4% (w/v) bromophenol blue, 40% (v/v) glycerol) was added to proteins before separation by SDS-PAGE. Gel electrophoresis was carried out in 1 X running buffer (25 mM Tris, 20 mM Glycine, 3 mM SDS) for 2 h at 20 mA.

2.2.2 Silver staining

The polyacrylamide gel was fixed for 10 min in 50% (v/v) methanol, 12% (v/v) acetic acid and 0.05% (v/v) formalin. The gel was washed three times in 35% (v/v) ethanol for 5 min. After sensitizing in 0.02% (w/v) Na₂S₂O₃ polyacrylamide gel was washed three times in H₂O for 5 min. 0.2% (w/v) AgNO₃ and 0.076% (v/v) formalin was used to stain the gel for 20 min. After staining the gel was washed two times in H₂O for 1 min before developing in 6% (w/v) Na₂CO₃, 0.05% (v/v) formalin and 0.0004% (w/v) Na₂S₂O₃. The development of the gel was carried until protein bands became visible. The development of the gel was stopped using 50% (v/v) methanol and 12% (v/v) acetic acid for 5 min. The gel was stored in H₂O.

2.2.3 Western blot

Proteins separated on SDS-PAGE were electrophoretically transferred onto an Amersham Protran 0.45 NC nitrocellulose membrane (GE Healthcare, cat. No. 10600007) at 150 mA for 2 h in 1 X transfer buffer (25 mM Tris, 20 mM Glycine, 3.5 mM SDS, 20% (v/v) methanol). The transfer was blocked with either 5% (w/v) milk or 3% (w/v) BSA (in the case of biotinylated proteins) for 1 hour. The membrane was treated with the primary antibody (1:1000 dilution) for 4 hours, followed by three 5 minute washes with TBST buffer (20 mM Tris (pH 7.8), 150 mM NaCl, 0.1% (v/v) TWEEN® 20 (Sigma, cat. No. P1379-1L)) and incubation with the secondary antibody (1:10000 dilution) for 40 min. Biotinylated proteins were incubated with streptavidin-800 for 40 min. Proteins were visualised by using a Li-cor Odyssey Sa fluorescence scanner.

2.3 GSH transport assay (roGFP)

2.3.1 Preparation of microsomes

Fully confluent HT1080 cells expressing super-folded roGFP1-iE-KDEL were trypsinised, washed two times with ice cold PBS and resuspended in Buffer A (50 mM Tris-HCl (pH 7.4), 0.25 M sucrose, 25 mM KCl, 0.5 mM MgCl, 1 mM EDTA). HT1080 cells were harvested from four T225 cm² flasks, combined and then homogenised using a ball-bearing homogeniser (12 µM ball, 4 passes) and centrifuged at 6000 x g for 8 minutes to yield the postnuclear supernatant (PNS). PNS was centrifuged at 150,000 x g (Beckman Optima™ MAX-XP Ultracentrifuge, rotor TL 100.3) for 40 min at 4°C to sediment microsomes. The pellet was resuspended in 500 µl of Buffer A by pipetting. Microsomes were frozen using liquid nitrogen and stored at – 80 C° or used immediately.

2.3.2 Optimising the concentration of reducing agents

Two aliquots of microsomes were treated with different concentrations of dithiothreitol (DTT, Melford, cat. No. MB1015), tris(2-carboxyethyl)phosphine (TCEP, Thermo Scientific, cat. No. 20490) or GSH (Sigma, cat. No. G4215). The

first aliquot consisted of intact microsomes while the second aliquot was solubilised by 0.15% (v/v) Triton X-100 (Sigma, cat. No. T8523). The absorbance of both aliquots was measured using PHERAstar® FS after approximately 1 hour after addition of reducing agents.

2.3.3 roGFP transport assay of reducing agents across the ER membrane

To measure the rate of transport of individual reducing agent microsomes were loaded into a 96 well flat bottom plate. Each reducing agent (DTT, TCEP and GSH) was added to a different well to a final concentration of 0.2 mM DTT, 0.2 mM TCEP, 5 mM GSH and the fluorescence of roGFP was measured at 390 nm and 460 nm every 30 seconds for 55 minutes using PHERAstar® FS. In order to assess how the presence of ER membrane affects transport the experiment was repeated after addition of a detergent (Triton X-100) to microsomes (the final concentration- 0.15% (v/v)) before adding reducing agents.

2.3.4 Serine protease digestion of microsomes

Microsomes were treated with a concentration range (25 µg/ml - 100 µg/ml) of either proteinase K, trypsin, or chymotrypsin and incubated at room temperature for approximately 20 min. After protease treatment a transport assay was performed.

2.3.5 Alkylation of glutathione

200 mM of N-Ethylmaleimide (NEM) was added to 500 µl of 200 mM GSH and incubated for 10 min at room temperature. The sample was analysed and purified using RP-HPLC performed on an AKTA Explorer 10 instrument. 100 µl of each sample was flowed through a Jones Chromatography HPLC C8 Column using a 200 µl/min flow rate with gradients of increasing concentration (0-100%) of methanol (containing 0.1% trifluoroacetic acid).

2.3.6 Inhibition of transport by N-ethylsuccinimido-S-glutathione (ESG)

Microsomes were treated with a concentration range (25 µg/ml - 100 µg/ml) of ESG and incubated at room temperature for approximately 20 min. After ESG treatment a transport assay was performed.

2.3.7 GOH synthesis

GOH was synthesised using Solid Phase Peptide Synthesis (SPPS) with BOP as a coupling reagent, N,N-Diisopropylethylamine (DIPEA) as non-nucleophilic base and Dichloromethane (DCM) as an organic solvent. The first step of the synthesis involved addition of Boc-Ser to HCl-Gly. Boc-Ser (25 mM), HCl-Gly (30 mM), Bop (30 mM) and DiPEA (60 mM) were added to 100 ml of DCM. The mixture was placed on ice before adding DiPEA to avoid ester bond formation between Boc-Ser. The solution was mixed for 2 h and analysed by thin layer chromatography (TLC) in 6 ml Ethyl Acetate, 4 ml Hexane 4-5 drops of Acetic Acid (AcOH) were added, checked under UV light and then stained with Ninhydrin. The solvent was evaporated under vacuum at +40°C. Acid-Base extraction was performed using 80 ml of Ethyl Acetate, followed by 100 ml of KHSO₄ and 100 ml of NaHCO₃ and 100 ml of Brine. Solvent was dried by adding Magnesium Sulfate and filtered. Mixture was evaporated under vacuum at +40°C and purified using a silica (geduran si 60) column. Purified fractions were collected and analysed using TLC. Fractions containing the compound were combined into a 1L flask, evaporated under vacuum at +40 °C and then left overnight under high vacuum. Finally, the structure of Boc-SerGly-OtBuBoc was confirmed by ¹H NMR. The Boc protective group was removed by HCl/dioxane as described by Han, G. et al (Han et al., 2001). Boc-Glu-OtBu was added to purified SerGly-OtBu. Boc-Glu-OtBu (5.5 mM), SerGly-OtBu (4.5 mM), Bop (5.5 mM) and DiPEA (11 mM) were mixed in 20 ml DCM. The reaction and purification proceeded as described above for SerGly-OtBu with additional TFA/DCM step to remove OtBu protection groups before removal of Boc by HCl/dioxane. 5 ml of TFA and 5 ml of DCM was added per 100 mg of compound. The mixture was mixed for 1 hour and evaporated under vacuum at +40 °C in a fume hood. Next Ether was added to the mixture and the evaporation was repeated. After evaporation the mixture was freeze dried overnight. Structure of GOH was confirmed by ¹H NMR (Figure 2.1). GOH was freeze dried and stored at room temperature.

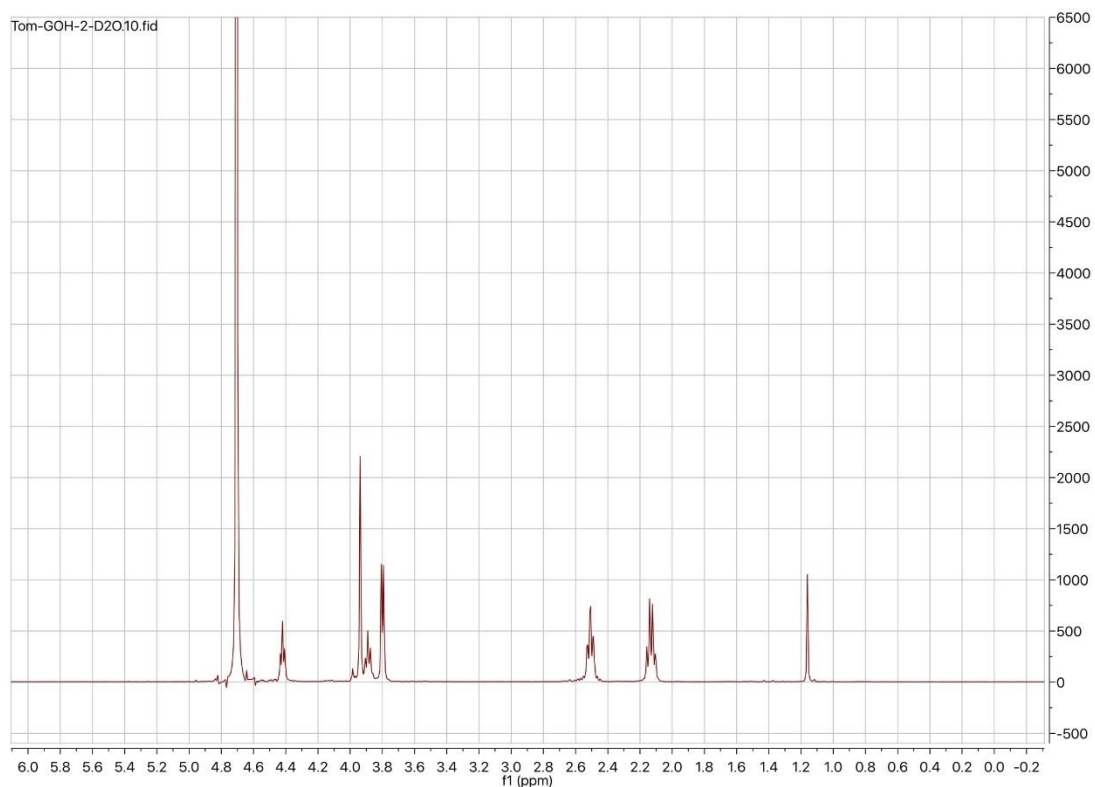


Figure 2.1 ^1H NMR spectrum of GOH.H NMR (D_2O , 400 MHz) δ 4.52 (t, $J = 5.3$ Hz, 1H), 4.04–4.01 (m, 3H), 3.90 (d, $J = 5.3$ Hz, 2H), 2.62 (td, $J = 7.2, 2.3$ Hz, 2H), 2.27–2.22 (m, 2H)

2.3.8 GOH inhibition of GSH transport

Different concentrations (5 mM – 50 mM range) of GOH and 5 mM GSH were simultaneously added to microsomes and a transport assay was performed as described above.

2.4 Generation of stable cell line expressing GSTP1-1A in the ER

2.4.1 GSTP1-1A plasmid construct designing

A GSTP1-1A-KDEL construct was designed using the GSTP1-1A sequence (accessed online at <https://www.ebi.ac.uk/ena/data/view/AAA56823>). An EcoRI restriction site followed by IgG signal sequence were added to the 3' end of GSTP1-1A sequence. Flag tag followed by KDEL sequence and NotI restriction site were added to the 5' end of the sequence. The designed construct was ordered using GeneArt™ Plasmid Construction Service in the pMA-RQ vector.

2.4.2 Transformation

Plasmids were transformed into *E. coli* rubidium chloride competent cell. 100 ng of GSTP1-1A-KDEL_pMA-RQ plasmid was added to 50 µL of competent cells and left on ice for 30 min. Cells were exposed to a heat shock at 42°C for 45 secs and placed on ice for 2 min. LB broth (850 µl) was added and the cells were incubated for 1h at 37°C. 100 µL of bacteria were plated on 1% agar plates containing Ampicillin (100 µg/ml).

2.4.3 Plasmid purification

A single colony was picked from the agar plate and incubated overnight at 37°C in 2 ml of LB broth containing Ampicillin (100 µg/ml). Cells were pelleted and resuspended in GTE buffer (25 mM TrisCl pH8, 50 mM glucose, 10 mM EDTA) with RNase A (10 mg/ml) followed incubation at RT for 2 min. 200 µL of freshly made NaOH/SDS (0.2 M NaOH, 1% (w/v) SDS) was added and cells were placed on ice for 5 min and 150 µl of 5 M potassium acetate solution (pH 4.8) was added. The resulting solution was centrifuged at 16,000 x g for 5 min. The supernatant was transferred into a clean Eppendorf tube containing 450 µl phenol:chloroform:isoamyl alcohol (25:24:1), mixed and centrifuged at 16,000g for 2 min. The upper phase was transferred to a new tube containing 450 µl chloroform:isoamyl alcohol, mixed and centrifuged at 16,000 x g for 2 min. The upper phase was transferred to a new tube containing 800 µl 95% (v/v) ethanol and 16,000g for 5 min. The pelleted DNA was

washed with 1 ml 70% (v/v) ethanol and air-dried. Plasmid DNA was resuspended into 30 µl dH₂O and stored in -20°C.

2.4.4 Restriction digest

Double restriction digest of GSTP1-1A-KDEL_pMA-RQ and empty pcDNA3.1 vector was performed using EcoRI and NotI endonucleases manufactured by NEB. The double digestion was performed following the manufacturer's guidelines using CutSmart® Buffer.

2.4.5 Agarose gel electrophoresis

10 µL of SYBR™ Safe DNA Gel Stain (Invitrogen, cat. No. S331103) was mixed with 100 ml of 1% agarose gel (Bio-Rad cat. No. 1613102). 6X blue/orange loading dye (Promega, cat. No. G1881) was added to DNA before analysis. A 1 Kb plus DNA ladder (Invitrogen, cat. No. 10787018) or a 100 bp DNA ladder (NEB, cat. No. N3231S) were used to estimate DNA fragment size.

2.4.6 DNA gel extraction/purification

Endonuclease digested DNA was extracted from a 1% agarose gel and purified using QIAquick Gel Extraction Kit (QIAGEN, cat. No. 28706) following the manufacturer's protocol. The concentration of purified DNA was determined by measuring the OD at 260 nm using the Spectrostar nano plate reader (BMG Labtech).

2.4.7 Ligation

GSTP1-1A-KDEL sequence was ligated into 100 ng of empty pcDNA3.1 vector. 3:1 or 5:1 insert vector ratio was calculated using the following formula:

$$\frac{\text{ng of vector} \times \text{kb size of insert}}{\text{kb vector size}} \times \frac{\text{molar ratio of insert}}{\text{ng of vector}} = \text{ng of insert}$$

The volume of the ligation mixture contained vector, insert DNA, ligation buffer (250 mM Tris-HCl (pH 7.6), 50 mM MgCl₂, 5 mM ATP, 5 mM DTT, 25% (w/v) polyethylene glycol-8000) (Invitrogen, cat. No 46300018), 1 unit T4 DNA ligase (Invitrogen, cat. No 46300018) was brought to 10 µl with dH₂O. The ligation mixture was incubated overnight at 4°C.

2.4.8 Plasmid purification and sequencing

GSTP1-1A-KDEL_pcDNA3.1 plasmid was transformed into *E.coli* as described above. Plasmid DNA was extracted and purified from a single colony incubated overnight in LB broth containing Ampicillin (100 µg/ml) using the Qiagen® Plasmid Midi Kit (QIAGEN, cat. No. 12143) following the manufacturer's protocol. Purified GSTP1-1A-KDEL_pcDNA3.1 plasmid was sequenced using T7 forward primer and BGH reverse primer by the GATC biotech Sanger sequencing service.

2.4.9 Transfections into HT1080

The GSTP1-1A-KDEL_pcDNA3.1 plasmid was transfected into HT1080 cells using MegaTran 1.0 (OriGene, cat. No. TT200003) following the manufacturer's protocol.

2.4.10 Selection

Various concentrations (1:10 to 1:10,000) of transfected HT1080 cells were plated on 15 cm² dishes. Cells were grown in Dulbecco's Modified Eagle Medium (ThermoFisher, cat. No. 21969035) supplemented with 10% fetal bovine serum, 50 U/ml of penicillin, 50 µg/ml streptomycin, 2 mM L-glutamine until confluent and 200 µg/ml Hygromycin B until colonies appeared. Single colonies were picked and transferred to 12 well plate using Scienceware® cloning discs (Sigma, cat. No Z374431-100EA). Cells were grown until confluent and then transferred to 25 cm² flask and then 75 cm² flask when confluent. The presence of GSTP1-1A was confirmed by Western blot using ANTI-FLAG® M2 antibody (Sigma, cat. No F316S).

2.4.11 Cultivation

Cells were cultivated as described in section in 2.1

2.5 Cloning and purification of GSTP1-1A

2.5.1 Polymerase chain reaction (PCR)

GSTP1-1A-KDEL sequence was amplified by PCR in order to remove the IgG signal sequence and the KDEL sequence, using the following conditions: 5 min of initial denaturation at 94°C, 35 cycles each consisting of 30 sec denaturation at 94°C, annealing at 66°C for 60 sec, 1 min extension at 72°C, and final extension at 72°C for 10 min. Each PCR tube contained: 50 ng of template DNA, 1 X Accuzyme buffer (60 mM TrisHCl, 6 mM (NH₄)₂SO₄, 10 mM KCl, 2 mM MgSO₄, pH 8.3) (Bioline, cat. No. BIO-21052), 2 mM MgCl₂ (Bioline, cat. No. BIO-21052), 10 mM dNTP mix, 2% (v/v) DMSO, 2.5 units Accuzyme (Bioline, cat. No. BIO-21052), 10 μM forward primer (3'GGCCATGGATGCCGCCCTAC5'), 10 μM reverse primer (3'GACGACAAGTGAGAATTCCGG5'), dH₂O was added to make the total reaction volume of 50 μl.

2.5.2 PCR product analysis and purification

5 μl of the PCR product was analysed on a 1% Agarose gel as described above. The remaining 45 μl was purified using the QIAquick PCR Purification Kit (QIAGEN, cat. No. 28104) following the manufacturer's protocol.

2.5.3 Cloning into pET28 expression vector

pET28 and the PCR product were digested using EcoRI and NotI endonucleases manufactured by NEB. The double digestion was performed following the manufacturer's guidelines using CutSmart® Buffer. The PCR product and pET28 were gel purified and ligated as described above.

2.5.4 Transformation

GSTP1-1A _pET28 plasmids were transformed using BL21(DE3) Competent Cells (Agilent Technologies, Cat. No. 200131) using the company's protocol.

2.5.5 GSTP1-1A Expression

For the protein expression and solubility test bacteria were grown in 10 ml of medium containing kanamycin (50mg/μl) until the OD 600 = 0.6 - 0.8 and then induced with 0.4 mM IPTG. Before IPTG induction 1ml of each sample was taken and stored for further analysis (uninduced sample). After IPTG induction the bacteria were further incubated at 37°C for 4 h. Bacteria were pelleted by centrifugation (16,000g for 5 min) and lysed by boiling in 4X sample buffer (200 mM TrisHCl pH 6.8, 8% (w/v) SDS, 0.4% (w/v) bromophenol blue, 40% (v/v) glycerol). Cell debris were pelleted by centrifugation (16,000 x g for 10 min) and the remaining supernatant was analysed on 12.5% SDS-PAGE.

2.5.6 Purification of GSTP1-1A

GSTP1-1A_pET28 BL21(DE3) competent cells were grown overnight in 500 ml of autoinduction medium (6g Na₂HPO₄ (~42 mM), 3g KH₂PO₄ (~22 mM), 10g Tryptone, 5g yeast extract, 5g NaCl (85 mM), 10ml 60% v/v Glycerol, 5 ml 10% w/v Glucose, 25 ml 8% w/v lactose per one litre of medium) containing kanamycin (50 mg/μl). Cells were harvested by centrifugation at 15000 x g for 50 min and lysed by repeated freeze/thaw cycles. 500 ml of cell lysate was incubated with GST beads for 1 hour and washed 3 times with 50 ml of 50 mM Tris-HCL (pH 8.0). GSTP1-1A was eluted with 10 mM GSH (pH 8.0). Eluted proteins were analysed on 12.5% SDS-PAGE followed by Coomassie blue staining (10% (v/v) phosphoric acid, 10% (v/v) ammonium sulfate, 0.12% (w/v) Coomassie G250, and 20% (v/v) methanol). Purified GSTP1-1A was concentrated to ~2.8 μg/ml using Vivaspin® Turbo 10k MWCO (Sartorius, cat. No. VS15T01). The concentration was measured using Spectrostar nano plate reader (BMG Labtech).

2.5.7 Purified GSTP1-1A activity

1 mM of GSH and CDNB (1 mM) or Cl-BODIPY (150 nM) were added to various concentration (50 nM – 500 nM) of purified GSTP1-1A in PBS buffer (cat. No. 14190250) and the increase in absorption at 340 nm (CDNB) or 530 nm (Cl-

BODIPY) was measured every 30 seconds for 60 minutes using a PHERAstar® FS plate reader (BMG Labtech).

2.6 GSH transport assay (GST)

2.6.1 Estimate concentration of GSTP1-1A inside microsomes

GSTP1-1A microsomes were lysed and separated by 12.5% SDS-PAGE and subjected to Western blotting. Increasing concentration of purified GSTP1-1A (25 nM – 250 nM) was added to the blot to help estimate the concentration of GSTP1-1A inside microsomes. Band intensities were compared and analysed using ImageJ software.

2.6.2 *In vivo* activity of GST

HT1080-GSTP1-1A-KDEL cells were lysed and incubated with glutathione Sepharose® 4B (Sigma-Aldrich cat. No. 17-0756-01) for 30 min at room temperature. Glutathione Sepharose® 4B beads were washed 3 times with PBS and then eluted with GSH (50 mM). Eluted samples were analysed on 12.5% SDS-PAGE gel followed by silver staining, as described in section 2.2.2.

2.6.3 GST based transport assay using CI-BODIPY as substrate (fluorescence spectra)

0.1 mM GSH was added to 100 µl of GSTP1-1A microsomes pre-treated with 100 nM CI-BODIPY. Emission spectra was measured every 15 minutes using Fluorolog® fluorometer (Horiba) to observe the increase fluorescence at 540 nm and the decrease in fluorescence at 512 nm.

2.6.4 Mass spectrometry identification of conjugates

GSH was added to GSTP1-1A microsomes (1 mM final concentration) pre-treated with CI-BODIPY (150 nM) or CDNB (250 µM) and microsomes were incubated for

2 h at room temperature. Microsomes were centrifuged at 150,000 x g (Beckman Optima™ MAX-XP Ultracentrifuge, rotor TL 100.3) for 40 min at 4°C to sediment. Microsomal pellet was washed 3 times with ice cold PBS before solubilising in 0.5% Triton X-100 and analysed by mass spectrometry. Purified GSTP1-1A incubated with Cl-BODIPY (150 nM) or CDNB (250 µM) was used as a positive control. Microsomes prepared from HT1080 cells (not expressing GSTP1-1A) were used as a negative control. The conjugated product was analysed using liquid chromatography mass spectrometry (LCMS) carried out on a Thermo Scientific LCQ Fleet quadrupole mass spectrometer with a Dionex Ultimate 3000 LC using a Dr. Maisch Reprosil Gold 120 C18 column (110 Å, 3 µm, 150×4.0 mm) and a 0-100% linear gradient of buffer B (acetonitrile/H₂O 95:5 with 0.1% TFA) into buffer A (acetonitrile/H₂O 5:95 with 0.1% TFA) at a flow rate of 1.0 ml·min⁻¹

2.6.5 GST based transport assay endpoint and time course (CDNB and BODIPY)

GSH (1 mM) was added to GSTP1-1A microsomes pre-treated with Cl-BODIPY (150 nM) or CDNB (250 µM). For the endpoint samples were incubated for 2 hours at RT following precipitation using 10% TCA. For the time course samples were collected at different time points and precipitated using 10% TCA. Samples were centrifuged, and the absorbance of the supernatant was measured at 530 nm (Cl-BODIPY) or 340 nm (CDNB).

2.6.6 Inhibition of GSTP1-1A activity using GOH

GSH (1 mM) and CDNB (250 µM) were added to 250 nM of GST incubated with various concentrations of GOH (0.2 mM – 1 mM). The increase in 340 nm absorbance was measured and plotted over time.

2.7 Isolating a GSH transporter

2.7.1 Preparation of rat liver microsomes (RLM)

Rat liver(s) was washed thoroughly with homogenisation buffer (50 mM Tris (pH 7.5), 25 mM KCl, 1 mM EDTA (pH 7.5)) weighed and then chopped. The liver tissue was homogenised in a volume of homogenising buffer equal to three times the weight of the liver using a Potter Elvehjem homogeniser. The homogenate was centrifuged at 13,000 x g (Beckman Optima™ XL-80K Ultracentrifuge, rotor 70.1 Ti) for 10 min at 4°C. Floating lipids were carefully removed from the top of the supernatant using Pasteur pipette and the supernatant was transferred into a clean tube taking care not to disturb the bottom pellet. This step was repeated to make sure that lipids and heavy molecular weight materials were removed. The supernatant was centrifuged at 150,000 x g (Beckman Optima™ XL-80K Ultracentrifuge, rotor 70.1 Ti) for 90 min at 4°C to sediment microsomal membranes. The supernatant was discarded and microsomes resuspended in 0.2M potassium phosphate buffer (pH 7.0). The concentration of microsomes was measured by measuring OD at 280 nm using Spectrostar nano plate reader (BMG Labtech). The concentration of miceosomes were adjusted to approximately 0.5 mg/ml by addition of 0.2M potassium phosphate buffer (pH 7.0). Microsomes were either frozen using liquid nitrogen and stored at – 80 C° or used immediately.

2.7.2 Isolation of proteins using glutathione Sepharose beads.

RLM were incubated with glutathione Sepharose® 4B (Sigma-Aldrich cat. No. 17-0756-01) for 30 min at room temperature and solubilised with TWEEN20 (0.2%). Glutathione Sepharose® 4B were washed 3 times with washing buffer (TrisHCl (pH 7.5), 1% (v/v) Triton X-100). GSH binding proteins were eluted with 35 µl of GSH (50 mM). Eluted samples were analysed on 12.5% SDS-PAGE gel followed by silver staining.

2.7.3 Mass spectrometry identification

Fraction of eluted samples or proteins cut from silver stained polyacrylamide gel using scalpel and were sent to the proteomics facility at the University of St Andrews.

2.7.4 Conjugation of GSH to Mts-Aft-Biotin

Mts-Aft-Biotin (Santa Cruz, cat. No. SC-223339) was incubated with excess of GSH for 1 h at room temperature. The resulting GS-Mts-Aft-Biotin was analysed by high-pressure liquid chromatography (HPLC) carried out on a Shimadzu instrument comprising a communication module (CBM-20A), autosampler (SIL-20HT), pump modules (LC-20AT), UV/Vis detector (SPD-20A) and system controller (Labsolutions V5.54 SP), with a Phenomenex Gemini C18 column (110 Å, 5 µm, 250×4.60 mm). UV measurements were recorded at 214 and 254 nm, using a standard protocol: 100% buffer A (acetonitrile/H₂O 5:95 with 0.1% TFA) for 2 min followed by a linear gradient of buffer B (acetonitrile/H₂O 95:5 with 0.1% TFA) into buffer A (0-100%) over 28 min at a flow rate of 1.0 ml·min⁻¹. Purification of GS-Mts-Aft-Biotin was performed on an Agilent Technologies 1260 infinity preparative system using both UV and ELSD detectors with a Phenomenex Gemini C18 column (110 Å, 10 µm, 250×20 mm). Auto-collection of fractions was used based on the UV measurements at 214 or 254 nm, using a standard protocol: 100% buffer A for 5 min followed by a linear gradient of buffer B into buffer A (20-100%) over 65 min at a flow rate of 12.5 mL·min⁻¹ using the same buffers as described for analytical HPLC. The presence of GS-Mts-Aft-Biotin in purified sample was confirmed by liquid chromatography mass spectrometry (LCMS) carried out on a Thermo Scientific LCQ Fleet quadrupole mass spectrometer with a Dionex Ultimate 3000 LC using a Dr. Maisch Reprosil Gold 120 C18 column (110 Å, 3 µm, 150×4.0 mm) and a 0-100% linear gradient of buffer B into buffer A with the same flow rate and buffers as described for analytical HPLC. GS-Mts-Aft-Biotin was freeze dry and stored in -20°C.

2.7.5 Photocrosslinker isolation of GSH binding proteins

RLM were incubated with GS-Mts-Aft-Biotin (250 µM) for 30 min at RT occasionally mixed. RLM were placed on ice and then exposed to UV light (Spectroline® Model SB-100P/FB 365 nm) for 5 min. Samples were centrifuged at 150,000x g (Beckman bench top ultracentrifuge, rotor TL 100) for 40 min at 4°C. Microsomes were washed 3 times with ice cold PBS prior to solubilisation in 500 µl of immunoprecipitation (IP) buffer (50 mM Tris-HCl (pH 7.5), 1% (v/v) Triton X-100, 150 mM NaCl, 2 mM EDTA, 0.5 mM PMSF, 0.02% (w/v) Na-azide). RLM were incubated with streptavidin beads

rotating at RT for 30 min. RLM were washed 3 times with radioimmunoprecipitation (RIPA) buffer (10 mM Tris-Cl (pH 8.0), 1 mM EDTA, 0.5 mM EGTA, 1% (v/v) Triton X-100, 0.1% SDS, 140 mM NaCl, 1 mM PMSF) containing 1 mM DTT and eluted with Biotin (20 mM). The samples were separated on 12.5% SDS-PAGE and visualised by silver staining.

Chapter 3

roGFP assay for GSH transport

3.1 Introduction

To answer the question about how GSH is transported across the ER membrane a transport assay able to distinguish between GSH and other thiols was needed. The existing assays for glutathione transport rely on light scattering methods or radioactive GSH assays using filtration (Banhegyi et al., 1999, Inoue et al., 1984). However, these techniques are not GSH specific and are not GSH sensitive. Therefore, the first part of my project was focused on developing a GSH assay specific for GSH that would allow a further investigation of an ER localised GSH transporter.

In 2004 Cline (Cline et al., 2004) conducted a study in which they characterised, as well as describing the synthesis, of three different methyl ester derivatives of tris(2-carboxyethyl)phosphine (TCEP). Part of the study was focused on membrane permeability of the newly synthesised compounds using liposomes containing 5,5-dithio-bis-(2-nitrobenzoic acid) (DTNB, also known as Ellman's Reagent), a compound that absorbs strongly at 412 nm upon reduction. In their publication, *Cline et al.* demonstrated that GSH and TCEP were not able to cross a liposomal lipid bilayer while dithiothreitol (DTT) simply diffused across the bilayer.

We decided to modify the method described by *Cline et al.* to make it more suitable for our research. The GSH transport assay we developed relies on selective permeability of cellular membranes (Cooper, 2000). Cell membranes determine the boundary of cells and all the organelles within the cell, allowing separated environments to exist inside the cell (Shi, 2013). Lipid membranes function as a physical barrier for molecules within the cell, the hydrophilic exterior and hydrophobic interior of the membrane makes it permeable to small molecules with no charge, on the other hand polar substances cannot cross a membrane (Shi, 2013). However, a group of proteins specialised in mediating the exchange of molecules across the membranes have evolved (Shi, 2013). The main function of transport proteins (often called transporters) is to carry molecules, such as lipids, ions, sugars, peptides or fully folded proteins, across the lipid bilayer, however, they also play an important role in energy conversion, signal transduction, diseases, drugs delivery and more (Rubio-Aliaga and Daniel, 2008, Shi, 2013). There are a great variety of different transporters, some of them are very specific, for example the GLUT family of glucose transporters is specialised in transporting glucose and

some of the other hexoses (Hebert and Carruthers, 1992, Oka et al., 1990). However, many transporters have a broad spectrum of substrates. Examples include cationic amino acid transporter (CAT) family of transporters which is responsible for the transport of cationic L-amino acids, ATP-binding cassette (ABC) transporters which transport a variety of molecules at the expense of ATP, and the peptide transporter (PTR) family that facilitate uptake of di- and tripeptides (Borst and Elferink, 2002, Hatzoglou et al., 2004, Tsay et al., 2007). There is strong evidence suggesting that GSH is not able to cross a phospholipid bilayer (Cline et al., 2004) thus GSH transport is likely to be facilitated by a transport protein.

Cellular membranes differ greatly from each other in both lipid and protein composition (Van Meer et al., 2008). The ER membrane contains a relatively low concentration of sphingolipids and sterols, however it is rich in phosphatidylcholine (Van Meer et al., 2008). There are many membrane proteins found exclusively in the ER membrane of mammalian cells, for example translocating chain-associated membrane protein (TRAM) (Zimmermann et al., 2011, Shao and Hegde, 2011). To investigate GSH transport we needed a system which mimics the properties of the ER membrane. Therefore, we decided to use microsomes which are widely used in studies investigating processes occurring in the ER, especially processes involving ER membranes, such as translocation of newly synthesised proteins (Walter and Blobel, 1981). Microsomes are small vesicles isolated from the ER following fragmentation by homogenisation of the cell and separated by centrifugation. They were first recognised and described by Albert Claude in 1941 (Claude, 1941). Microsomes contains all the ER luminal proteins and most important for our research they have the same lipid and protein composition as ER membrane.

To establish an assay for GSH transport we also needed a molecule or protein sensitive to redox changes which would report the transport of GSH across microsomal membrane, such as DTNB used by Cline et al. in liposomes. We decided to take advantage of the properties of a redox sensitive Green Fluorescent Protein (roGFP) (Meyer and Dick, 2010). This modified version of GFP contains two genetically engineered cysteines (in the place of Ser¹⁴⁷ and Gln²⁰⁴) that allow formation of a disulfide bond (Meyer and Dick, 2010). Disulfide formation influences the fluorescent properties of the protein (Ostergaard et al., 2001). The ratio of

emission intensities between two excitations peaks (390 nm and 460 nm) reflects the redox status of the protein. The 390/460 ratio increases when roGFP is oxidised and decreases upon reduction. Importantly, ratiometric measurements are independent of the amount of protein, changes in pH or photobleaching effects. roGFP has been widely used in the redox biology field (Meyer and Dick, 2010b). The ER localised version of roGFP (roGFP-iE) was selected as a probe for the experiment. Thanks to several engineered amino acids (C48S, Q80R, S147CE, H148S, Q204C) the redox potential of roGFP-iE is similar to the redox potential found within the ER lumen (Lohman and Remington, 2008). roGFP-iE had been successfully used to monitor changes in the ER in both yeasts and mammalian cells (Birk et al., 2013, Delic et al., 2010). The superfolder roGFP-iE (SFroGFP-iE) used contains another four amino acids substitutions (S30R, Y39N, T105N and I171V) which improve protein folding, thermostability and enhanced the dynamic range of redox change (Hoseki et al., 2016).

3.2 roGFP transport assay

Microsomes were prepared from HT1080 cell line expressing superfolder roGFP-iE localised in the ER (ER retention sequence - KDEL) (Birk et al., 2013). Therefore, if GSH is transported it should be able to reduce roGFP-iE and a decrease in 390/460 ratio should be observed. Because of the fast equilibration of roGFP-iE and GSH we assumed that the rate of roGFP-iE reduction would be directly proportional to the transport rate of GSH across the ER membrane. In order to validate the results of the assay we included two potent reducing agents DTT and TCEP. DTT is widely used membrane permeable thiol reducing agent (Cleland, 1964). It has been demonstrated in many instances that DTT can reduce disulfide bonds in intact cells, therefore, it was used as a positive control in our assay (Cline et al., 2004). Because of its charge density at neutral pH, TCEP is not able to cross a lipid bilayer, therefore TCEP was used as a negative control in our assay (Cline et al., 2004). In our hypothesis, we assumed that GSH will only be able to cross the microsomal membrane, and reduce roGFP-iE, if a GSH transporter is present. We also used permeabilised microsomes (with 0.15% Triton-X) as a control, this should allow all the reducing agent to fully reduce roGFP-iE at the maximum rate. The approach is summarised in Figure 3.1.

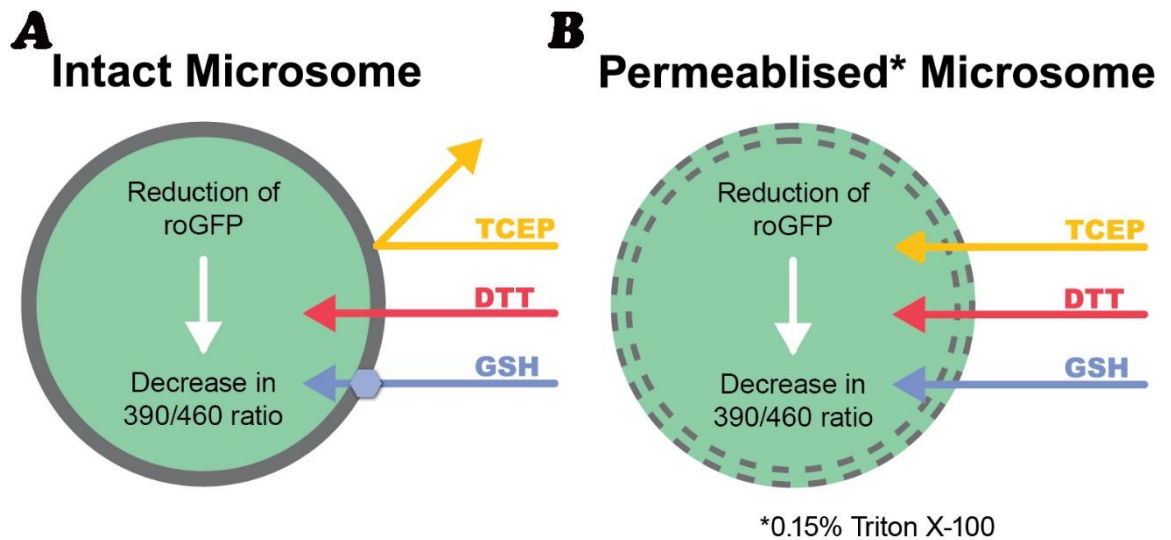


Figure 3.1. GSH transport in microsomes. Superfolder roGFP-iE, present inside microsomes, will become reduced upon addition of different reducing agent (TCEP, DTT and GSH), the rate of reduction is directly proportional to the rate of reducing agent passing through the ER membrane. A) Intact Microsomes. Due to its polarity TCEP will not be able to cross the microsomal membrane and reduce roGFP-iE. DTT will diffuse across the membrane and reduce roGFP-iE at a very fast rate. GSH will only be able to cross the membrane if the protein responsible for GSH transport is present. Since GSH is transported, it should be able to reduce roGFP-iE at a moderate rate. B) Permeabilised Microsomes. Microsomes will be permeabilised with 0.15% of Triton X-100. The membrane is no longer a barrier for reducing agents, therefore, all of them should be able to reduce roGFP-iE at their maximal rate.

3.2.1 Optimising the concentration of reducing agents

In order to determine the minimum concentration of TCEP needed to fully reduce roGFP-iE a simple titration method was carried out (Figure 3.2).

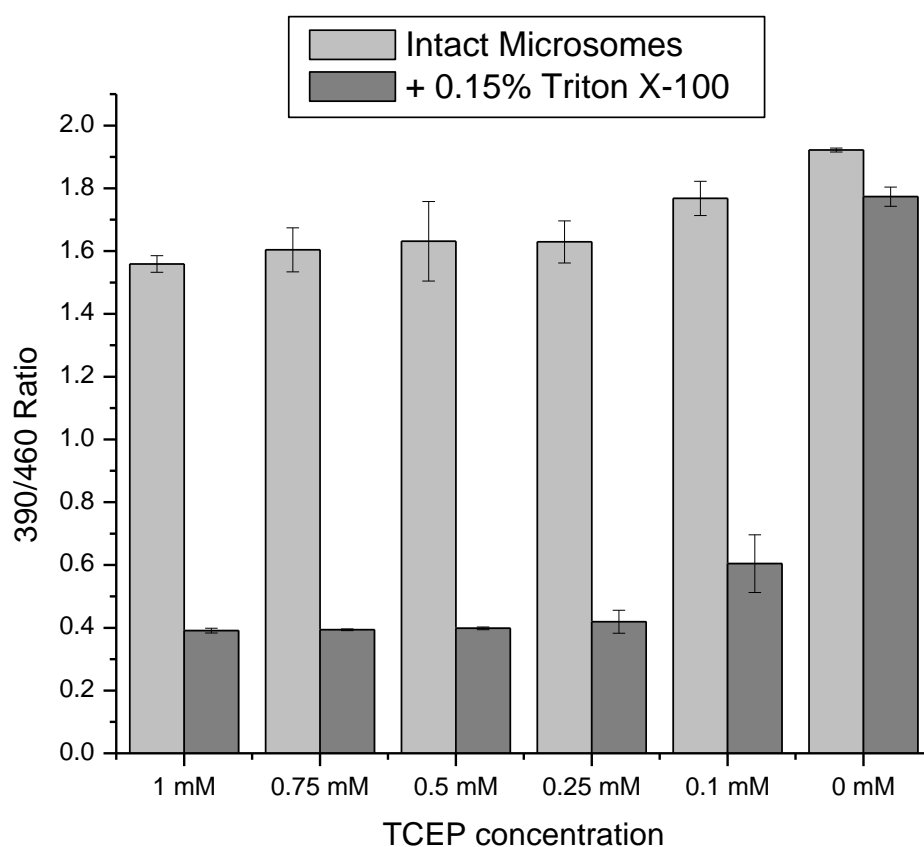


Figure 3.2. Optimising the concentration of TCEP. Microsomes were treated with different concentrations of TCEP and fluorescence at 390 nm and 460 nm was measured approximately 1 hour after treatment. Triton X-100 permeabilises the membrane allowing TCEP to reduce roGFP-iE at its maximal potential. The 390/460 ratio was calculated, and the concentration of 0.15 mM was chosen for further experiments as it was able to fully reduce roGFP-iE. The data was plotted using three technical replicates, error bars represents standard deviation.

TCEP is not able to cross the membrane of intact microsomes therefore there were only minor differences between each sample. In permeabilised microsomes almost all concentrations of TCEP are able to fully reduce roGFP-iE. The decrease in roGFP-iE ratio starts at concentration 0.1 mM and gets higher as TCEP concentration increases. Thereafter 0.15 mM TCEP was used in all experiments as this concentration is sufficient to fully reduce roGFP-iE but does not significantly reduce roGFP-iE in intact microsomes.

A similar titration was carried out using GSH (Figure 3.3). When compared to TCEP none of the GSH concentrations used could fully reduce roGFP-iE, therefore, a concentration with the greatest difference of roGFP-iE reduction between intact microsomes and detergent treated microsomes was used. A concentration of 5 mM GSH was used in all future experiments for two reasons. First, GSH at 5 mM significantly reduces roGFP-iE in detergent treated microsomes and there is considerable difference in 390/460 ratio between intact and permeabilised microsomes. Second, 5 mM GSH is within the concentration range of GSH found in the cytosol (Birk et al., 2013). DTT was able to fully reduce roGFP-iE at all tested concentrations therefore a concentration of 0.2 mM was chosen, and used in all experiments, to have a better comparison with TCEP (Figure 3.4).

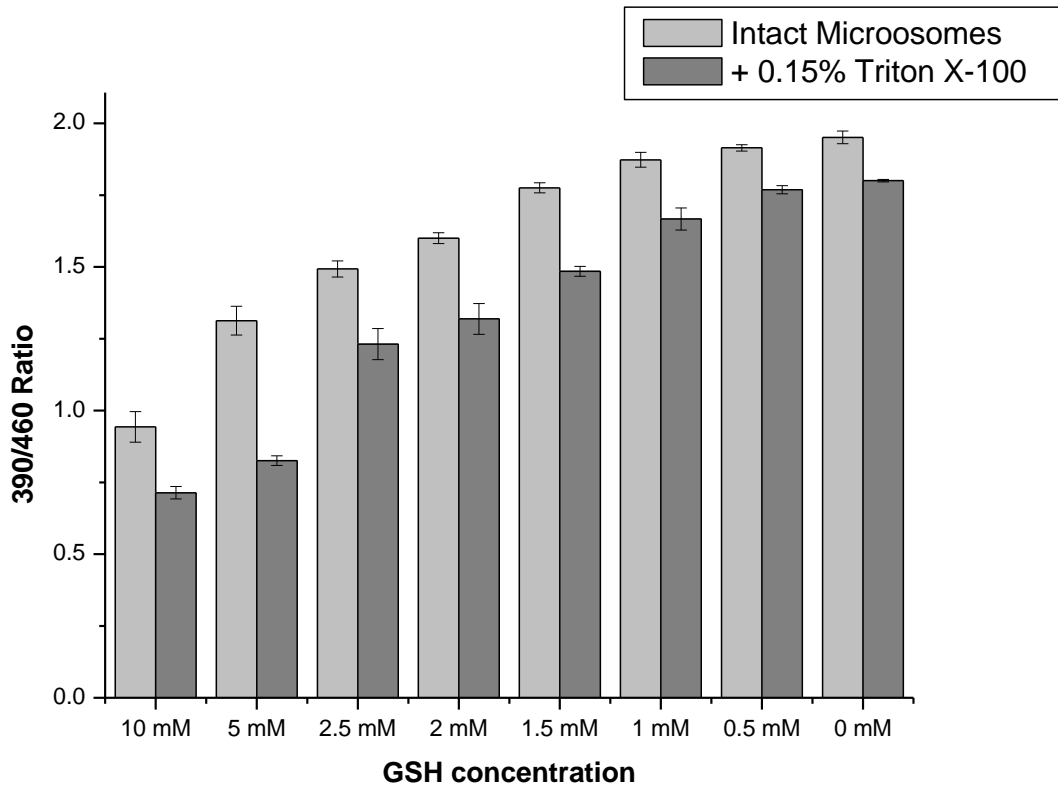


Figure 3.3. Selecting an optimum concentration of GSH for the transport assay. Microsomes were treated with different concentrations of GSH and fluorescence at 390 nm and 460 nm was measured approximately 1 h after addition of GSH. Triton X-100 permeabilises the microsomal membrane allowing GSH to reduce roGFP-iE. The 390/460 ratio was calculated and the concentration with the greatest difference between permeabilised and intact microsomes was chosen for further experiments. The data was plotted using three technical replicates, error bars represents standard deviation.

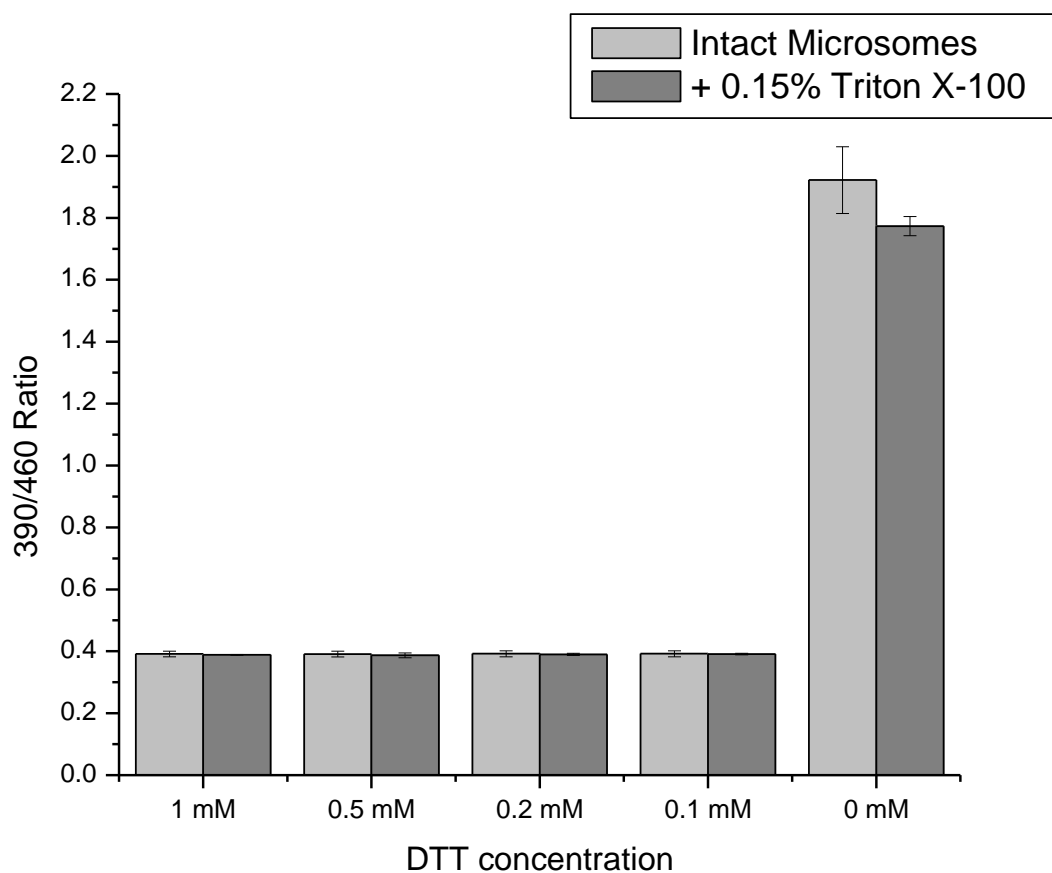


Figure 3.4. Optimising the concentration of DTT. Microsomes were treated with different concentrations of DTT as indicated and fluorescence at 390 nm and 460 nm was measured approximately 1 h after treatment. Triton X-100 permeabilises the microsomal membrane allowing DTT to reduce roGFP-iE. The data was plotted using three biological technical, error bars represents standard deviation.

3.2.2 Kinetics

Intact microsomes were resuspended in PBS and each of the reducing agents (DTT, TCEP and GSH) was added to individual aliquots of microsomes (Figure 3.5a). Upon addition of DTT (0.2 mM final concentration), roGFP-iE within microsomes became rapidly reduced. This result can be explained by the fact that DTT is able to diffuse across ER membrane. The rate of roGFP-iE reduction after addition of TCEP (0.15 mM) was very slow, almost undetectable, when compared to DTT. GSH was able to reduce roGFP-iE at a moderate rate.

To assess how the microsomal membrane affects the transport of reducing agents the experiment was repeated after the addition of Triton X-100 (0.15%) (Figure 3.5b). In the previous experiment TCEP was not able to cross the membrane and reduce roGFP-iE but after Triton X-100 treatment TCEP is able to reduce roGFP-iE as effectively as DTT and at similar rate. There is no difference between intact and permeabilised samples treated with DTT; this confirms that the ER membrane is not a barrier for DTT and the compound is able to diffuse across the lipid bilayer. After treating microsomes with Triton X-100 GSH is able to reduce roGFP-iE at a higher rate and reaches steady state much faster compared to intact microsomes. This further confirms that the ER membrane is a barrier for GSH and GSH is not able to diffuse across the membrane by its own and requires transport. GSH reduces roGFP-iE very rapidly because of much higher concentration, this can be observed by fast drop of 390/460 ratio in Figure 3.5b, however, because GSH has a higher reduction potential than DTT and TCEP, it is not able to reduce roGFP as effectively as other reducing agent used in the experiment and reaches 390/460 ratio equal to 0.91 compared to 0.44 reached by TCEP and DTT.

A)

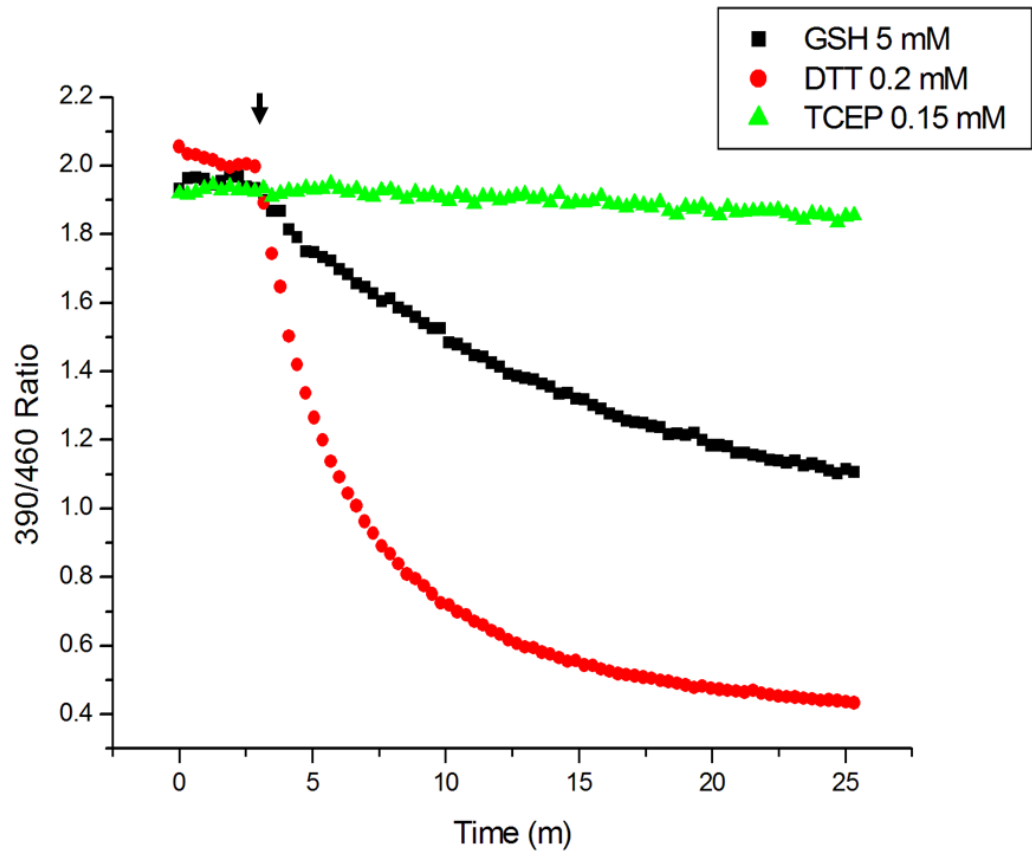


Figure 3.5a. roGFP-iE based GSH transport assay in intact microsomes. A) Kinetics of roGFP-iE reduction in intact microsomes. GSH (5 mM), DTT (0.2 mM) and TCEP (0.15 mM) were added (indicated by arrow) to intact microsomes. The average change of 390/460 ratio was plotted over time, representing the rate of transport across the microsomal membrane. GSH is able to cross microsomal membranes at moderate speed compared to DTT. DTT diffuses through membrane at relatively high rate. Due to its polarity TCEP cannot cross the membrane. The data was plotted using three biological replicates to make sure the results are replicable.

B)

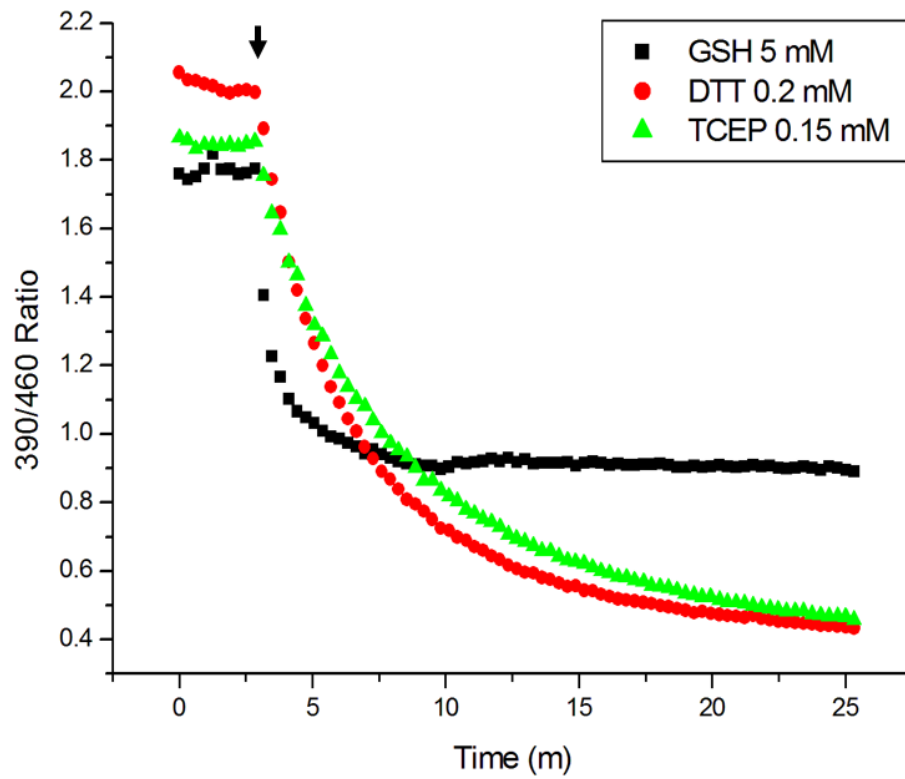


Figure 3.5b. roGFP-iE based GSH transport assay in permeabilised microsomes. Kinetics of roGFP-iE reduction in Triton X-100 permeabilised microsomes. 5 mM GSH, 0.2 mM DTT and 0.15 mM TCEP were added (indicated by arrow) to permeabilised microsomal membrane therefore all reducing agents can reduce roGFP-iE at maximum rate. The change of 390/460 ratio was plotted over time, representing the overall rate of transport across microsomal membrane. The data was plotted using three biological replicates to make sure the results are replicable.

3.3 Inhibition of GSH transport

The previous experiment demonstrated that GSH is transported across the microsomal membrane rather than diffusing. If this really is the case there must be a protein responsible for transporting GSH. Therefore, it should be possible to inhibit GSH transport. This is a very important step in validating our previous results.

3.3.1 Broad range proteases inhibition

Because there is very little information available related to mammalian GSH ER transporters, we speculated that a broad range proteases may be successful in inhibiting GSH transport. Trypsin, chymotrypsin and proteinase K are all well studied and characterised (Muller et al., 1994, Rawlings and Barrett, 1994). All three proteases used in the experiment have broad substrate specificity, therefore, we assumed that they might digest the protein responsible for GSH transport and thus inhibit its transport.

Proteinase K (EC 3.4.21.64) from *Tritirachium album* belongs to family of serine proteases known as the subtilases family (Ebeling et al., 1974). Proteinase K cleaves peptide bonds adjacent to the carboxylic group of aliphatic and aromatic amino acids (Ebeling et al., 1974).

Microsomes were treated with different concentrations (25 µg/ml – 100 µg/ml) of proteinase K and the transport assay was performed as normal (Figure 3.6). When compared to the untreated sample roGFP-iE initially was reduced only slightly slower, however after 40 minutes all the samples reached the same point and progressed at the same rate. Although there are some differences in the reduction rate of roGFP-iE between proteinase K treated samples and untreated sample, especially at the beginning of the assay, they are not significant enough to be considered to inhibit GSH transport. Moreover, there are no differences in samples treated with different concentrations of proteinase K, this further confirmed the protease has no effect on GSH transport across microsomal membrane.

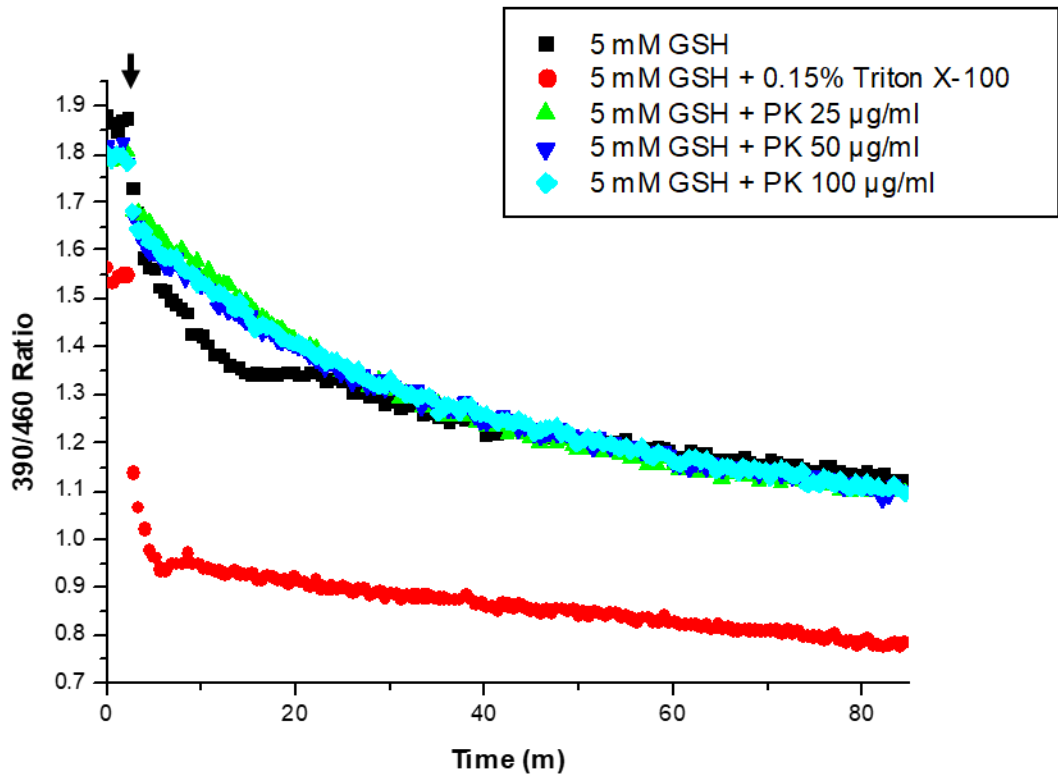


Figure 3.6. Proteinase K treatment of intact microsomes. Intact microsomes were treated with various concentrations (25 µg/ml – 100 µg/ml) of proteinase K for 20 min prior to carrying out a transport assay with the addition (indicated by arrow) of GSH (5 mM). Triton X-100 (0.15%) was added to one of the sample to represent the maximum rate of roGFP-iE reduction. The average change of 390/460 ratio was plotted over time, representing the overall rate of transport across microsomal membrane. The data was plotted using three biological replicates to make sure the results are replicable.

The same approach was tested using the of serine proteases, trypsin (EC 3.4.21.4) and chymotrypsin (EC 3.4.21.1). Trypsin and chymotrypsin are digestive enzymes, both are very similar in structure, but each have a different substrate specificity (Hedstrom et al., 1992). Trypsin cleaves peptides at lysine and arginine residues while chymotrypsin prefers to cleave the peptide at tyrosine, tryptophan, and phenylalanine residues (Rawlings and Barrett, 1994).

Microsomes were treated with different concentrations (25 µg/ml – 100 µg/ml) of trypsin and chymotrypsin, after the treatment a transport assay was performed as previously (Figure 3.7). In all samples treated with serine proteases roGFP-iE was reduced at the same rate as untreated sample. There is almost no difference in the initial rate of roGFP-iE reduction in all 3 samples as well as in the level of reduction in all samples.

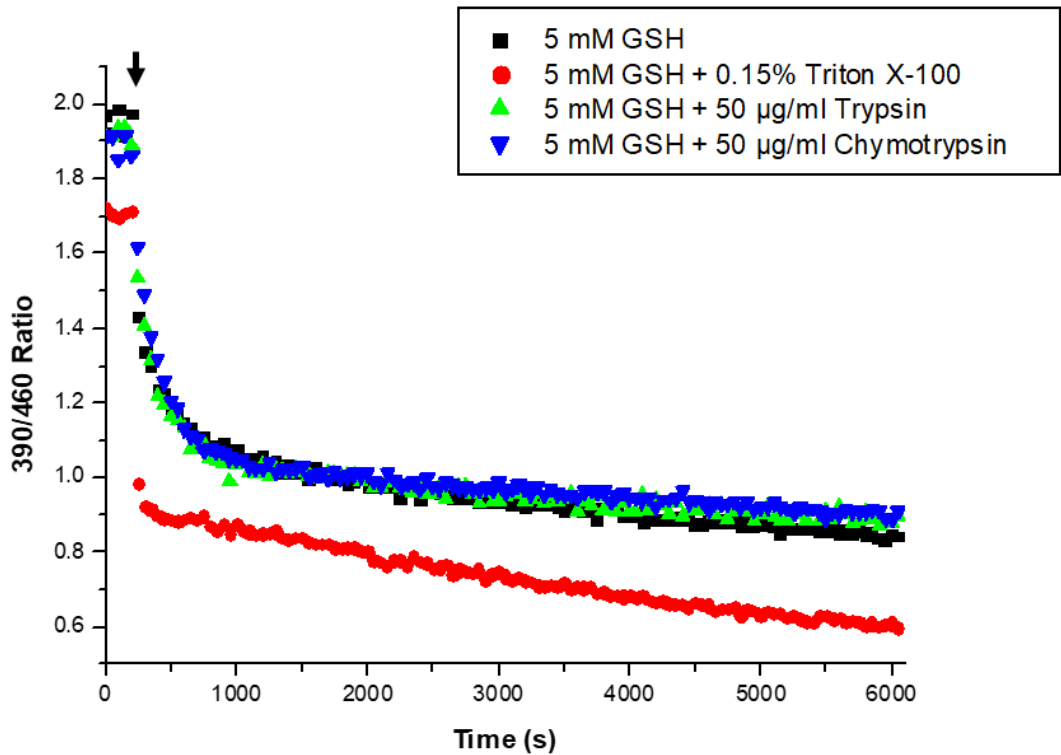


Figure 3.7. Trypsin and chymotrypsin treatment of intact microsomes. Intact microsomes were treated with trypsin and chymotrypsin (50 µg/ml) and incubated for 20 min prior to carrying out a transport assay in the presence of 5 mM GSH (indicated by arrow). Triton X-100 (0.15%) was added to one of the sample to represent the maximum rate of roGFP-iE reduction. The change of 390/460 ratio was plotted over time, representing the overall rate of transport across microsomal membrane. The data was plotted using three biological replicates to make sure the results are replicable.

3.3.2 Alkylation of GSH

Treating microsomes with broad substrate specificity serine proteases did not inhibit GSH transport. Therefore, the next approach we tried involved relying on modifying GSH itself using stoichiometric amounts of N-ethylmaleimide (NEM) to create a competitive inhibitor of GSH transport. NEM is an alkylating agent able to react with the thiol group of cysteines. NEM forms an irreversible covalent bond with cysteine therefore preventing disulfide bond formation. When GSH reacts with NEM it forms N-ethylsuccinimido-S-glutathione (ESG) (Figure 3.8) and it loses its ability to reduce thiols and proteins (Mojica et al., 2008).

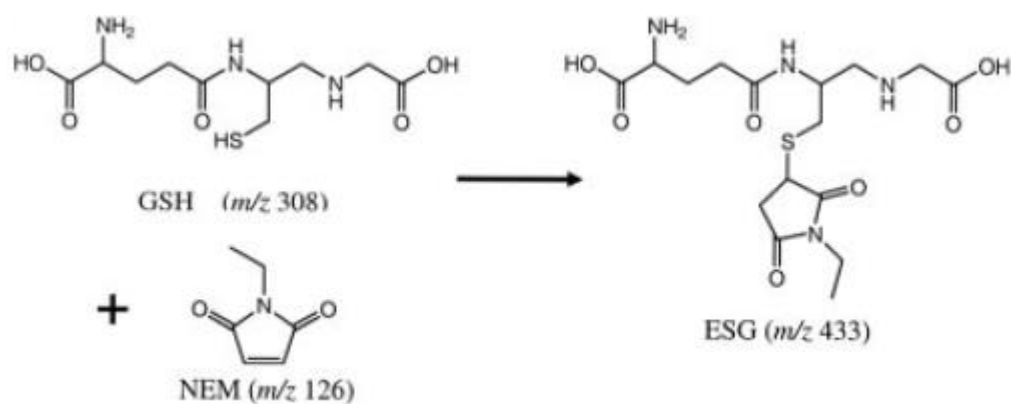


Figure 3.8. Reaction of GSH with NEM to form N-ethylsuccinimido-S-glutathione (ESG)

Alkylated GSH will not be able to reduce roGFP-iE but may still be transported across microsomal membranes acting as a competitive inhibitor for GSH transport. GSH and NEM were mixed in 1.2:1 ratio to make sure no free NEM was present and all NEM will react with GSH. Reversed phase high-performance liquid chromatography (RP-HPLC) was used to make sure alkylation of GSH is completed and there is no excess of either GSH or alkylating agent, but also to purify ESG (Figure 3.9a). RP-HPLC is a powerful technique used to separate molecules based on their hydrophobicity. Separation of molecules relies on the hydrophobic binding of the solute molecule from the mobile phase to the immobilised hydrophobic ligands attached to the stationary phase. When introduced to the sorbent molecules are in aqueous buffer. The molecules are then eluted by increasing the concentration of organic solvent (acetonitrile).

The chromatographic properties of GSH were also determined (Figure 3.9b) and NEM (Figure 3.9c) alone to determine their elution profiles. By comparing all three chromatographs it was possible to identify each peak present in ESG sample (Figure 9a).

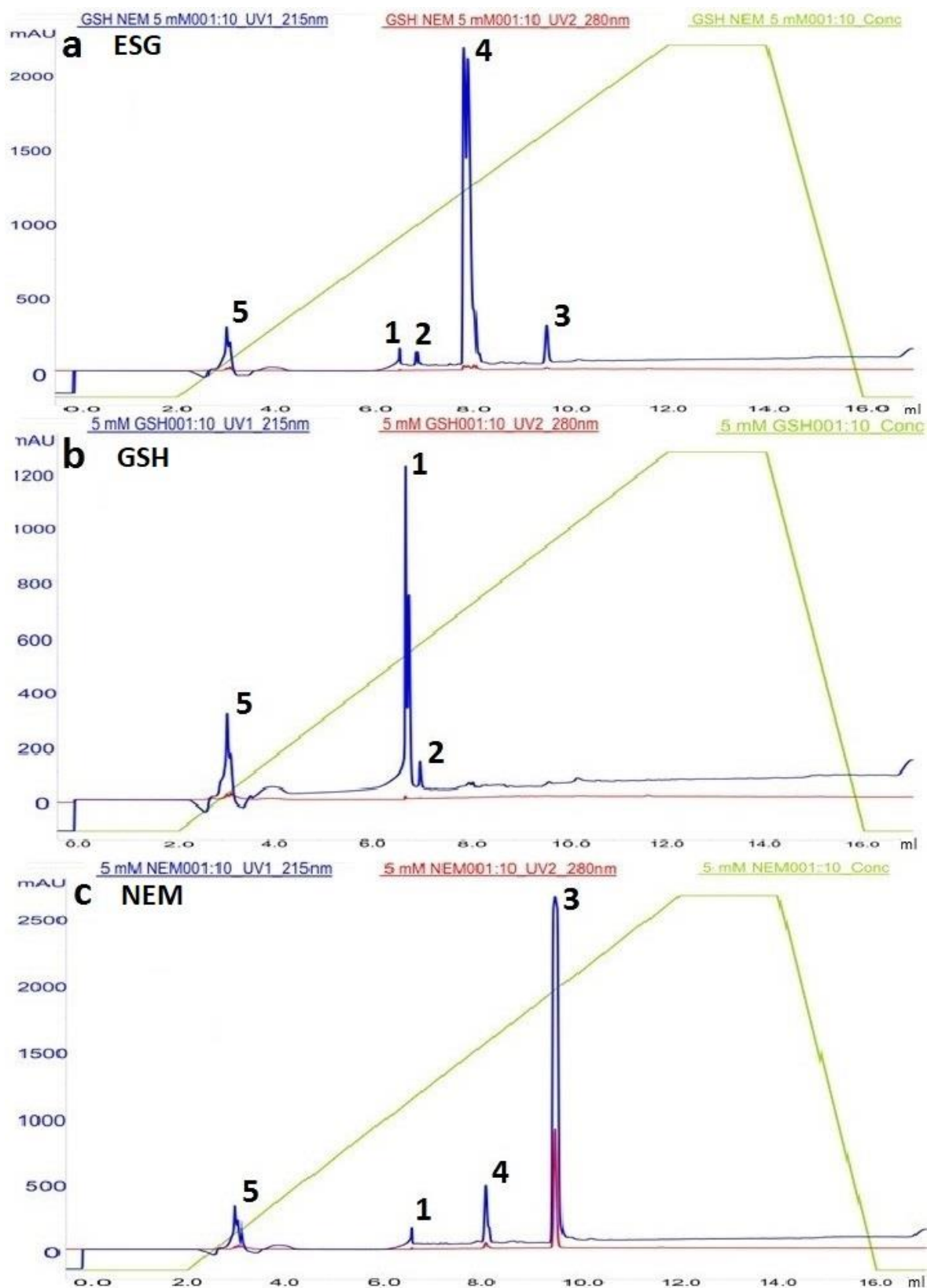


Figure 3.9. RP-HPLC chromatogram of ESG (a), GSH (b) and NEM (c). 1 – GSH, 2 – GSSG, 3 – NEM, 4 – ESG, 5 – peak due oversaturation of the column.

In the GSH sample (Figure 9b) the strong peak (1) represents GSH, the minor peak (2) may represent GSSG. In the NEM only sample (Figure 9c) the sharp peak (3) corresponds to NEM, the small peaks (1) and (4) may correspond to GSH/GSSG and ESG, respectively. The presence of GSH in the NEM sample could be simply contamination from previous analysis. In ESG sample (Figure 9a) ESG is represented by two sharp peaks (4), these two peaks may represent protonated and deprotonated version of ESG, two minor peaks around (1 and 2) are representing remaining GSH and GSSG, respectively, while the small peak (3) corresponds to unreacted NEM. The peak present at the beginning of every sample (5) is probably caused by over saturation of the column. The purified sample from collected fractions were combined and freeze dried. Alkylated GSH was used in the transport assay and added to microsomes (Figure 3.10).

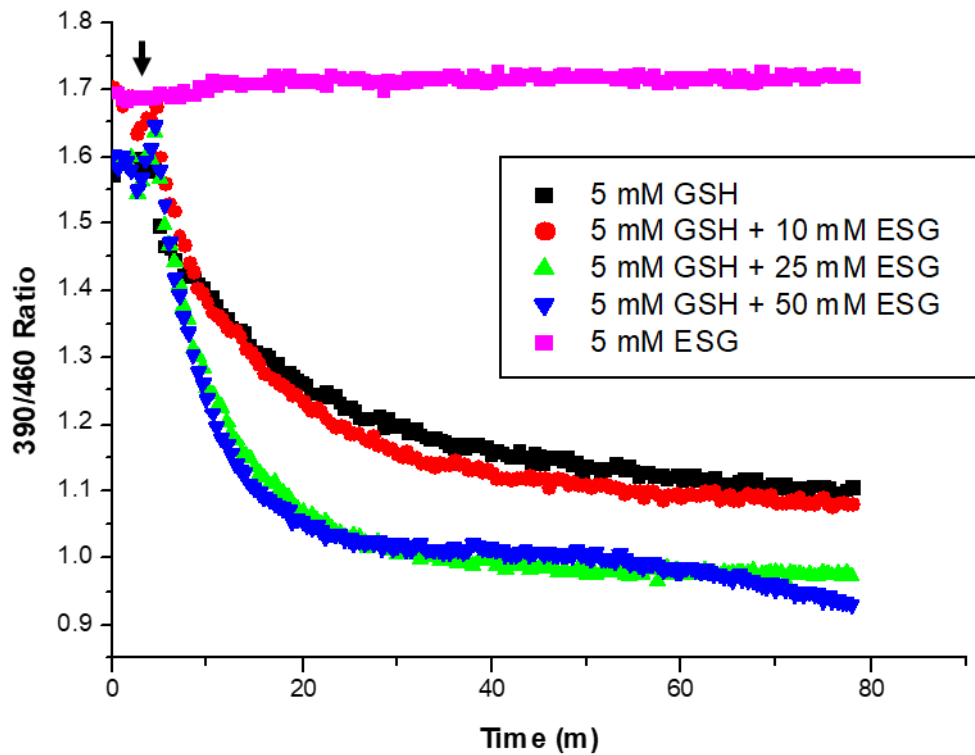


Figure 3.10. ESG inhibition of GSH transport. Various concentrations of ESG were added to intact microsomes and incubated for approximately 15 min. Following the addition (indicated by arrow) of GSH (5 mM) the change of 390/460 ratio was measured and plotted over time, representing the overall rate of transport across microsomal membrane. The data was plotted using three biological replicates to make sure the results are replicable.

The effects of adding ESG to microsomes were opposite to what was expected. Samples with high concentration of ESG displayed an increase in the rate of roGFP-iE reduction and were able to reach lower 390/460 ratio, thus they were reducing roGFP-iE greater and faster than the control sample with no ESG added. If ESG would act as an inhibitor of GSH transport the drop in the transport rate should be observed. Interestingly no change in 390/460 ratio was observed in the sample treated with ESG alone.

3.3.3 Glutathione analogue synthesis

ESG was not able to inhibit GSH transport, however the results were unexpected and very interesting. It was possible that the addition of quite bulky NEM to GSH was the reason why we saw no inhibition. By altering the GSH structure a new competitive inhibitor was designed, and this time the alterations were subtler. The analogue was synthesised using a simplified version of solid-phase peptide synthesis (SPPS) from its precursor amino acids glutamate, serine and glycine therefore its structure is very similar to GSH (Figure 3.11) (Coin et al., 2007). The only difference between GSH and the analogue was the substitution of the **-SH** for an **-OH** group, therefore the new compound was named GOH.

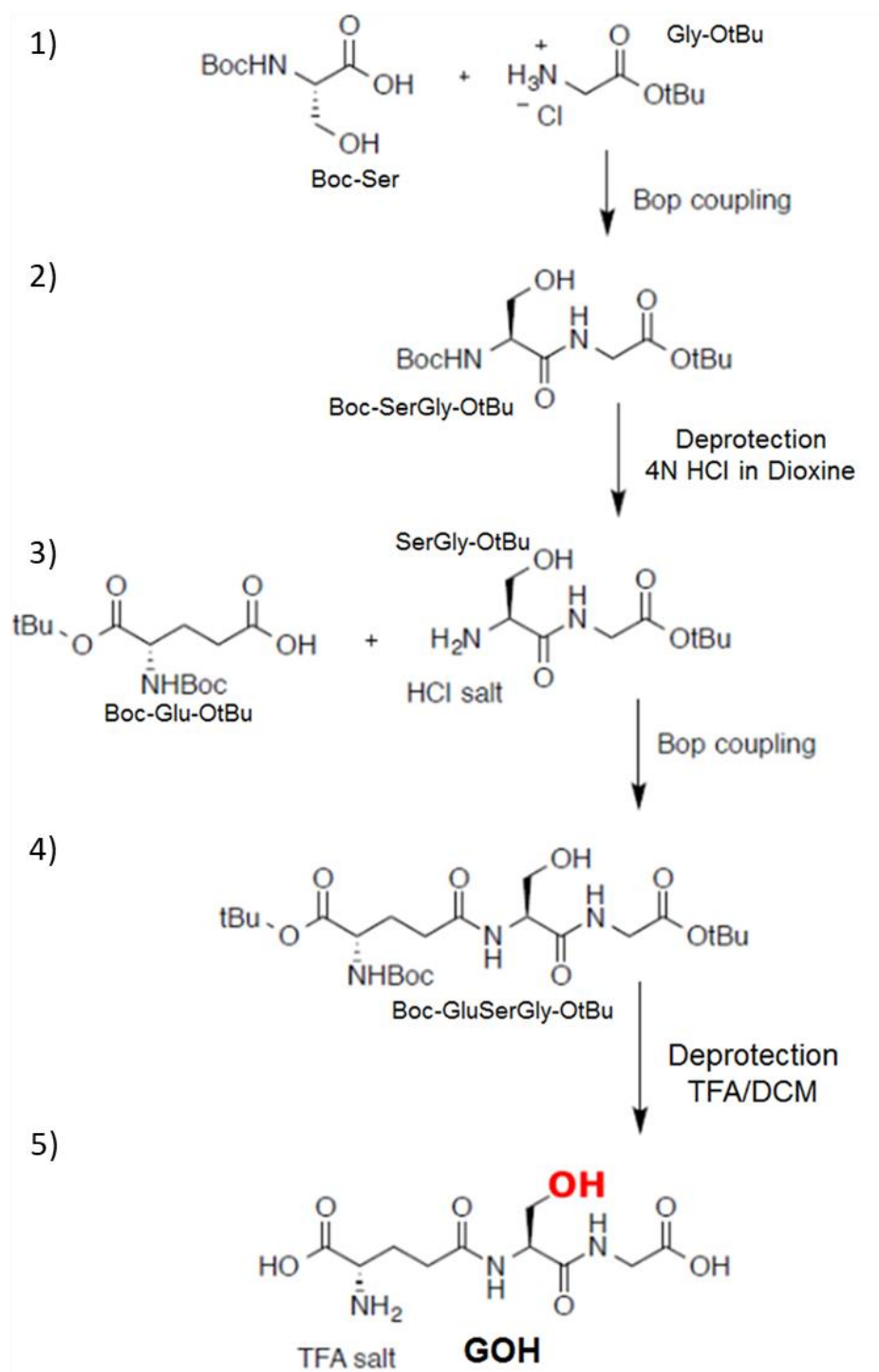


Figure 3.11 GOH synthesis. GOH was synthesised using a simplified version of solid-phase peptide synthesis from its precursor amino acids glutamate, serine and glycine. **1)** Boc-Ser and Gly-OtBu coupled together using BOP reagent. **2)** Boc group removed from Boc-SerGly-OtBu by 4M HCl in dioxane. **3)** Boc-Glu-OtBu coupled to SerGly-OtBu using BOP reagent. **4)** All the protection groups are removed by trifluoroacetic acid (TFA) and dichloromethane (DCM) solution. **5)** GOH together with TFA salt are formed.

GOH was purified by HPLC, the compound was freeze dried and analysed by both mass spectrometry and proton nuclear magnetic resonance (^1H NMR) (Fig 2.1). A synthesis of GOH was already described in previous study (Jao et al., 2006). However, the Jao et al. used a different method to synthesise the product and the purpose of the study was also different. Because the results from ^1H NMR were already published, it was possible to simply match them with our results confirming that indeed the synthesised product was the compound of interest.

3.3.4 GOH effect on GSH transport

After confirming that the synthesised compound was indeed GOH, its effect on GSH transport was tested by adding GOH to microsomes and performing our standard transport assay (Figure 3.12).

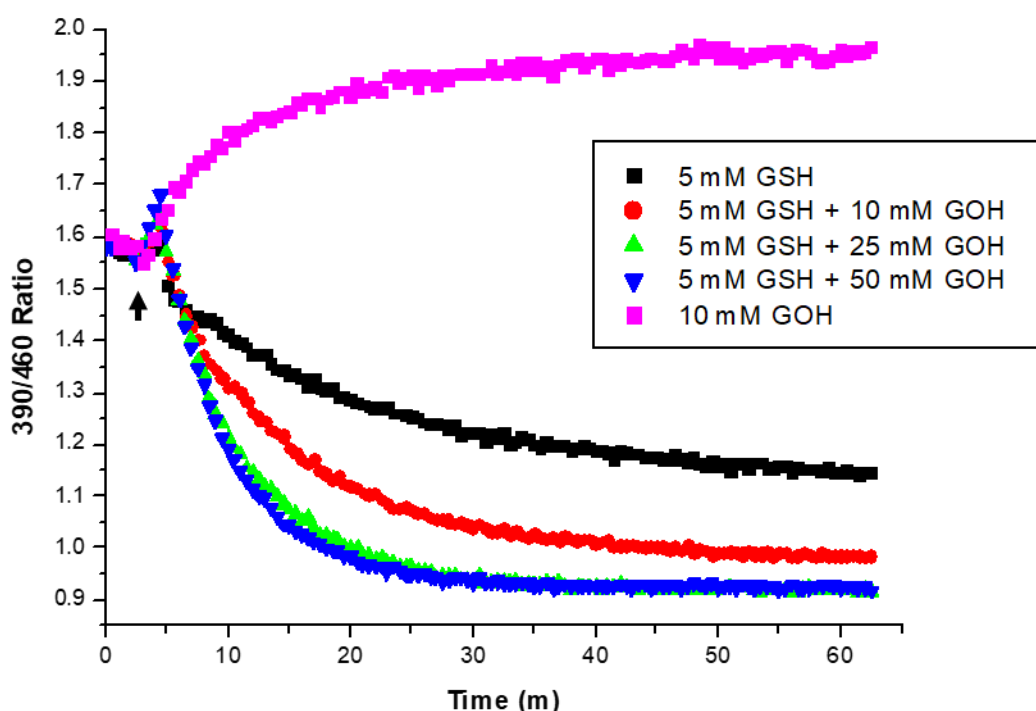


Figure 3.12. GOH effect on GSH transport in intact microsomes. Various concentrations of GOH were added to intact microsomes and incubated for approximately 15 min. Following addition (indicated by arrow) of GSH (5 mM) the change of 390/460 ratio was measured and plotted over time, representing the overall rate of transport across microsomal membrane. The increased concentrations of GOH have accelerated the rate of GSH transport and lowered 390/460 ratio when compared with GSH only sample. The data was plotted using three biological replicates to make sure the results are replicable.

When microsomes were treated with GOH only, roGFP-iE became more oxidised with the 390/460 ratio increasing much faster than the untreated sample. In microsomes treated with GOH and GSH, roGFP-iE was more reduced (reached lower 390/460 ratio) than in the sample with only GSH added, moreover the rate of reduction was also increased when compared with the sample treated with GSH only. Because of the structural similarities it was expected GOH to act as a competitive inhibitor when included in the GSH transport assay, however GOH seems to have an opposite effect and accelerates GSH transport. This effect seems to be concentration dependent as increasing the concentration of GOH also increased the rate of reaction and degree of roGFP-iE reduction. These results were similar to the results obtained from ESG experiment.

We wanted to make sure that GOH has an effect on GSH transporter or the microsomal membrane rather than roGFP-iE itself. To do that microsomes were permeabilised by adding Triton X-100 (0.15%) to all microsomes and treated with different concentrations of GOH (Figure 3.13).

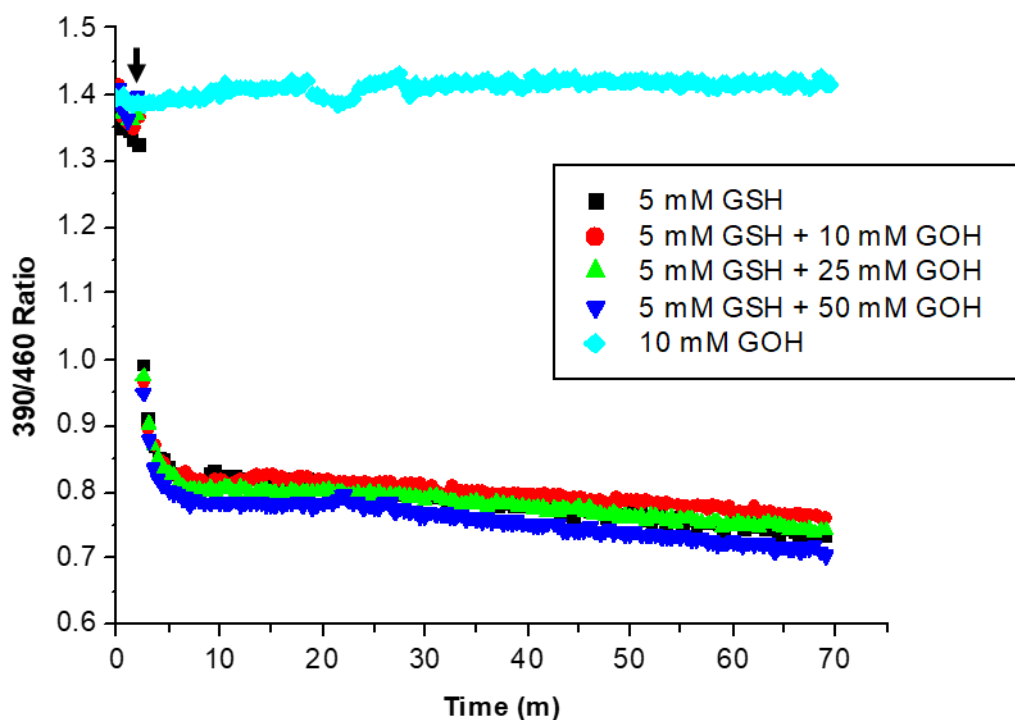


Figure 3.13. GOH effect on GSH transport in permeabilised microsomes.

Various concentrations of GOH were added to microsomes (indicated by arrow) permeabilised using Triton X-100 (0.15%) together with 5 mM of GSH. The change of 390/460 ratio was plotted over time, representing the overall rate of transport across microsomal membrane. The increased concentrations of GOH had no significant effect on the rate of GSH reduction when compared with GSH only sample. GOH on its own had no effect on roGFP. The data was plotted using three biological replicates to make sure the results are replicable.

All samples reduced roGFP-iE at the same rate and were able to reduce roGFP-iE to the same level while GOH on its own did not affect 390/460 fluorescence ratio of roGFP. This finding indicated that GOH does not affect roGFP-iE directly. Thus, the effect of GOH on GSH transport remains unknown.

3.4 Glutaredoxin roGFP fusion

It was not possible to inhibit GSH transport in previous experiments. The reason for that maybe a low specificity of roGFP-iE towards GSH. Contrary to the previously stated hypothesis, the rate of roGFP-iE reduction measured in the experiment may not correspond to GSH transport across microsomal membrane. It is possible that a cascade effect, in which GSH reduces another substrate and then the unknown substrate reduces roGFP-iE, is taking place. In order to increase the specificity of the GSH assay we used roGFP fused to glutaredoxin (GRx). In this instance roGFP-iL was used (Figure 3.14). roGFP-iL is very similar to roGFP-iE and has been used to monitor redox changes in the ER (Lohman and Remington, 2008, Van Lith et al., 2011). roGFP is able to exchange disulfide bonds with a variety of thiols and does not have specificity for GSH (Meyer and Dick, 2010). Therefore by fusing roGFP with a protein which reacts highly specifically with GSH it is possible to increase roGFP specificity towards GSH (Meyer and Dick, 2010). The fused protein GRx is part of the family of proteins with glutathione-disulfide oxidoreductase activity, that interact very specifically with GSH (Fernandes and Holmgren, 2004, Meyer et al., 2009). roGFP probes can equilibrate with GSH, however, this equilibration is slow and requires endogenous redox catalysts, such as GRx (Meyer and Dick, 2010). Therefore, the availability of endogenous GRx can limit the intracellular response of non-fused roGFP, thus the covalently attachment of GRx to roGFP facilitate the equilibration between roGFP and GSH, making it more rapid and complete (Meyer and Dick, 2010). roGFP fused to GRx not only becomes catalytically self-sufficient but also have a very high specificity for GSH because the presence of GRx in close proximity ensures that the interaction between roGFP and other redox couples do not occur (Meyer and Dick, 2010). Taking all of it together, Grx_roGFP-iL offers several advantages over SFroGFP-iE, especially a higher specificity for GSH and faster equilibration rate (Meyer and Dick, 2010).

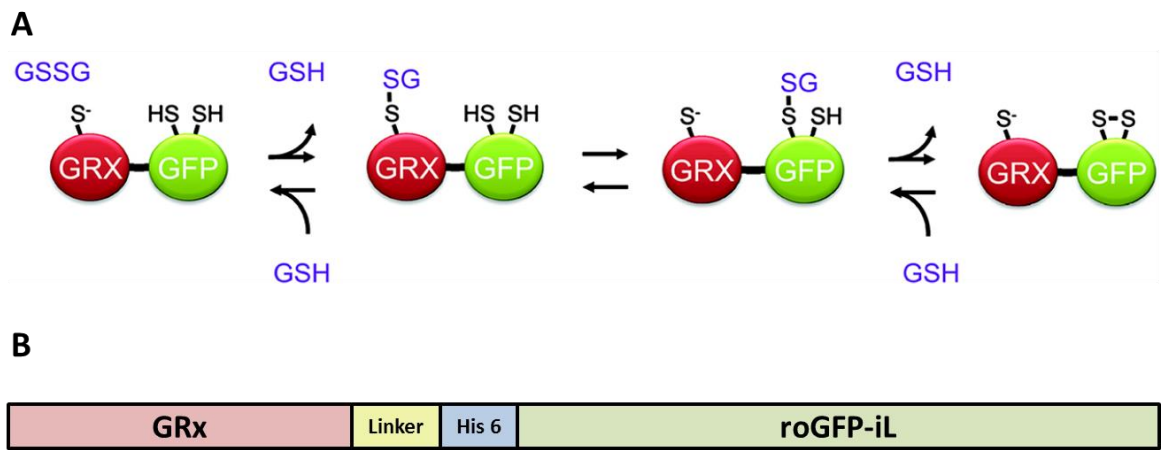


Figure 3.14. **(A)** Molecular mechanism of the Grx1–roGFP. Each individual step of the three-step thiol-disulfide exchange is fully reversible. **(B)** Diagrammatic representation of Grx1–roGFP-iL, a His-Tag was introduced to allow purification of the protein.

Because the fusion protein is more specific for GSH lower concentrations of GSH can be used. After carrying out a GSH titration 1 mM of GSH was used in all further experiments involving ER localised GRx_roGFP-iL. The GSH transport assay was performed as described previously, to find out if there are any differences between SFroGFP-iE and GRx_roGFP-iL (Figure 3.15a and figure 3.15b).

A)

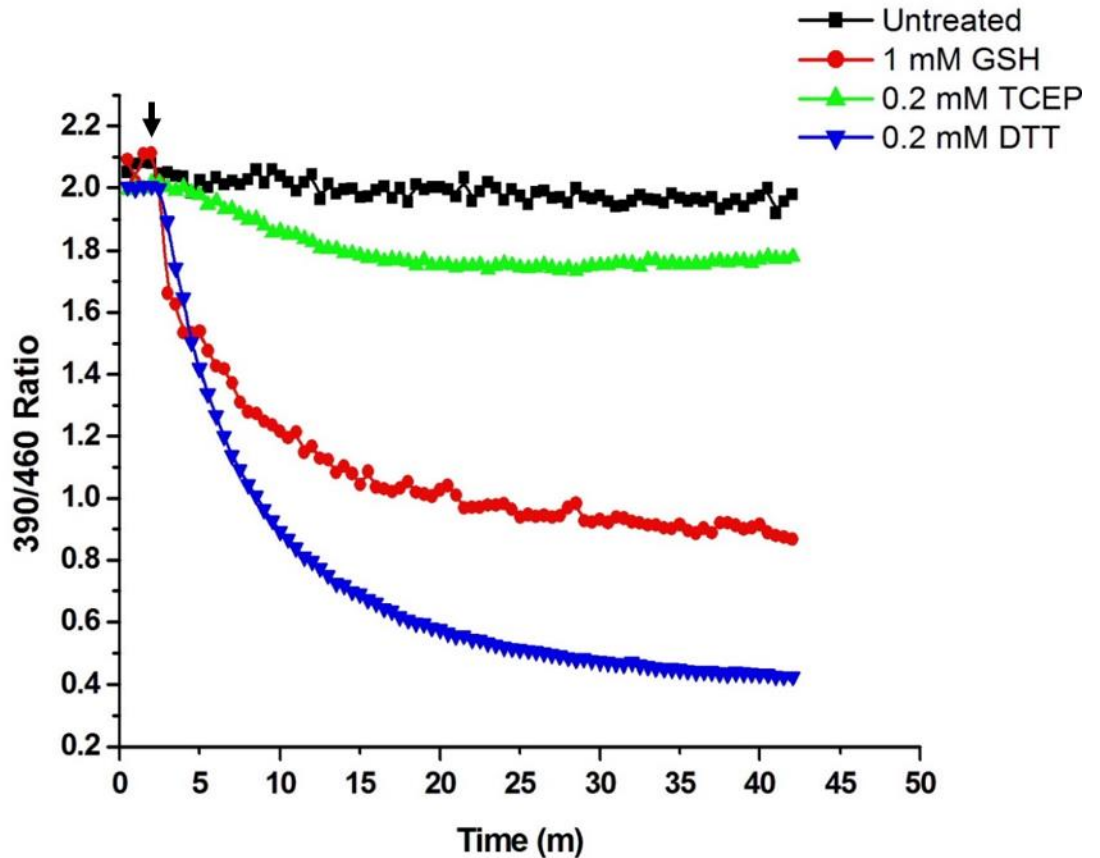


Figure 3.15a. Kinetics of GRx_roGFP-iL reduction in intact microsomes. 1 mM GSH, 0.2 mM DTT and 0.2 mM TCEP were added (indicated by arrow) to intact microsomes. The change of 390/460 ratio was plotted over time, representing the overall rate of transport across the microsomal membrane. GSH is able to cross the microsomal membrane at moderate speed compared to DTT which diffuses through the membrane at high rate. TCEP is membrane impermeable, therefore, there is no drop in 390/460 ratio. Untreated microsomes were stable over time and 390/460 ratio did not change over time. The data was plotted using three biological replicates to make sure the results are replicable.

B)

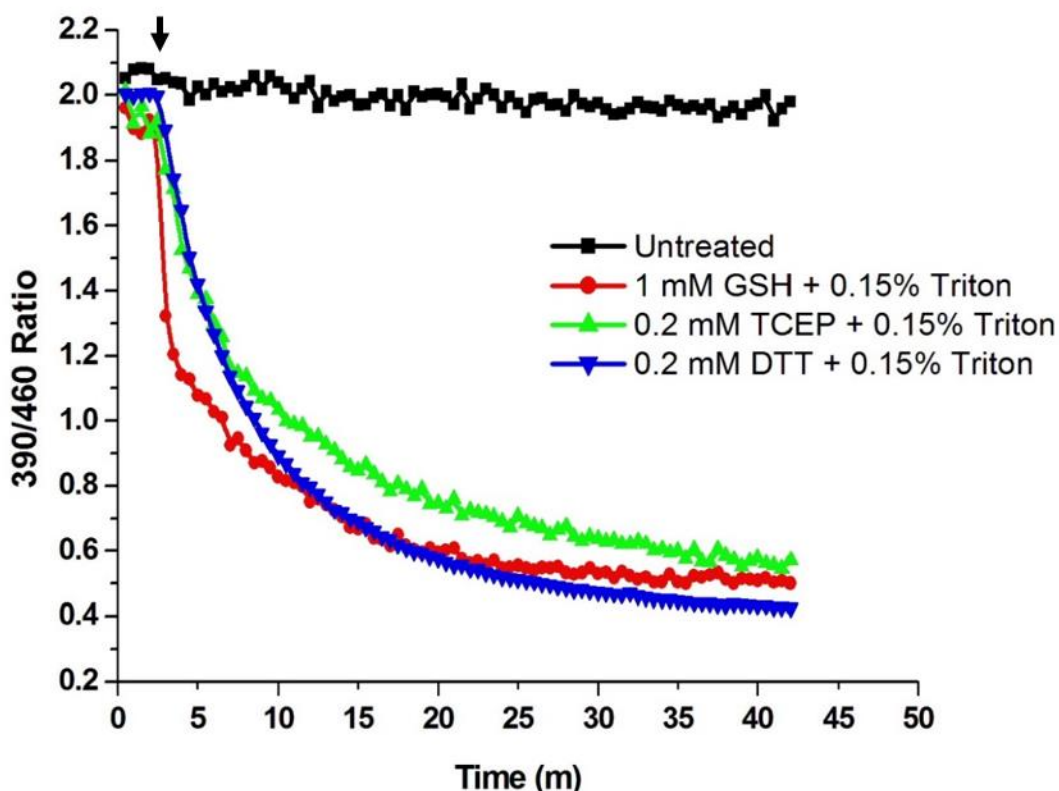


Figure 3.15b. Kinetics of GRx_roGFP-iL reduction in Triton X-100 permeabilized microsomes. 1 mM GSH, 0.2 mM DTT and 0.2 mM TCEP were added (indicated by arrow) to permeabilised microsomes so all reducing agents can reduce roGFP at maximum rate. The change of 390/460 ratio was plotted over time, representing the rate of roGFP reduction. Untreated microsomes were stable over time and 390/460 ratio did not change over time. The data was plotted using three biological replicates to make sure the results are replicable.

The assay results were very similar to the results obtained from roGFP-iE. However, this time GRx_roGFP-iL was reduced by GSH almost as effectively as DTT. This happens not only because fusing GRX increased roGFP-iL specificity for GSH but also because roGFP-iL has a slightly lower reduction potential than roGFP-iE, therefore roGFP-iL is more easily reduced (Meyer and Dick, 2010b).

3.4.1 Glutaredoxin roGFP fusion – GOH inhibition

After confirming that GRx_roGFP-iL is in fact more specific for GSH we decided to test how GOH will affect the transport of GSH in this model (Figure 3.16). The same ratios of GSH:GOH were used as in previous experiment (1:2, 1:5 and 1:10).

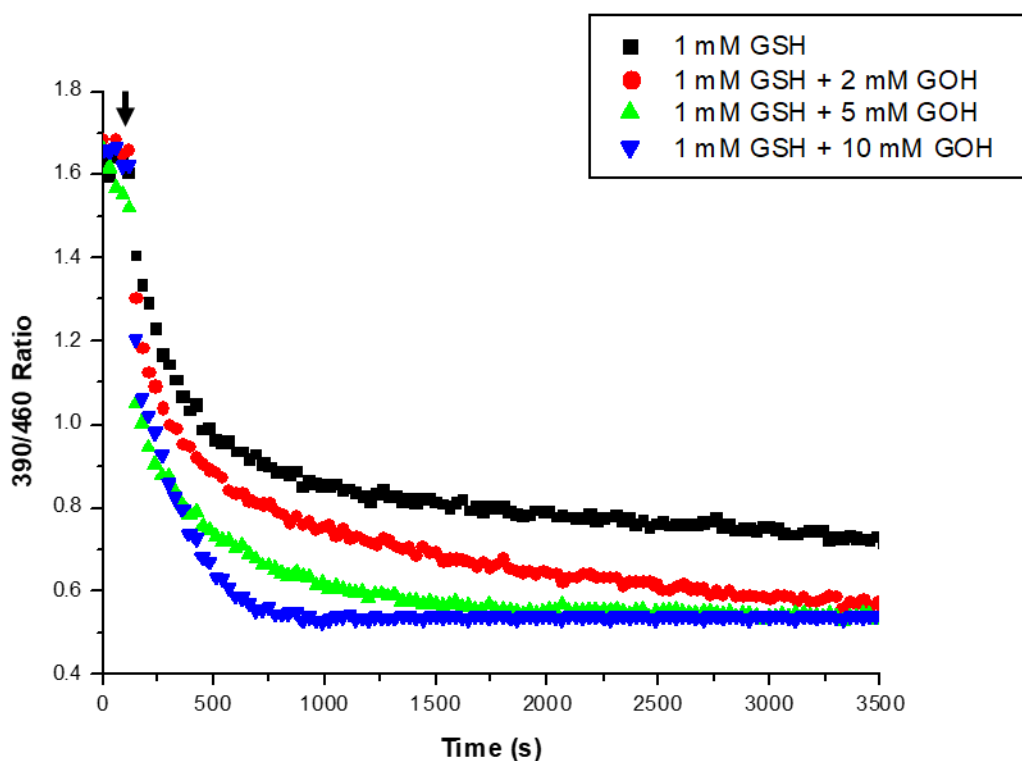


Figure 3.16. GOH effect on GSH transport in GRx_roGFP-iL intact microsomes. Various concentrations of GOH were added (indicated by arrow) to intact microsomes together with 1 mM of GSH. The change of 390/460 ratio was plotted over time, representing the overall rate of transport across the microsomal membrane. The increased concentrations of GOH accelerated the rate of GSH transport and lowered 390/460 ratio when compared with GSH only sample. The data was plotted using three biological replicates to make sure the results are replicable.

The results matched the result obtained by using roGFP-iE. The higher the concentration of GOH the faster the GSH transport and 390/460 ratio becomes lower.

3.5 Discussion

How glutathione is transported from the cytosol to other cellular compartments is still unknown. In my PhD project we were trying to tackle this important question. The assay which is described in this chapter might be used as a basis to identify a GSH transporter in the future.

The assay presented allows us to monitor the transport of reducing agents across the ER membrane. The overall change in roGFP redox state measured over time reflects the rate of transport of reducing agents. By using this system it was demonstrated that the ER membrane constitutes a barrier for GSH. It was also shown that GSH does not simply diffuse through the ER membrane and transport is necessary for GSH to cross the ER membrane. This assay is not limited to reducing agents only and can be used to monitor the transport of any compounds able to alter the redox status of roGFP.

The results, in respect to DTT and TCEP, are similar to those presented by *Cline et al.* in their assay, however GSH behaves different in our assay because of the difference between liposomes and microsomes. Liposomes used by *Cline et al.* do not contain any proteins embedded into bilayer thus any molecule that requires transport is not able to cross the lipid bilayer. Microsomes, in contrast to liposomes, contain all the membrane proteins normally present in the ER, therefore, it is assumed that a GSH transporter present in the ER membrane is also present in microsomes and allows GSH to move across the membrane. The different results from liposomes and microsomes indicates that GSH is transported across the ER membrane rather than by simple diffusion.

A potential drawback of the assay is the variation between each batch of prepared microsomes. Therefore, each experiment was repeated at least three times to make sure the results are replicable. Indeed, the results were replicable as each batch followed the same trend, however, different batches tend to behave slightly different, for example the starting 390/460 ratio of roGFP differs between each batch and needs to be tested prior to conducting any experiment. Usually the differences are not significant but may lead to confusion and misinterpretation of the data. The microsomes are prepared as mixture of intact and disrupted vesicles (Burchell et al., 1988). If the microsomes are not intact, the membrane is disrupted and GSH may be able to get inside microsomes by other means than being transported and

thus lead to false positive signal in the transport assay. It is very interesting that despite being a membrane impermeable reducing agent, TCEP was still able to reduce roGFP to some degree. This indicates a possible leakage of microsomes, thus it is possible to use TCEP to assess the intactness of our microsomes. If microsomes were very leaky TCEP would be able to reduce roGFP more, however if microsomes are intact the degree of roGFP reduction by TCEP would not be significant (for examples see appendix). DTT also played an important role as a control, it shows the maximum rate of roGFP reduction that can be achieved.

The biggest challenge was to inhibit GSH transport. Trying to inhibit it with broad range serine proteases was not effective. We were afraid that factors like temperature, pH, and in the case of proteinase K, presence of calcium, could compromise the activity of the proteinases used. However, proteinase K is very stable (optimal activity between pH 7.5 and 12 and temperature range of 20°C - 60°C) and despite requiring calcium for its stability the catalytic activity is not compromised in the absence of calcium. Therefore, our conditions were within the activity range of all proteinases. The activity of proteinase K can be stimulated when up to 2% SDS or up to 4 M urea is added into the buffer (Hilz et al., 1975), however adding these compounds would most likely affect our transport assay. Trying to digest the GSH transporter with serine proteases has other flaws. GSH transporting protein is most likely a membrane embedded protein, therefore could be protected from digestion.

The fusion of GRx to roGFP makes the roGFP more specific towards GSH, thus making the assay more sensitive allowing the use of lower concentrations of GSH. This seemed to be an improvement, however, the fluorescence of GRx_roGFP-iL is weaker than SFroGFP-iE, due to the lack of the superfolder mutations. The fluorescence brightness appeared to be an issue in GRx_roGFP-iL as the signal was weak. We are planning to solve this problem by fusing super folded roGFP to GRx. This will eliminate the drawback of GRx_roGFP-iL.

Probably the most unexpected results came from testing ESG and GOH effect on GSH transport. The results from ESG experiment could be simply explained by the fact that NEM group is bulky and maybe ESG gets “stuck” and somehow makes the transporter stay in an open conformation. However, because of the structural similarities between GOH and GSH it was expected that GOH would act as an inhibitor of GSH transport. However, samples with high concentration of GOH

displayed an increase in transport rate and were able to reach lower 390/460 ratio, thus they were reducing roGFP greater and faster than control sample with no GOH added. The results are not fully explained but one of our hypotheses is similar to what may happen to ESG. GOH is able to bind to the GSH transporter and keep it in an open conformation thus allowing GSH to enter microsomes freely, reducing roGFP greater and faster than normally. Other possible reason for the increase in reduction rate of roGFP is a simple gradient effect. As a greater amount of analogue was added this could cause GSH to move inside microsomes faster.

Chapter 4

GST assay for GSH transport

4.1 Introduction

The previous chapter described the development of novel assay for glutathione transport in which redox sensitive GFP was used as reporter protein. The assay proved that the ER membrane is a barrier for GSH and that GSH is transported across the ER membrane. To validate these findings, it was necessary to inhibit the transport process, however, despite taking different approaches to inhibit GSH transport we did not succeeded in this task. We tried crude methods using broad ranged serine proteases but also more targeted methods like inhibiting the transport with a GSH analogue.

We had some concerns about the roGFP assay and we were careful to restrict our interpretation of the results. Because disulfide exchange reactions are dynamic and there are many proteins and/or molecules in the ER lumen able to exchange disulfides, these can be potential substrates which can reduce roGFP. We wanted to make sure GSH interacts directly with the reporter protein in our assay. Therefore, we decided to change our approach and develop a new assay, alongside roGFP assay, which will be more specific. To complement the roGFP assay we developed an assay that uses glutathione transferase (GST) targeted to the ER lumen.

Glutathione transferases (EC 2.5.1.18), formerly named glutathione S-transferases, are a family of isoenzymes whose primary role is detoxification of xenobiotics by nucleophilic reactions with glutathione (Keen and Jakoby, 1978). GSTs can bind a variety of exogenous and endogenous ligands non catalytically, they can also protect cells against H₂O₂ induced cell death, and have isomerase and peroxidase activities (Sheehan et al., 2001). GSTs are classified into 3 main families, cytosolic (classes alpha, zeta, theta, mu, pi, sigma, and omega), mitochondrial (class kappa) and membrane-associated proteins in eicosanoid and glutathione metabolism (MAPEG) which consist of four subgroups (I-IV) (Hayes et al., 2005). The three-dimensional structure of cytosolic and mitochondrial classes of GSTs are very similar, however MAPEG classes of GSTs share no structural similarities to other GSTs classes (Ladner et al., 2004, Holm et al., 2002). The typical structure of the cytosolic family of GSTs consists of a C-terminal region rich in α -helices and an $\beta\alpha\beta\alpha\beta\alpha$ topology of a N-terminal thioredoxin-like domain (Oakley, 2011). The structure of mitochondrial kappa class of GSTs is very similar to cytosolic GSTs enzymes, it also contains a thioredoxin-like domain, however it has a DsbA-like α -

helical domain inserted between helix- α 2 and strand- β 3 (Oakley, 2011). In order to become catalytically active cytosolic and mitochondrial GSTs form homodimers (Oakley, 2011). Because MAPEG class of GSTs consists of membrane associated proteins they are very different in structure when compared to cytosolic and mitochondrial GSTs. All MAPEG GSTs have helical bundles (four left-handed α -helices) assembled into trimers and orientated orthogonally in the plane of the membrane (Oakley, 2011). However structurally different, all three GSTs families have similarities when it comes to catalytic activity, such as glutathione peroxidase activity, or conjugation of GSH with 1-chloro-2,4-dinitrobenzene (CDNB) (Hayes et al., 2005).

In our assay, we decided to use cytosolic GST class-pi (GSTP1-1) for the following reasons. Most importantly, GSTP1-1 is expressed in more tissues than any other GST (Suzuki et al., 1987). Among all GSTs, GSTP1-1 was the first one for which a three-dimensional structure was determined at 2.3 angstrom resolution by multiple isomorphous replacements (Reinemer et al., 1991). Since then GSTP1-1 was studied extensively, to date GSTP1-1 is probably the most characterised member of the GST family. Different polymorphic variants of GSTP1-1 differ in substrate affinity however we decided to use wild type GSTP1-1A (Ile105, Ala114). Compared to other cytosolic GSTs, GSTP1-1A has moderate peroxidase activity and high affinity for CDBN ($K_m = 0.33 \text{ mM}$, $V_{max} = 62.3 \mu\text{mol}^{-1}\text{mg}^{-1}$) and GSH ($K_m = 0.45 \text{ mM}$) (Aliosman et al., 1997, Seeley et al., 2006, Goodrich and Basu, 2012). Because the K_m for GSH is lower than the K_m for CDBN it is possible that GSH might be the rate limiting factor in the conjugation reaction. Because the moderate peroxidase activity of GSTP1-1A we knew it should not affect the redox state of ER.

Two suitable substrates for GST were selected, CDBN and the membrane permeable fluorescent dye 4,4-difluoro-4-bora-3a,4a-diaza-s-indacene (BODIPY). BODIPY has many qualities that make it a good choice as fluorescent probe, for example, resistance to photobleaching, narrow and high-intensity emission peaks, stability at physiological conditions and insensitivity to pH changes (Loudet and Burgess, 2007). Moreover, BODIPY also allows us to monitor changes not only in fluorescence but also in absorbance (Niu et al., 2012). To date many derivatives of the "core" BODIPY have been synthesised and characterised, we were interested in chloro-BODIPY (Cl-BODIPY) as it has properties making it selective for GSH and it has very low non-enzymatically activity between Cl-BODIPY and GSH (Loudet

and Burgess, 2007, Niu et al., 2012). GSTs catalyse the conjugation of GSH to Cl-BODIPY, this creates a shift in both emission (512 nm to 540 nm) and absorbance (503 nm to 530 nm), which allows for monitoring either a decrease or increase in emission/absorbance (Niu et al., 2012, Wang et al., 2014).

CDNB is the standard substrate choice for GSTs in the conjugation assay with GSH (Habig et al., 1974). The conjugation of CDBN to GSH results in a formation of stable product, GS-DNB conjugate, that absorbs strongly at 340 nm wavelength (Habig et al., 1974). The increase in absorbance at 340 nm reflects the enzymatic activity of GST. The process of conjugation of GSH to CDBN is well described and has become a standard method to assess activity of various GSTs (Aliosman et al., 1997, Suzuki et al., 1987). Moreover, CDBN is membrane permeable and can enter cells rapidly, which is very important for our assay (Lindwall and Boyer, 1987).

The principles of the new GST based transport assay are exactly the same as in previous roGFP based assay (Figure 4.1). As mentioned before there are many potential proteins and/or molecules involved in redox exchange reactions that could interact with GSH and then reduce roGFP. Since nothing else present inside the ER lumen/microsomes is able to conjugate GSH to Cl-BODIPY/CDBN the reaction can only be carried out by the ER localised GSTP1-1A. This makes the GSH transport assay using GST more direct than the previous assay based on roGFP reduction. Because of the dynamic state of roGFP it was impossible for a roGFP based transport assay to be quantitative. However, because GST based transport assay results in a stable product formation (GS-DNB/GS-BODIPY conjugate) the assay can be quantified and various other experiments can be carried out, for example product analysis by mass spectrometry or HPLC.

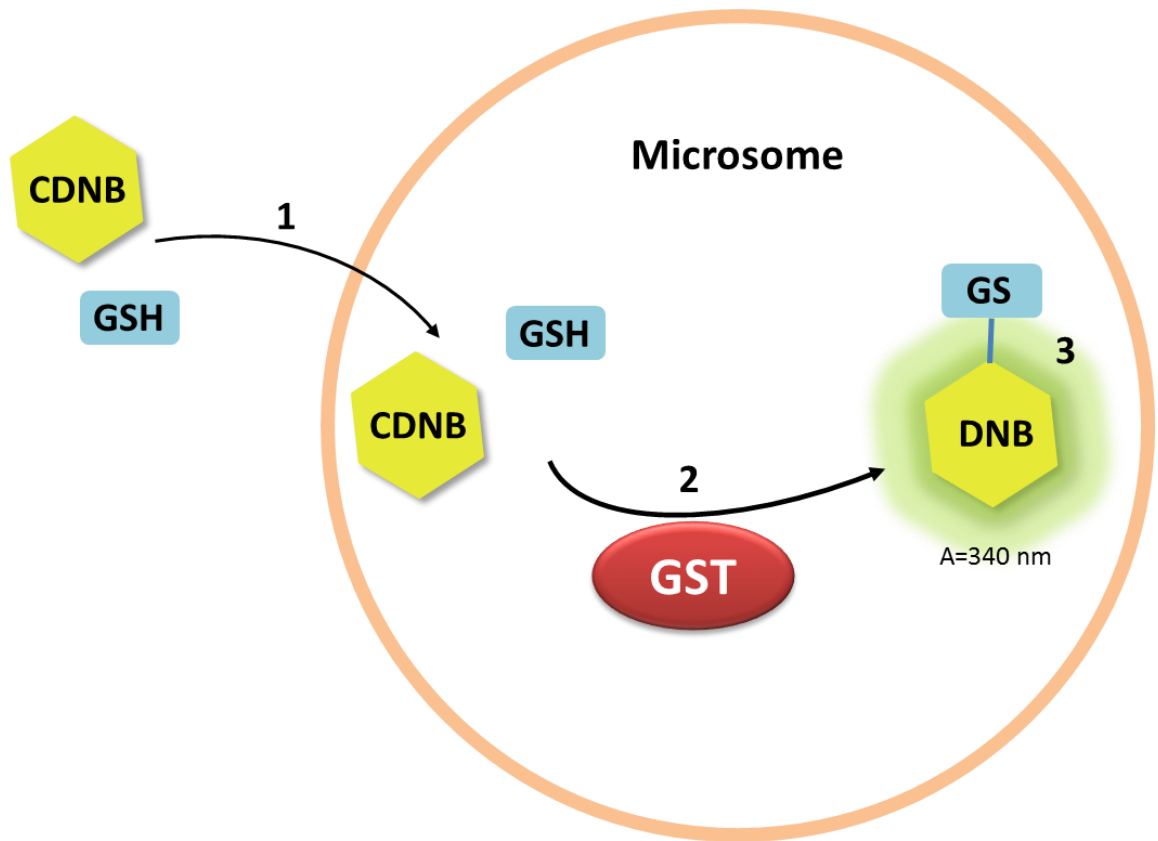


Figure 4.1. Principles of GSH transport based on conjugation of GSH to CDNB by GST. (1) GSH and CDNB are added to microsomes and cross the membrane. (2) GSH is conjugated to CDNB by GST. (3) GS-DNB conjugate is formed and absorbance at 340 nm can be measured.

4.2 GSTP1-A-KDEL cell line

A stable HT1080 cell line overexpressing GSTP1-A was created. A FLAG tag and KDEL sequence were added to C-terminus to make the protein easier to characterise on Western blot and to make sure GSTP1-1A stays in the ER (Hopp et al., 1988, Stornaiuolo et al., 2003). After isolating clones and confirming GSTP1-1A expression, by Western blot, microsomes were prepared and the presence of GSTP1-1A was confirmed by Western blot (Figure 4.2).

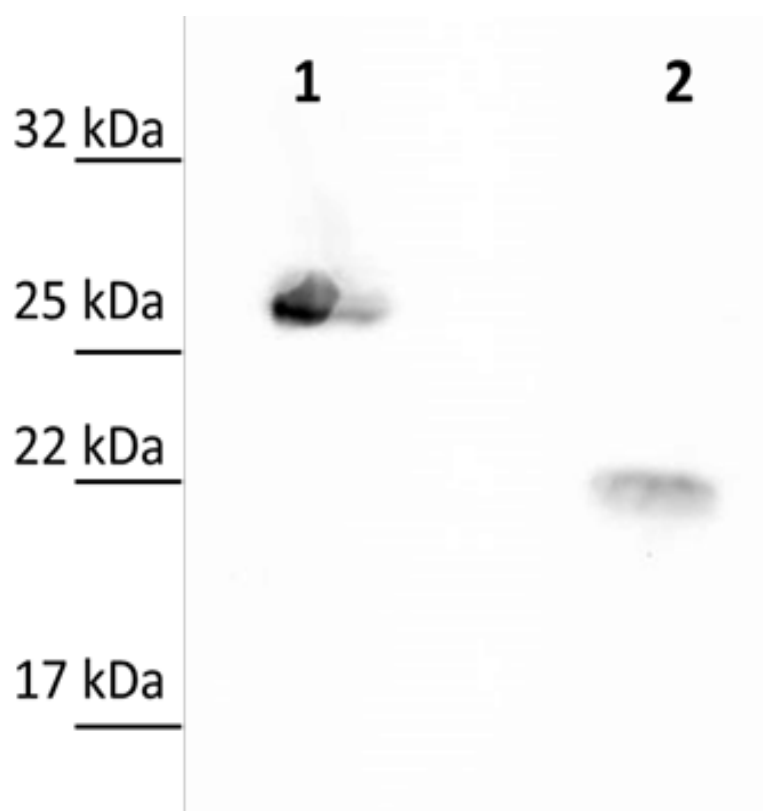


Figure 4.2. Immunofluorescence Western blot analysis of FLAG tagged GSTP1-1A. GSTP1-1A microsomes were lysed and separated by 12.5% SDS-PAGE and subjected to Western blotting. The blot was incubated with α -FLAG (Mouse) antibody (1:1000) for 4 hours followed by 40 minutes incubation with secondary α -mouse-800 antibody (1:10000). Lane 1 - GSTP1-1A (~25 kDa). Lane 2 - a positive control - FLAG tagged SNARE protein.

4.3 GST based transport assay

Both CDNB and BODIPY assays were performed to check which one would be more suitable for monitoring GSH transport across the microsomal membrane.

Due to the high fluorescence intensity and poor water solubility a low concentration of BODIPY (100 nM) was used in the transport assay. Microsomes were treated with BODIPY (100 nM) and GSH (0.1 mM) was added. The change in fluorescence spectra was monitored over time (Figure 4.3). The relatively low concentration of 100 nM was enough to give a strong fluorescence signal and to observe a shift in emission peaks, indicating GS-BODIPY formation. There is a clear decrease in 512 emission peak, however, the increase in 540 emission peak is not as clear as seen in BODIPY related publications (Wang et al., 2014, Niu et al., 2012). Moreover, the shift in emission peaks in our assay requires much more time compared to previous publications and is still not completed even after 2 h (Niu et al., 2012). This could possibly indicate low activity of GSTP1-1A and its low specificity for Cl-BODIPY. If the rate of GSH to Cl-BODIPY conjugation is slower than GSH transport across membrane the rate of GS-BODIPY formation is measured instead of the rate of GSH transport.

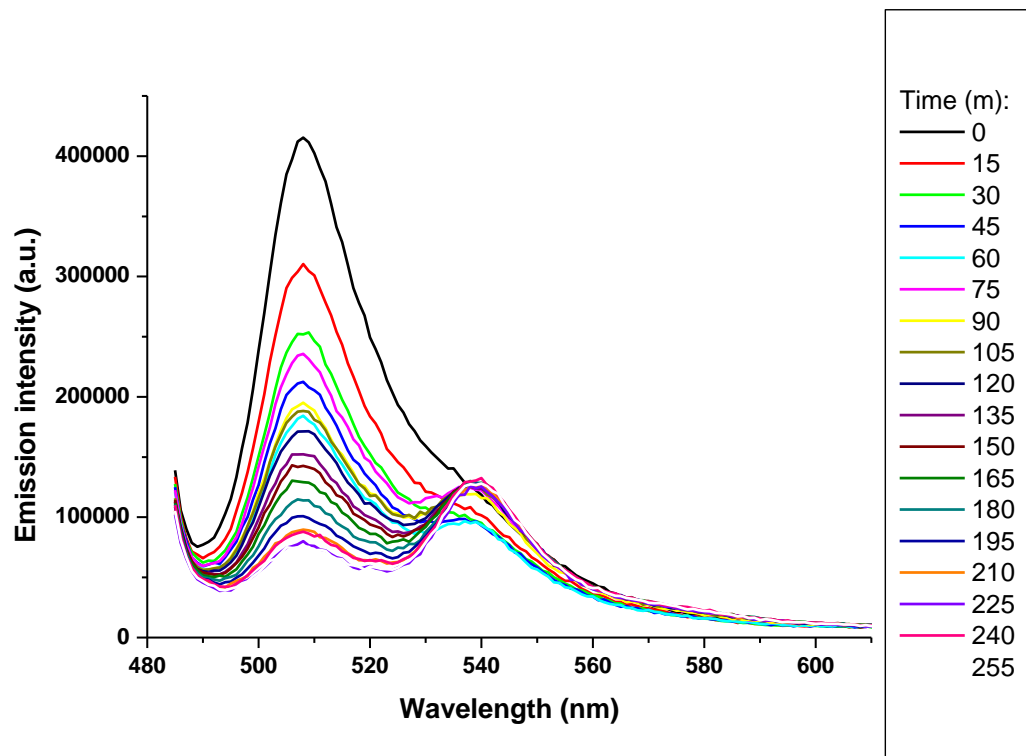


Figure 4.3. Fluorescence spectra of CI-BODIPY. To assess GSH transport across microsomal membrane 0.1 mM GSH was added to GSTP1-1A microsomes pre-treated with 100 nM CI-BODIPY. Fluorescence spectra was measured every 15 minutes. Different colours represent measurement at different time. Over time a slow shift in emission was observed (512 nm to 540 nm). The data was plotted using average of three technical replicates.

It has been reported that high concentrations of CDNB can disturb the cell membrane, therefore a low concentration of CDNB was used in the assay. Microsomes were treated with CDNB (250 μ M) and GSH (1 mM) was added. The change in in 340 absorbance was monitored over time (Figure 4.4). The experiment was carried out three times and all replicates are shown in Figure 4.4 to demonstrate the problem with this approach. The absorbance at 340 nm fluctuated dramatically. Even the untreated sample containing only microsomes shows a lot of variability over time. All three samples treated with CDNB and microsomes behave differently and it is difficult to draw any conclusions in regard to GSH transport. The reason for these fluctuations is most likely due to a high background turbidity from the added microsomes.

Both of CDNB and Cl-BODIPY assays did not provide information about GSH transport. The investigation of why the assays did not work and how to improve both approaches, was required.

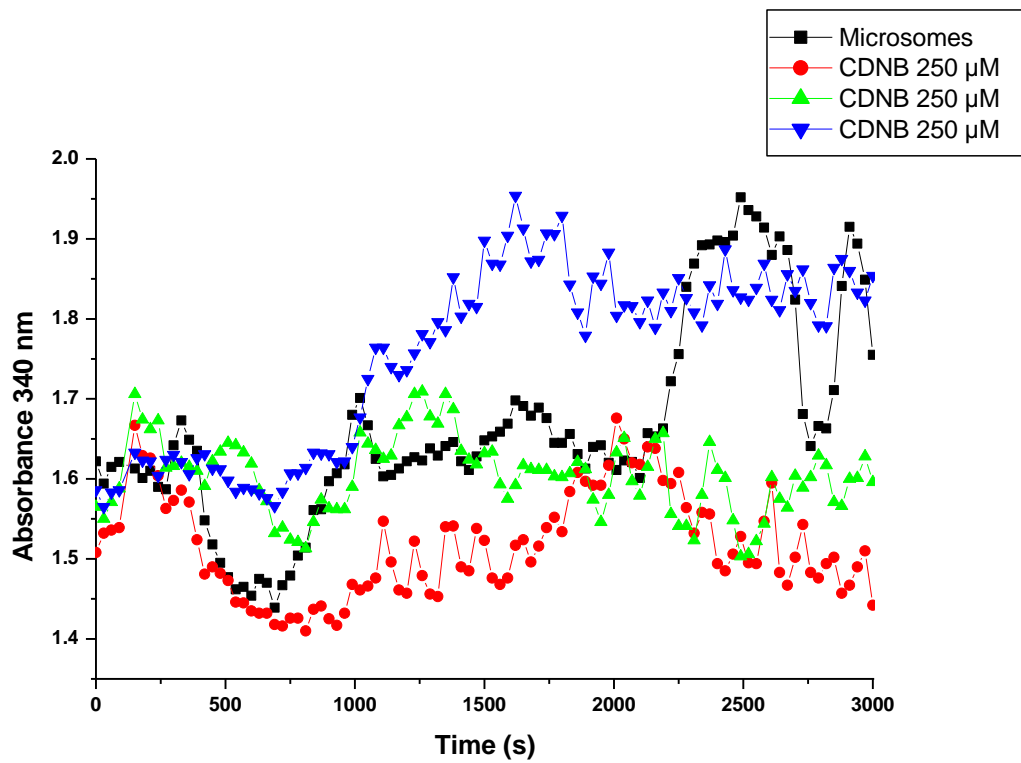


Figure 4.4 GST based assay of GSH transport across microsomal membranes.

To assess GSH transport across microsomal membranes 1 mM GSH was added to GSTP1-1A microsomes pre-treated with 250 μ M CDNB. The change in absorbance at 340 nm was plotted over time representing the activity of GSTP1-1A inside microsomes. All triplicates are included to show unreliability of the approach.

4.3.1 Purified GSTP1-1A activity

To evaluate the GSTP1-1A activity we overexpressed the protein in *E.coli* and carried out purification using glutathione Sepharose beads. Both FLAG tag and KDEL sequence were included in *E.coli* construct to make sure that activity of the protein is not affected by addition of these sequences.

To test how GSTP1-1A reacts with CDNB, GSH (1 mM) and CDNB (250 μ M) were added to different concentrations of GSTP1-1A (50 nM – 500 nM) the increase in 340 nm absorbance was monitored over time (Figure 4.5). As expected, the rate of GS-DNB conjugate formation is concentration dependent, as the concentration of GSTP1-1A increases the rate of GSH to CDNB conjugation also increases. In order to check the non-enzymatic activity between GSH and CDNB one sample without adding GSTP1-1A was included. The conjugation of GSH to CDNB without the presence of enzyme is slow and was treated as a background and results were normalised against it.

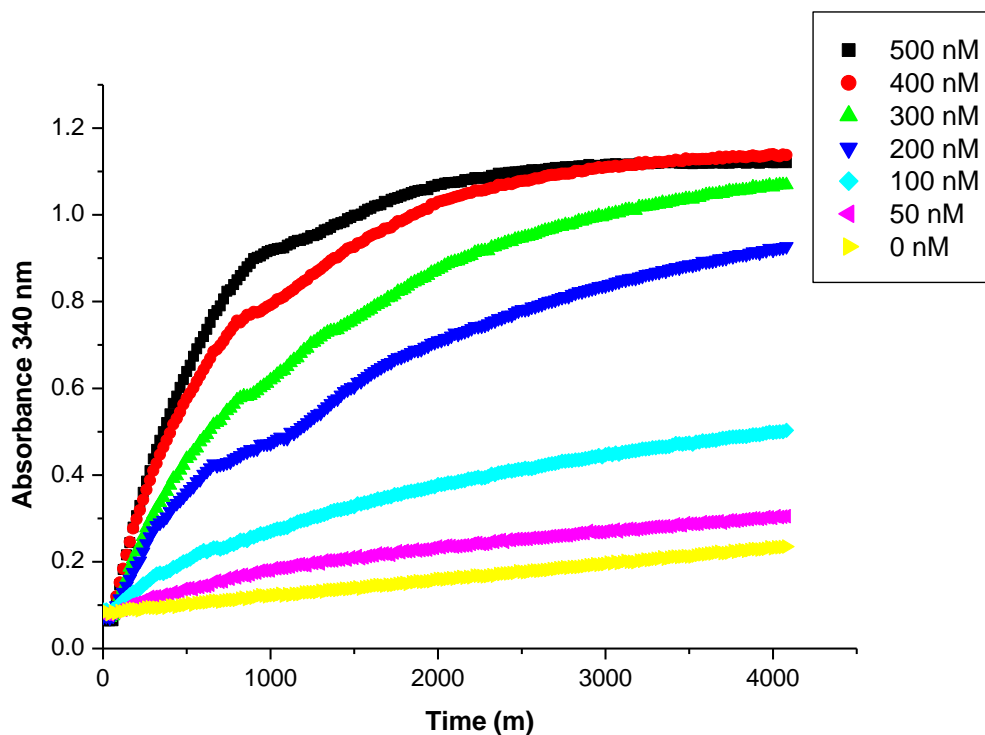


Figure 4.5. Purified GSTP1-1A activity. 1 mM of GSH and 250 μ M CDNB were added to different concentrations of GST. The increase in 340 nm absorbance was plotted over time, representing the overall GSTP1-1A activity. As the concentration of GSTP1-1A increases the rate of GSH to CDNB conjugation also increases together with the maximum absorbance. Sample with no GSTP1-1A added shows slow non-enzymatic conjugation of GSH to CDNB. The data was plotted using three biological replicates to make sure the results are replicable.

To test GSTP1-1A activity towards CI-BODIPY, GSH (1 mM) and CI-BODIPY (150 μ M) were added to different concentrations of GSTP1-1A (50 nM – 500 nM) the increase in 530 nm absorbance was monitored over time (Figure 4.6). When compared to CDNB the rate of GS-BODIPY conjugation was slow even at the highest concentration of GSTP1-1A. When plotted on the graph the slower rates did not resemble typical sigmoid curves seen in enzymatic reactions but were linear. The activity of low concentrations of GSTP1-1A are hard to distinguish from background non-enzymatic activity between CI-BODIPY and GSH. The slow and low activity of GSTP1-1A with CI-BODIPY can explain what was observed previously when CI-BODIPY was used with microsomes.

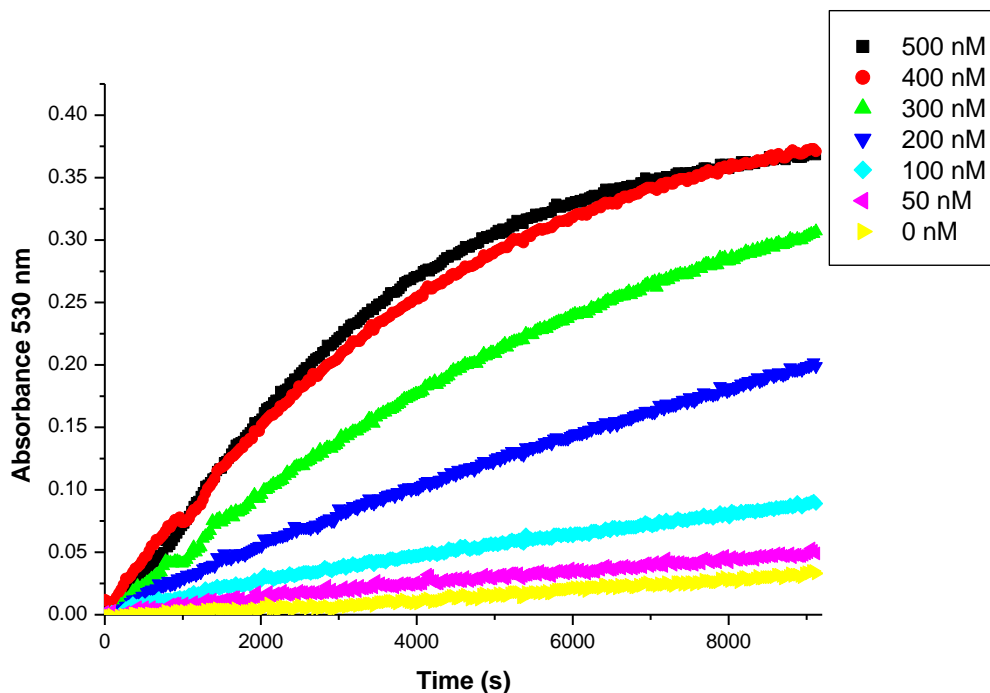


Figure 4.6. Purified GSTP1-1A activity towards CI-BODIPY. GSH (1 mM) and CI-BODIPY (150 nM) were added to different concentrations of GST. The increase in 530 nm absorbance was plotted over time, representing the overall GSTP1-1A activity. As the concentration of GSTP1-1A increases the rate of GSH to CI-BODIPY conjugation also increases together with the maximum absorbance. Lower concentrations of GSTP1-1A shows linear increase in absorbance. Sample with no GSTP1-1A added shows slow non-enzymatic conjugation of GSH to CI-BODIPY. The data was plotted using three biological replicates to make sure the results are replicable.

This result confirmed that GSTP1-1A is active and able to conjugate GSH to CDNB despite the presence of KDEL and FLAG sequences. However, CI-BODIPY is not a good substrate for GSTP1-1A. CI-BODIPY seems to react slowly with GSTP1-1A, because of this CI-BODIPY does not seem to be a good candidate for the GSH transport assay. Therefore, from now on the main focus of the project was on improving CDNB approach.

4.3.2 Estimate the concentration of GSTP1-1A inside microsomes

To have a rough idea of GSTP1-1A activity inside microsomes, estimating the concentration of GSTP1-1A inside microsomes was necessary. Solubilised microsomes were compared against the known concentration of purified GSTP1-1A on 12.5% SDS-PAGE followed by Western blot analysis (Figure 4.7). By comparing the bands intensities using ImageJ software, the concentration of GSTP1-1A inside microsomes was estimated to be around 150 nM. Compared to previous results from purified GSTP1-1A activity, 150 nM should still give enough activity to be able to monitor the increase in absorbance of CDNB. The concentration of 150 nM should also be enough to see changes in Cl-BODIPY absorbance/fluorescence, however, due to its slow kinetics it would be difficult.

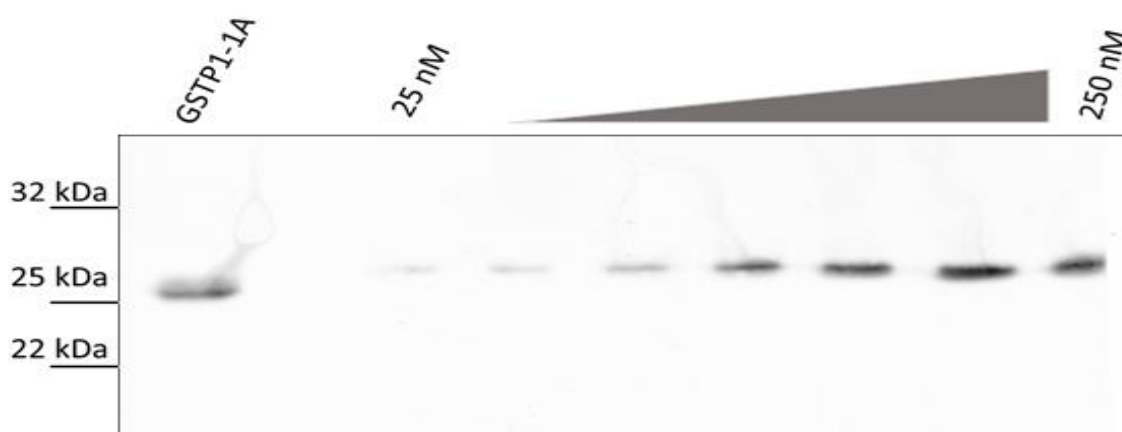


Figure 4.7 Western blot analysis of FLAG tagged GSTP1-1A. Lysed GSTP1-1A microsomes were separated on 12.5% SDS-PAGE and subjected to Western blotting. Increasing concentrations of purified GSTP1-1A were added to the blot to help estimate the concentration of GSTP1-1A inside the microsomes. The blot was incubated with α -FLAG (Mouse) antibody (1:1000) for 4 hours followed by 40 minutes incubation with secondary α -Mouse-800 antibody (1:10000).

4.3.3 In vivo activity of GSTP1-1A

Previous experiments proved GSTP1-1A to be active *in vitro*, however, an indication of protein being active *in vivo* was especially important for our GSH transport assay. A simple experiment using glutathione Sepharose beads was performed to find out if GSTP1-1A present inside the ER is able to bind GSH and thus be active and correctly folded. Glutathione Sepharose beads are normally used for purification of GSTs and GST tagged proteins but in this experiment it was used as an indication that GSTP1-1A had folded correctly and would be active. HT1080-GSTP1-1A-KDEL cells were lysed and incubated with glutathione Sepharose beads, washed 3 times with PBS then eluted with a high concentration of GSH. Both eluate and wash flow were analysed on 12.5% SDS-PAGE gel followed by silver staining (Figure 4.8). A strong band above 25 kDa in eluted sample corresponds to GSTP1-1A, other minor bands may represent endogenous cytosolic GSTs or proteins that bind GSH. The flow through sample contained a diffuse smear with a large number of bands present, this is not surprising as the majority of proteins do not interact with GST therefore were washed through. This indicates GSTP1-1A is active and able to bind GSH, otherwise it would not be possible to separate it from the rest of the proteins present in the lysate. As a control a mix of purified GSTP1-1A and ERp 27 was used. Because ERp27 does not bind GSH it should be possible to separate these 2 proteins based on GSH binding, thus ERp27 should only be seen in flow control. The elute control contained a strong band corresponding to GSTP1-1A while a band corresponding to ERp27 was only visible in the flow through control. This proved that the principles of the experiment work, it is possible to separate proteins based on GSH binding. In order to identify GSTP1-1A and ERp27 purified versions of these proteins were also run on the gel. Total cell lysate was also included as another control to check differences between the flow through samples. As expected a band corresponding to GSTP1-1A was present in total cell lysate sample. The results from the experiment are encouraging and showed that GSTP1-1A binds to GSH and is likely to be active *in vivo*, therefore it should be active in microsomes during GSH transport assay.

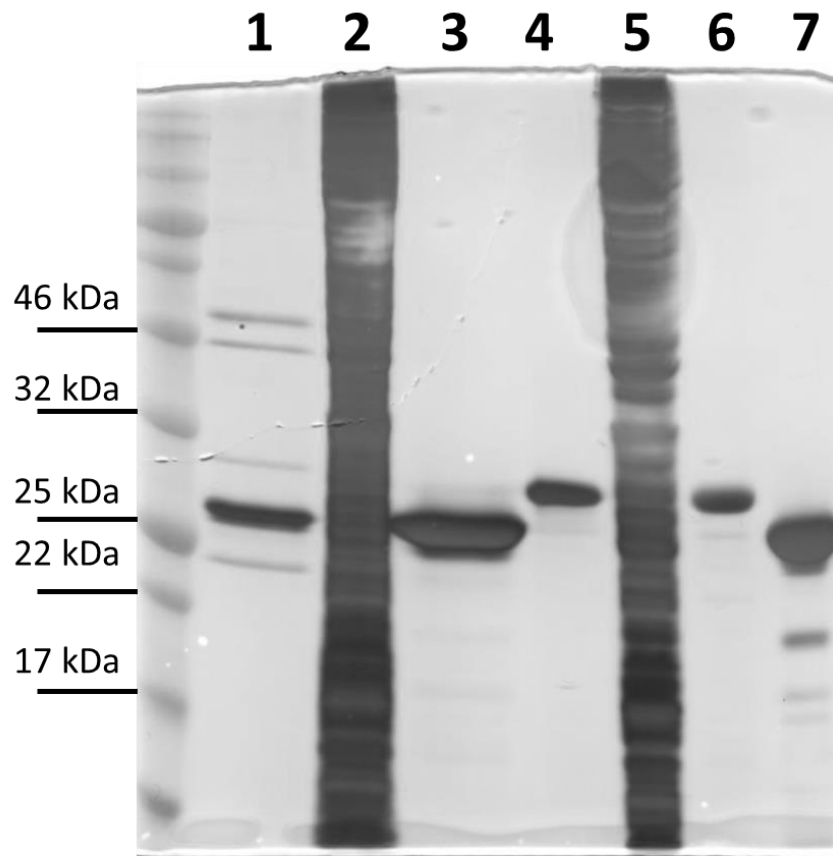


Figure 4.8 *In vivo* binding of GSTP1-1A to GSH-Sepharose. HT1080-GSTP1-1A-KDEL cells were lysed and incubated with GSH-Sepharose beads, washed 3 times with PBS then eluted with high concentration of GSH. Proteins were silver stained . Lane 1 - HT1080-GSTP1-1A-KDEL cell lysate eluted sample. Lane 2 - HT1080-GSTP1-1A-KDEL cell lysate unbound sample. Lane 3 – purified GSTP1-1A/ERp27 mix, GSH-eluted sample. Lane 4 – purified GSTP1-1A/ERp27 mix, unbound sample. Lane 5 - HT1080-GSTP1-1A-KDEL total cell lysate. Lane 6 – purified ERp27. Lane 7 – purified GSTP1-1A.

4.3.4 Mass spectrometry and HPLC identification of conjugated product

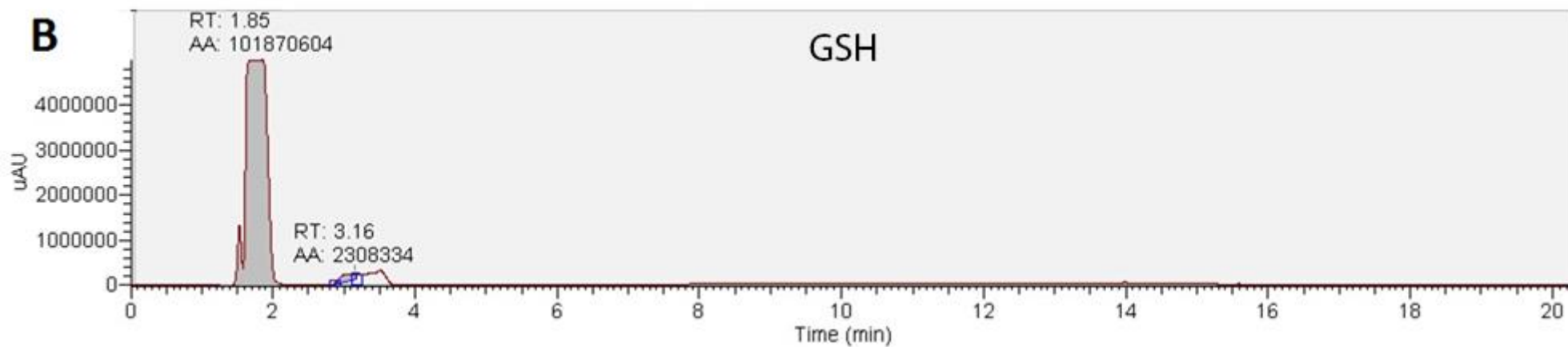
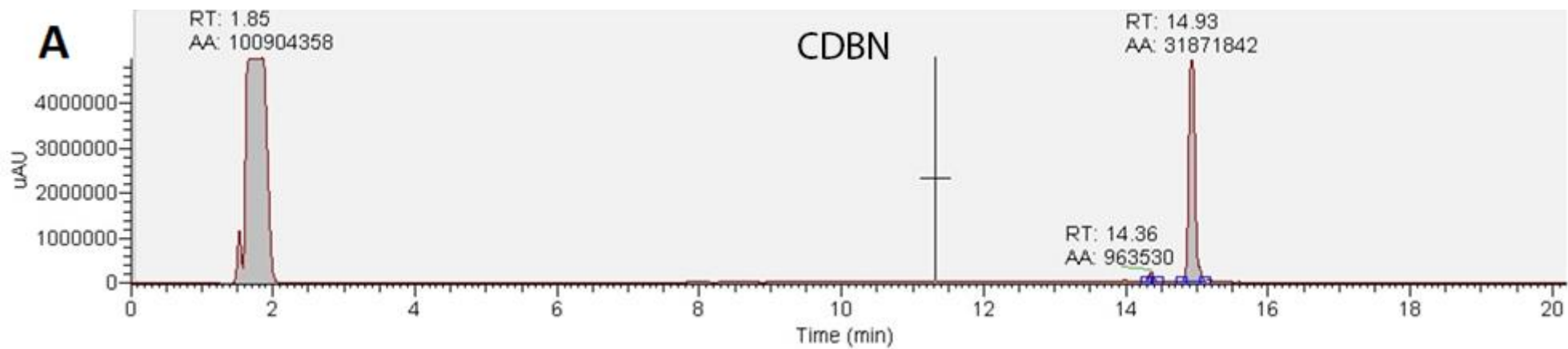
The main advantage of GST based transport assay is the formation of a stable GSH conjugated product, GS-DNB or GS-BODIPY. We decided to use this property of the GST based transport assay to detect the conjugated product using HPLC followed by mass spectrometry (Figure 4.9). Microsomes were treated with CDNB (250 μ M) and GSH (1 mM) for approximately 2 h and protein was precipitated using trichloroacetic acid (TCA) 10% v/v. Adding TCA precipitates protein but not small, water soluble molecules such as GSH. Therefore, following centrifugation the GSH-conjugate product remains in the supernatant ready for further analysis. After TCA treatment HPLC was performed followed by mass spectrometry. Peak areas were also indicated on chromatograms to allow quantification of any conjugate present in each sample. Overall 6 samples were analysed. CDNB alone was used to identify the peak corresponding to CDNB (Figure 4.9a), GSH alone to identify the peak corresponding to GSH (Figure 4.9b). A mixture of CDNB and GSH was included to identify the peak corresponding to the conjugated product and to determine the non-enzymatic background of conjugation (Figure 4.9c). A mixture of CDNB and GSH was incubated with GSTP1-1A to determine the maximum product that can be obtained from given concentrations of CDNB and GSH (Figure 4.9d). A sample containing GSTP1-1A microsomes incubated with CDNB and GSH was analysed (Figure 4.9e). A control sample containing microsomes made from untransfected HT1080 cell line, incubated with CDNB and GSH was included in analysis (Figure 4.9f). A chromatogram from the mass spectrometry of the sample containing GSTP1-1A microsomes treated with CDNB, and GSH is also included to demonstrate that the peak corresponding to GS-DNB conjugate contains the right product (Figure 4.9g).

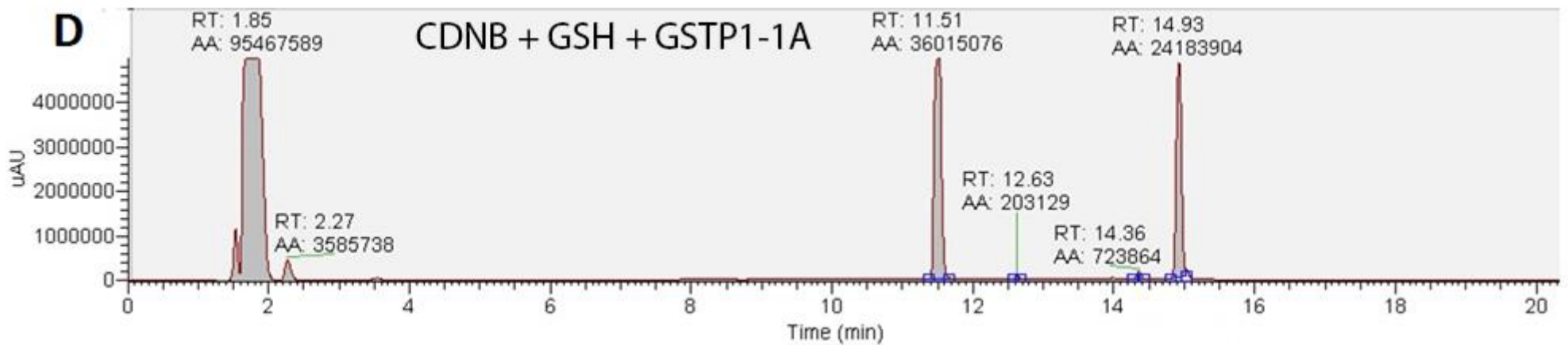
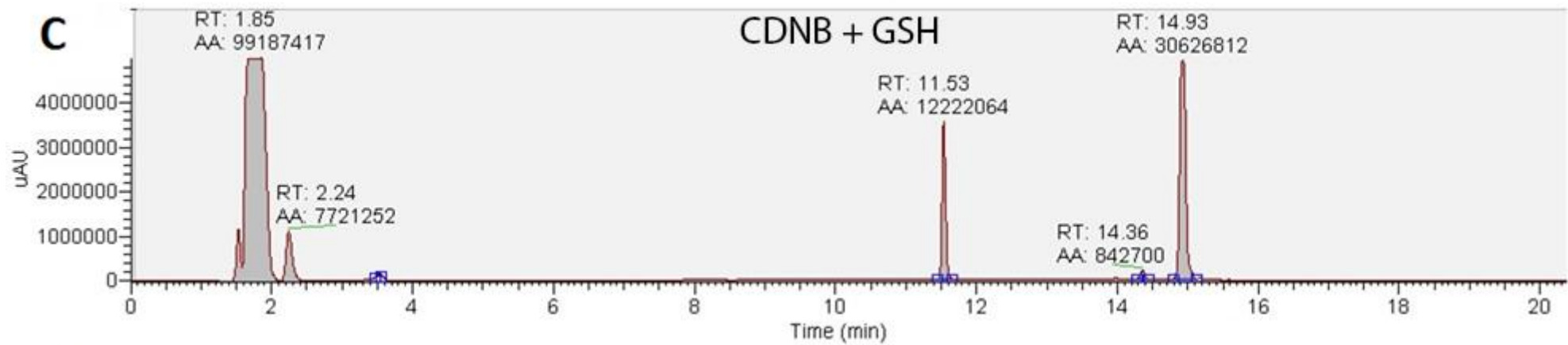
Because all samples were treated with high concentration of TCA (10%), an oversaturated peak (RT = 1.85) is present in every sample. CDNB is less polar than other molecules tested thus its retention time (RT) is longer (RT = 14.93), CDNB is represented by sharp peak, however a smaller peak (RT = 14.36) is also present. GSH was eluted earlier (RT ~ 2.26) after the TCA. For the reason still unclear in sample containing GSH only (Figure 4.7b), GSH is eluted later (RT = 3.16) than in any other tested sample. GS-DNB conjugate was identified as sharp peak (RT ~ 11.53) varying in size depending on the sample tested. Mass spectrometry analysis verified the GS-DNB peak (RT ~ 11.53) contain the right product by confirming its

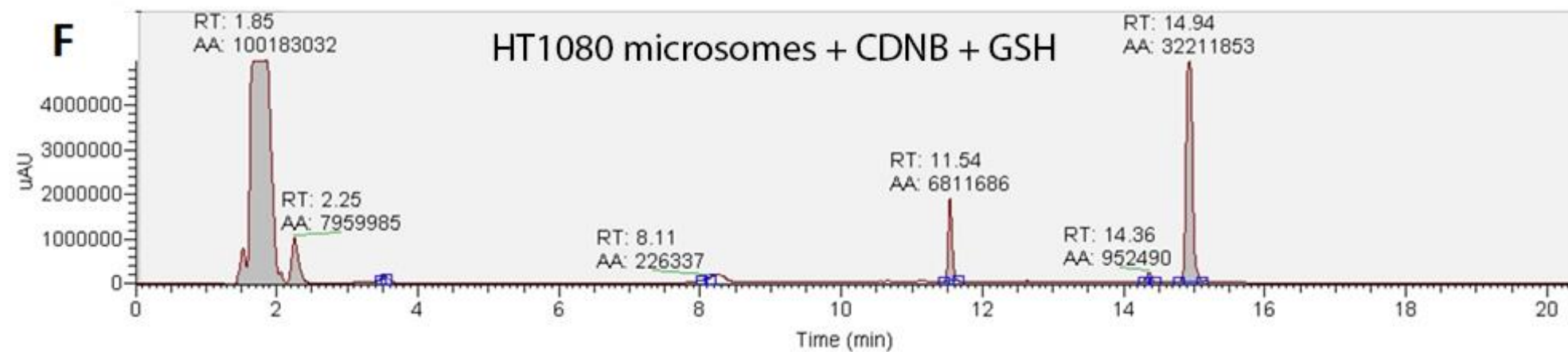
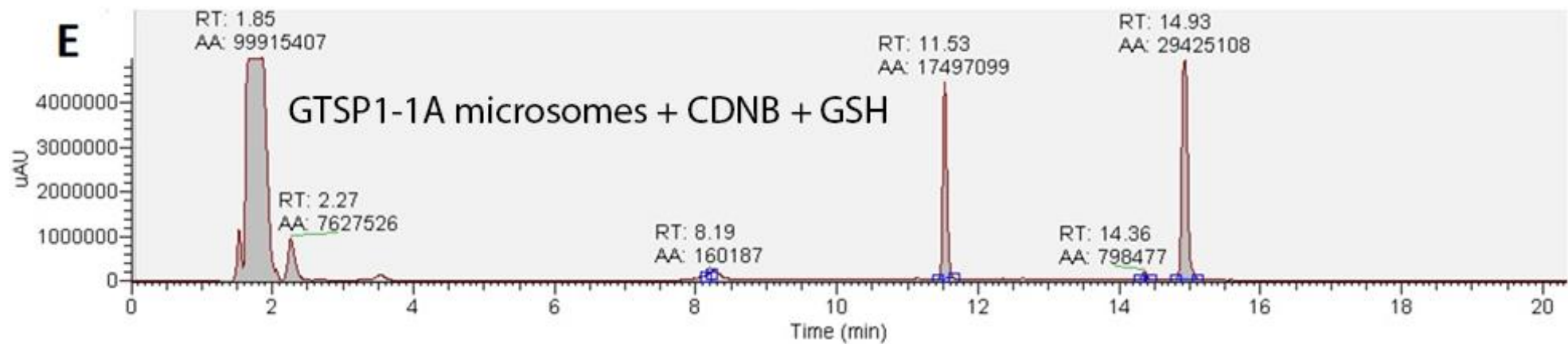
mass ($474 \text{ g}\cdot\text{mol}^{-1}$) (Figure 4.9g). In both microsomes samples, one additional small peak appeared (RT ~ 8.19), however, the origin of this peak is unknown.

By comparing peak areas values (indicated "AA" on chromatogram) it is possible to gain an estimate of how much GS-DNB conjugate has been formed and compare samples between each other. Microsomes containing GSTP1-1A (Figure 4.9e) can be compared to HT1080 microsomes (Figure 4.9f) as the only difference between them is presence of GSTP1-1A. Peak area value for GS-DNB conjugate in GSTP1-1A microsomes is equal to 17.5×10^6 while peak area value for HT1080 microsomes is equal to 6.8×10^6 . Making some simple calculations it is possible to estimate that there is approximately 2.5 times more GS-DNB conjugate formed in GSTP1-1A microsomes sample due to GSTP1-1A activity. However, it is important to remember that these numbers are not definitive and should only be used as an estimate/indication of relative abundance of compounds in each sample.

The HPLC/mass spectrometry experiment proved not only that GSH is transported inside microsomes and is conjugated to CDNB but also that GSTP1-1A is active inside microsomes and able to catalyse conjugation of GSH to CDNB. By comparing peak area values from different samples it became clear that in the presence of GSTP1-1A more product is formed. The presence of GSH to Cl-BODIPY conjugate was also confirmed by mass spectrometry (see appendix).







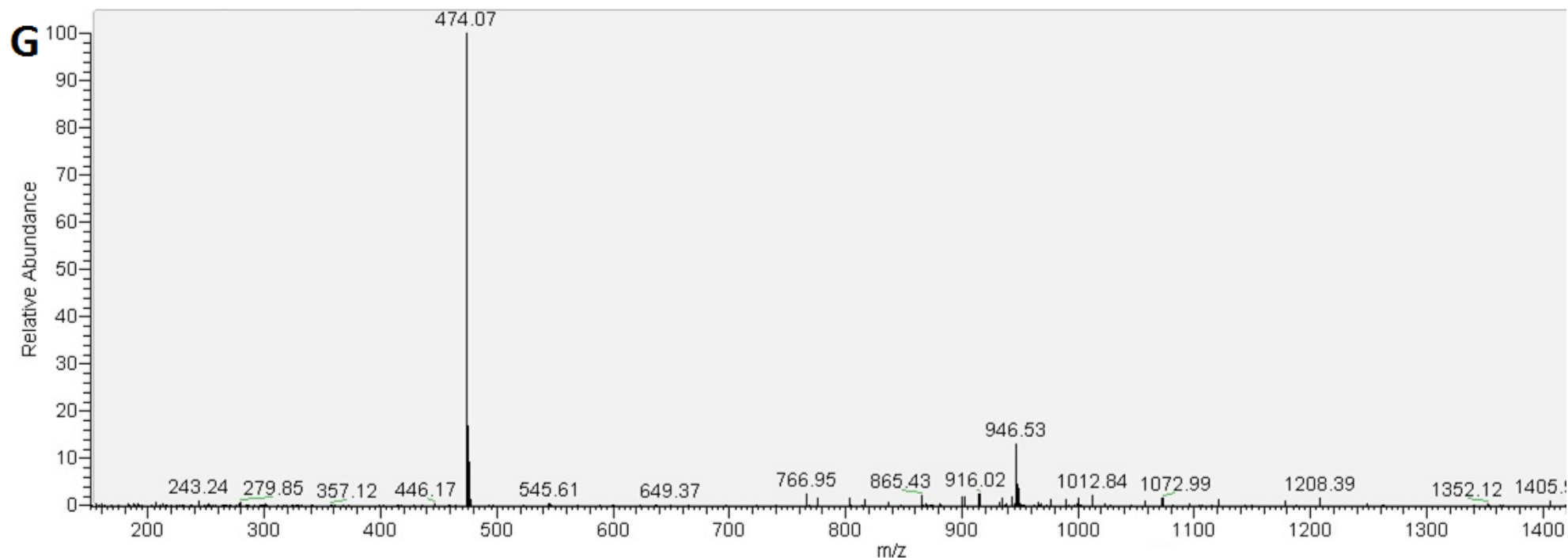


Figure 4.9 HPLC and mass spectrometry analysis of GS-DNB conjugate in different samples. A) CDNB, B) GSH, C) CDNB + GSH, D) CDNB + GSH + GSTP1-1A, E) GSTP1-1A microsomes + CDNB + GSH, F) HT1080 microsomes + CDNB + GSH G) Mass spectrometry chromatograph of GSTP1-1A microsomes + CDNB + GSH sample. Retention times (RT): CDNB = 14.93, GSH = ~2.25/3.16, GS-DNB = ~11.53, TCA = 1.85. GS-DNB mass = 474. AA = Peak area

4.3.5 Transport assay – endpoint

Experiments similar to previous mass spectrometry were then conducted, however this time the absorbance was measured after TCA treatment. This approach is much simpler than mass spectrometry or HPLC and gives us information related to amount of conjugated product present in each sample.

Microsomes were treated with CDNB (250 μ M) and GSH (1 mM) for approximately 2 h at RT until TCA was added to the final concentration of 10% v/v. Samples were centrifuged and the absorbance of supernatant was measured at 340 nm (Figure 4.10). The intensity of absorbance represents the amount of GS-DNB conjugate formed, higher absorbance means more GS-DNB is present in the sample. GSTP1-1A microsomes were compared against HT1080 microsomes and a purified GSTP1-1A sample. Background (non-enzymatic reaction between GSH and CDNB) was subtracted from all samples. When we compared GSTP1-1A microsomes to HT1080 microsomes the absorbance at 340 nm was almost 4 times higher in sample containing GSTP1-1A microsomes. This is very similar to what was observed with peak areas during HPLC experiment. The result is not surprising and is simply explained by the fact that HT1080 cell line do not express GSTP1-1A inside the ER, therefore there is no GSTP1-1A inside HT1080 microsomes, however there are still endogenous MAPEG enzymes present. Purified GSTP1-1A (500 nM) sample shows the maximum absorbance that could be obtained from given concentration of GSH (1mM) and CDNB (250 μ M) at the given timepoint is approximately 2.5 fold higher than in GSTP1-1A microsomes and 8-10 folds higher than in HT1080 microsomes.

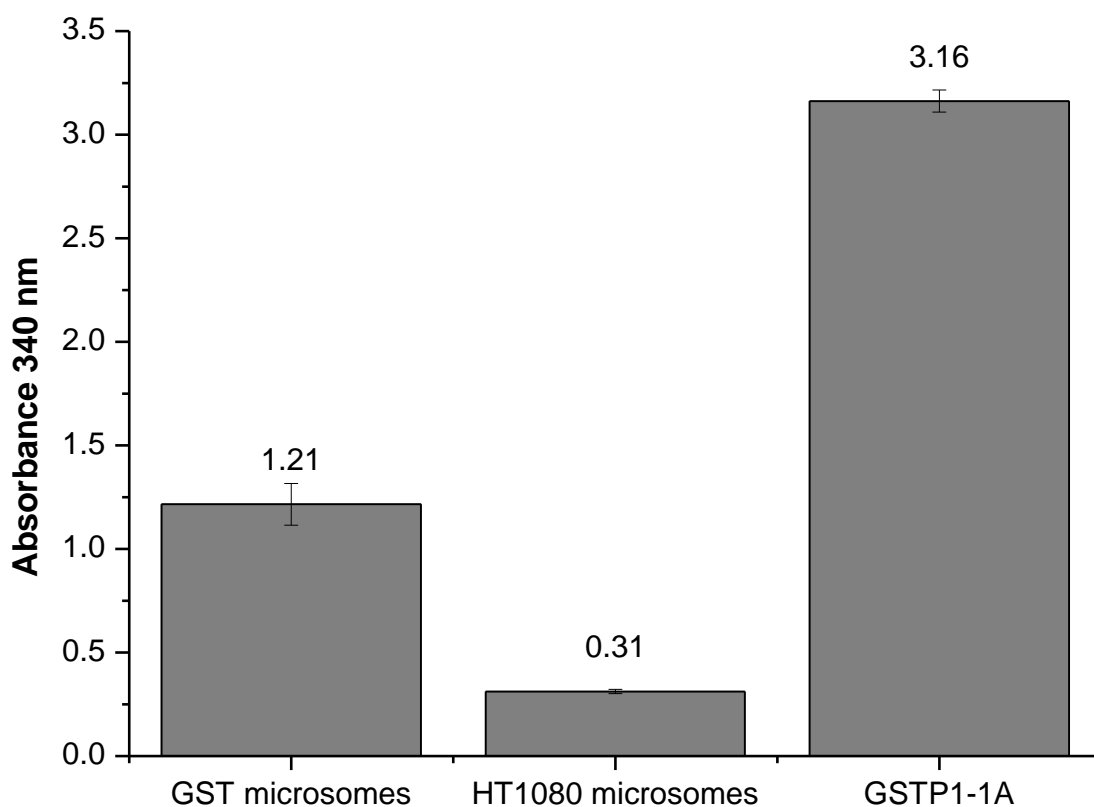


Figure 4.10 Endpoint measurement of GS-DNB conjugate after 2 h incubation. Microsomes treated with GSH (1 mM) and CDNB (250 μ M) were incubated for 2 h at RT and precipitated using TCA. Samples were centrifuged and the absorbance of the supernatant was measured at 340 nm. Average absorbance from 3 independent experiments were plotted on the histogram, the error bars represent standard deviation. Background (non-enzymatic reaction between GSH and CDNB) was subtracted from all samples.

It has been shown that the reaction between GSH and CI-BODIPY catalysed by GSTP1-1A is slower than that with CDNB, however, because the reaction kinetics are not measured in this experiment, CI-BODIPY was also analysed. Microsomes treated with CI-BODIPY (150 nM) and GSH (1 mM) were incubated for 2 hours at RT and precipitated using TCA. Samples were centrifuged and the absorbance of the supernatant was measured at 530 nm (Figure 4.11). Background (non-enzymatic reaction between GSH and CI-BODIPY) was subtracted from all samples.

The results from the CI-BODIPY experiment were very similar to what was observed when using CDNB. 530 nm absorbance from GSTP1-1A microsomes sample was equal to 0.12 ± 0.008 , it is 3.2 times higher than 530 nm absorbance measured in HT1080 microsomes sample (0.03 ± 0.0053). Purified GSTP1-1A (500 nM) sample shows the maximum absorbance (0.31 ± 0.0155) that could be obtained from given concentration of GSH (1mM) and CDNB (250 μ M).

The experiment confirmed the results from HPLC experiment about GSH being transported across microsomal membrane and GSTP1-1A being active inside microsomes.

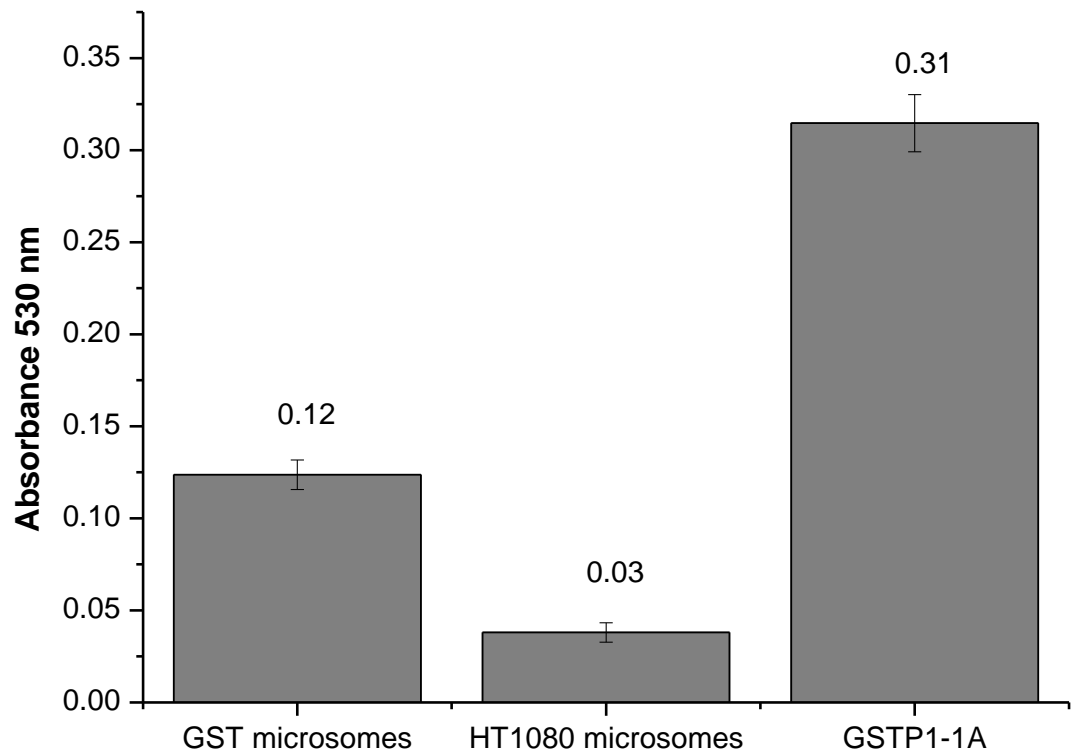


Figure 4.11 Endpoint measurement of GS-BODIPY conjugate after 2 h incubation. Microsomes treated with Cl-BODIPY (150 nM) and GSH (1 mM) were incubated for 2 h at RT and precipitated using TCA. Samples were centrifuged, and the absorbance of the supernatant was measured at 530 nm. Average absorbance from 3 independent experiments were plotted on the histogram, the error bars represent standard deviation. Background (non-enzymatic reaction between GSH and Cl-BODIPY) was subtracted from all samples.

4.3.6 Transport assay – time course

TCA precipitation has proven to be successful in removing the high background noise that was a problem in early attempts to monitor GSH transport. In the previous experiment samples were treated with TCA and end point absorbance was measured. In order to find out more about GSH transport several time points were collected. CDNB (250 μ M) and GSH (1 mM) were added to samples, TCA (10%) was added to each sample after specific time interval, samples were centrifuged, absorbance at 340 nm was measured and collected time points were plotted over time (Figure 4.12). Background (non-enzymatic reaction between GSH and CDNB) was subtracted from all samples. Three sets of samples were used, GSTP1-1A microsomes, permeabilised GSTP1-1A microsomes and HT1080 microsomes.

Compared to other samples the absorbance in HT1080 microsomes sample increased slowly and after 50 minutes reached 0.23, this is the lowest value of all tested samples. The sample containing GSTP1-1A microsomes reached absorbance equal to 0.71 after 50 minutes of incubation and the rate of reaction was higher when compared to HT1080 microsomes. To solubilise the microsomal membrane, which constitutes a barrier for GSH, 0.15% of detergent TWEEN20 was added to one of GSTP1-1A microsomes samples. Permeabilised GSTP1-1A microsomes displayed the highest rate of reaction and reached the highest absorbance of 0.94 after 50 minutes of incubation. Because CI-BODIPY is a poorer substrate for GSTP1-1A, than CDNB, it was not used in this experiment.

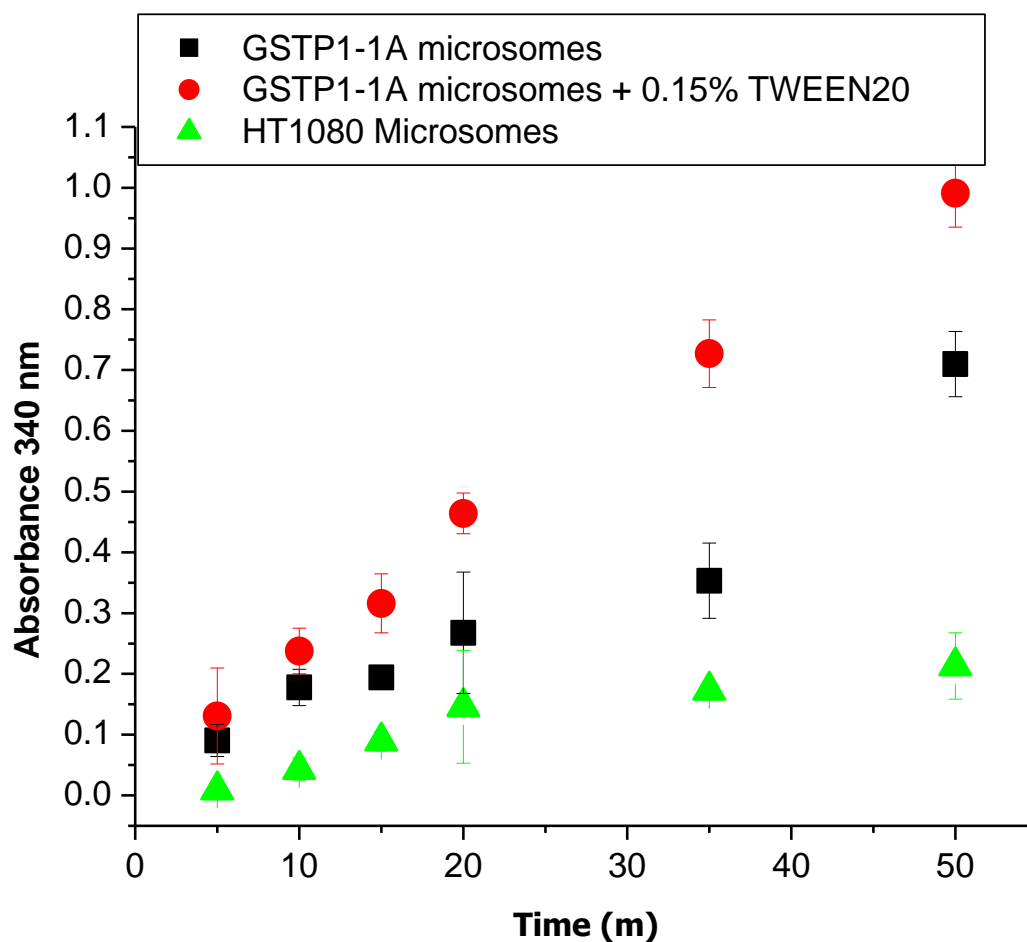


Figure 4.12 GST based assay of GSH transport across microsomal membranes. To assess GSH transport across microsomal membranes CDNB (250 μ M) and GSH (1 mM) were added to the samples, TCA (10%) was added to each sample after specific time interval, samples were centrifuged, absorbance at 340 nm was measured and collected time points were plotted over time. Average absorbance from 3 independent experiments were plotted on the graph, errors bars represent standard deviation. Background (non-enzymatic reaction between GSH and CDNB) was subtracted from all samples.

4.3.7 Inhibition of GSH transport

Inhibition of GSH transport is important validation step needed for further progress of GSH transporter identification. As stated in previous chapter, if a protein is responsible for transporting GSH, it must be possible to inhibit it. However, GSTP1-1A used in the assay has a high specificity for GSH. Therefore, using GSH analogues such as GOH may have direct effect on GSTP1-1A making it impossible to distinguish between the inhibition of a GSH transporter and inhibition of GSTP1-1A. A simple test in which different concentrations of GOH (0.2 mM – 1 mM) were added to GSTP1-1A (250 nM), GSH (1 mM) and CDNB (250 μ M), proved that GOH is in fact an inhibitor of GSTP1-1A activity (Figure 4.13). Both the rate of GSH to CDNB conjugation, as well as total conjugate formation, decreased proportionally to the amount of GOH added.

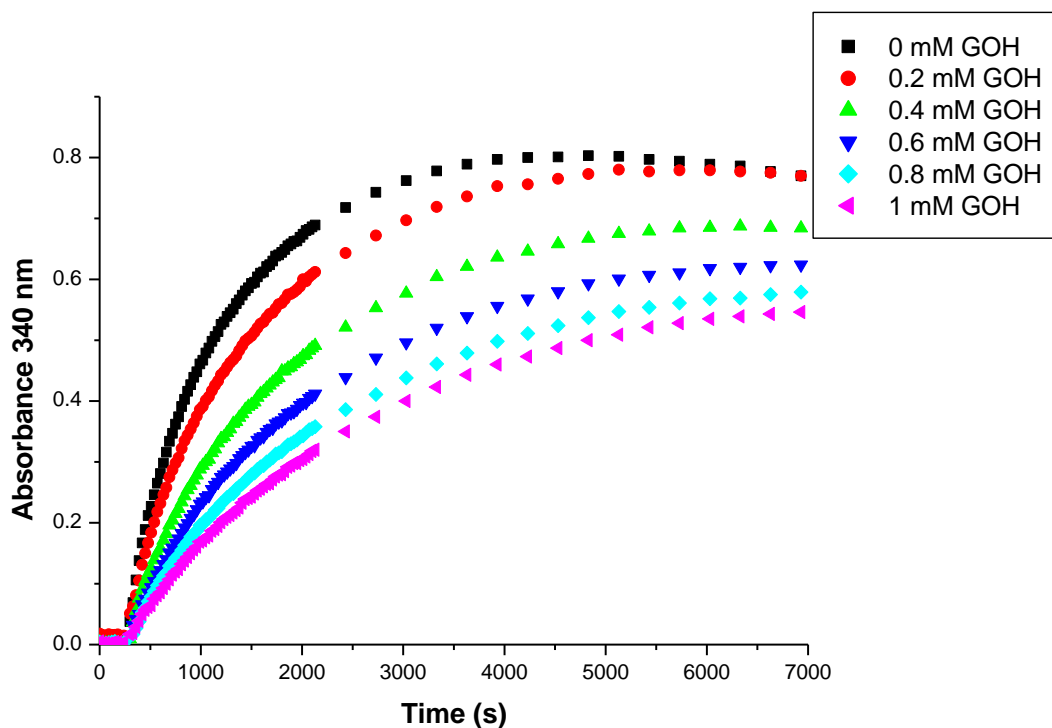


Figure 4.13. GOH inhibition of GSTP1-1A. GSH (1 mM) and CDNB (250 μ M) were added to 250 nM of GST incubated with various concentrations of GOH. The increase in 340 nm absorbance was plotted over time, representing the overall rate GSH to CDNB conjugation reaction. As the concentration of GOH increases the rate of GSH to CDNB conjugation decreases together with the maximum absorbance. Background (non-enzymatic reaction between GSH and CDNB) was subtracted from all samples. The experiment was repeated once.

4.4 Discussion

The GST based GSH transport assay presented in this chapter allows the monitoring of transport of GSH across the ER membrane. GSTP1-1A present inside microsomes can conjugate GSH to various substrates. In our experiments, CDNB and Cl-BODIPY were used as substrates. Overall CDNB turned out to be a better substrate for GSTP1-1A, thus CDNB was the main substrate used. By measuring the total absorbance over time it was possible to link the change in absorbance to GSH transport. Because the product of the conjugation is very stable it should allow further improvement. In one approach HPLC and mass spectrometry were performed to validate GSH transport and to detect the formation of GS-DNB conjugate to prove transport of GSH across the microsomal membrane.

There are a few drawbacks to this approach. First of all the results depend on concentration of GSTP1-1A expressed in HT1080 cell line. The low concentration proved to be an issue with Cl-BODIPY in which it was difficult to monitor kinetics of GSTP1-1A activity. It has been reported that CDNB induces cell permeability at high concentrations (Zou et al., 2002). This report looked at plasma membrane permeability however, high concentrations of CDNB may have an effect on microsomes and, therefore, it is advisable to use low concentrations of CDNB. In the transport assay HT1080 microsomes displayed activity above background. HT1080 microsomes do not contain GSTP1-1A however there are still endogenous MAPEG enzymes associated with ER membrane. These MAPEG enzymes display activity towards CDNB and GST, however, as shown in the experiment the activity is lower compared to GSTP1-1A microsomes (Bresell et al., 2005). Also it might be difficult to find an inhibitor of GSH transport that will affect GST transporter and will not affect GSTP1-1A activity. GOH used in the experiment is a good example of GSH analogue which inhibits GSTP1-1A and, therefore, cannot be used to inhibit GSH transporter, because if a drop in GSTP1-1A will be observed it will be impossible to distinguish between the drop in GSH transport and GSTP1-1A activity, however, GOH could be a good control if we can confirm that GOH is not transported across the microsomal membrane. To avoid confusion and to be able to distinguish between inhibition of GSH transporter and inhibition of GSTP1-1A activity, perhaps more specific inhibitor can be designed.

There are many ways in which the assay can be improved. There are many members of GSTs protein family, each have different specificity for different

substrates. Therefore, trying using different versions of GST might prove to be a better choice than GSTP1-1A used. However, different substrates can also be used. There are plenty of commercially available substrates for GSTs, some of them might be better than CDNB used in the experiment.

Chapter 5

Isolating putative GSH transporters

5.1 Introduction

In the previous two chapters, we focused on developing an assay able to monitor glutathione transport across the ER membrane. Two different approaches have been developed, one that relies on a change in fluorescence ratio of roGFP upon reduction by GSH, the other approach relies on conjugation of GSH to different substrates (CDNB or Cl-BODIPY) and measuring the change in absorbance. Both of these assays have advantages as well as limitations and can complement each other. However, the ultimate goal of the project was to identify the GSH transporter. To do this we decided to focus on the direct identification of a putative transporter.

GSH is an important molecule having crucial roles in many biological processes for example, apoptosis, signal transduction, gene expression, cell proliferation, differentiation and cell metabolism (Sies, 1999). Because glutathione is involved in so many biological processes it is important to maintain its normal homeostasis (Lushchak, 2012). The disturbance in GSH homeostasis has implications in several human diseases, including cancer, neurodegenerative diseases, diseases related to aging, inflammatory, immune and cardiovascular diseases (Lushchak, 2012). Therefore, finding an ER GSH transporter may lead not only to better understanding of GSH homeostasis but possibly also to controlling it, for example by designing an antagonist for GSH transport.

However, to date there is very little known about mammalian GSH transporters, especially the ER GSH transporters. Most of our knowledge comes from studies in yeast (Bachhawat et al., 2013). Multidrug resistance-associated protein (MRP) is a subclass of the ATP-Binding Cassette (ABC) transporter superfamily and has been identified as the first transporter capable of GSH transport (Rebbeer et al., 1998a, Rebbeer et al., 1998b). However, MRP is involved in efflux of GSH in the *Saccharomyces cerevisiae* vacuolar membrane and in the mammalian plasma membrane (Rebbeer et al., 1998a, Rebbeer et al., 1998b). Moreover, low affinity for GSH and primary efflux of GSH conjugates together with broad substrate specificity makes MRP not the best example of a GSH transporter (Ballatori et al., 2005). *Saccharomyces cerevisiae* Hgt1p/Opt1p was the first high affinity and high specificity GSH transporter to be discovered (Bourbouloux et al., 2000). Hgt1p/Opt1p is a member of a new oligopeptide transporter (OPT) family and has no mammalian homologue (Yen et al., 2001). Because of the importance of GSH

transport and our lack of understanding, there is an increasing demand in the field to identify a high affinity and high specificity mammalian GSH transporter (Bachhawat et al., 2013).

Knowing very little about the structure of mammalian ER GSH transporter, we decided to try to isolate the transporter relying on its properties of binding GSH. We aimed to isolate candidates based upon protein binding to modified ligand or/and substrate. Usually the ligand or/and substrate contains a unique feature that allows it to separate together with the protein of interest. This technique has been used widely in the biomolecular field to help identify many proteins with known ligands or known interactions with other proteins, the protein(s) are then further characterised by mass spectrometry (Gavin et al., 2002, Ho et al., 2002). We assumed that at some point during transport GSH must be with direct contact, and possibly bind, to the ER GSH transporter. Therefore, we decided to use GSH as an affinity ligand.

5.2 Glutathione Sepharose beads approach

In the previous chapter, a simple experiment using glutathione Sepharose beads was performed to determine whether GSTP1-1A present inside ER was able to bind GSH and thus being active and correctly folded. Although glutathione Sepharose beads are usually used to purify GSTs or GST tagged proteins, this experiment inspired us to use it in a different way.

Any putative GSH transporter should bind to glutathione Sepharose, but because GSH is immobilised, it cannot be transported. It is possible that the interaction between GSH transporter and GSH will be strong enough that the transporter will remain attached to GSH even after solubilisation of microsomes, allowing us to elute it with excess GSH (Figure 5.1). This approach was chosen as a starting point in our attempts to identify the mammalian ER GSH transporter because of its simplicity.

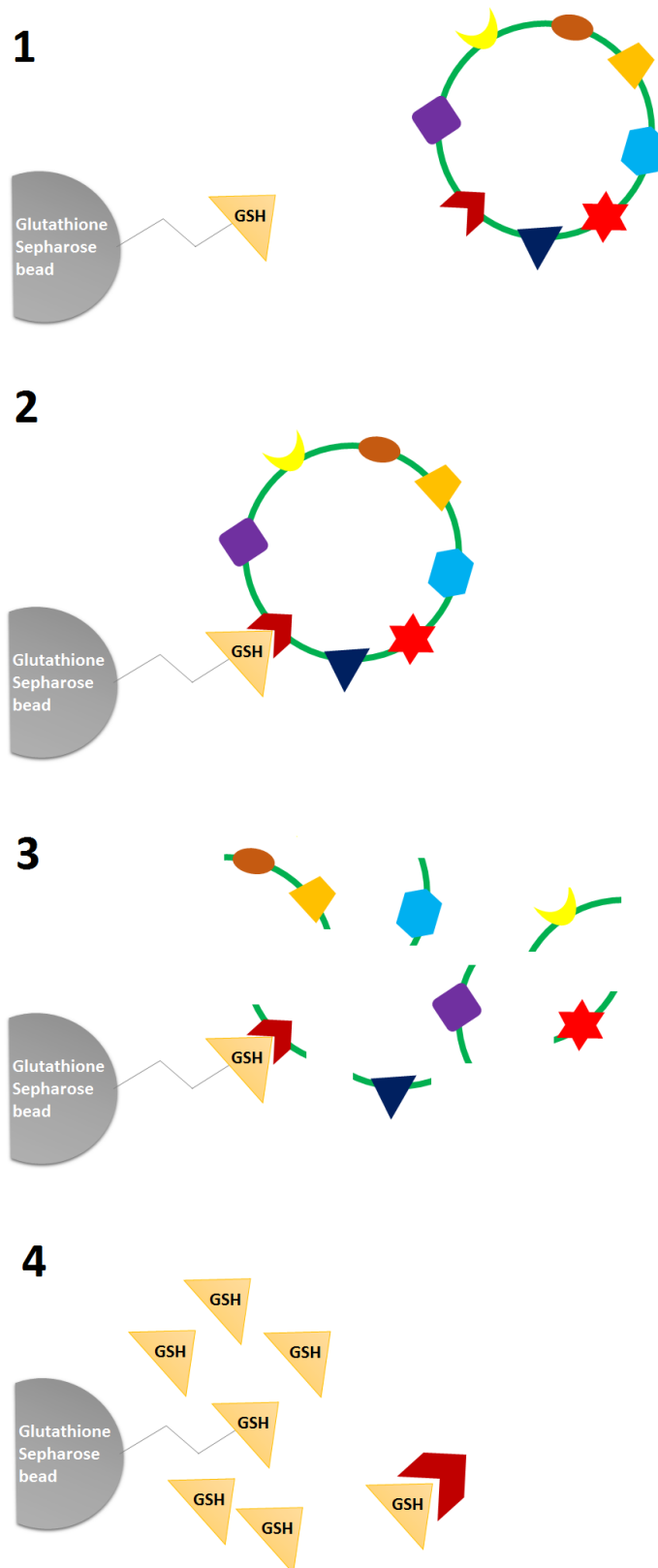


Figure 5.1 Isolation of putative glutathione transporter. 1) Rat liver microsomes incubated with glutathione Sepharose beads. **2)** Glutathione transporter binds to GSH linked to Sepharose beads. **3)** Rat liver microsomes solubilised with detergent. GSH transporter remains bound to GSH linked to Sepharose beads. **4)** Unbound proteins are washed away and GSH transporter is eluted with excess of GSH.

5.2.1 Isolating GSH interacting proteins using glutathione Sepharose beads

As a preliminary experiment, rat liver microsomes (RLM) were solubilised prior to the incubation with glutathione Sepharose beads to see if it was possible to isolate bound proteins. Glutathione Sepharose beads were washed once with PBS, samples were eluted with high concentration of GSH (50 mM) and analysed on 12.5% SDS-PAGE followed by silver staining (Figure 5.2). There are many clear bands present in the eluted sample (lane 1) especially around 25 kDa and above 46 kDa. The unbound fraction (lane 2) did not show any difference to total sample present in lane 3, which was not subjected to incubation with glutathione Sepharose beads.

This simple experiment has suggested that it is possible to isolate proteins based on their properties of binding GSH and using glutathione Sepharose beads. To develop the approach further we increased the number of washes and several controls were added.

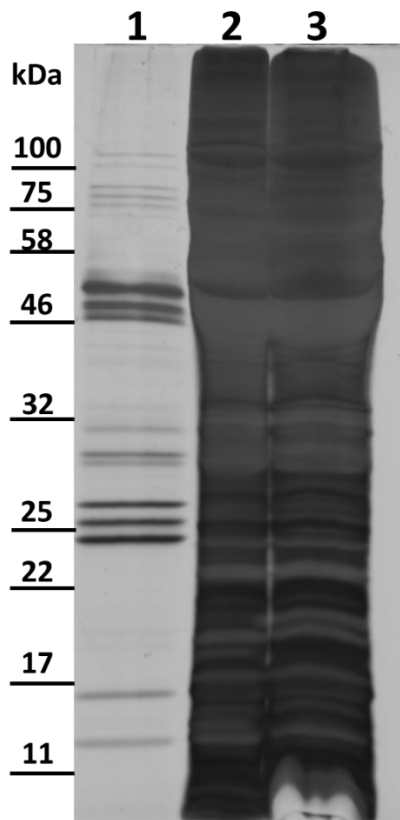


Figure 5.2 RLM proteins bound to glutathione Sepharose beads analysed on 12.5% SDS-PAGE followed by silver staining. RLM were solubilised with Triton X-100 (0.2%) and incubated with glutathione Sepharose beads for 30 min at RT. Samples were gently washed once with PBS, eluted with GSH and analysed on 12.5% SDS-PAGE. Lane 1 – RLM proteins bound to glutathione Sepharose beads eluted with GSH. Lane 2 – Unbound proteins. Lane 3 – Total RLM proteins.

RLM were incubated with glutathione Sepharose beads for approximately 30 minutes prior to the addition Triton X-100 (0.2%) to solubilise the microsomes. GSH transporter is most likely a membrane protein, therefore by solubilising the membrane while the transporter is still interacting with GSH may help to preserve its native conformation, and of course separate it from the membrane. Glutathione Sepharose beads were washed three times with TrisHCl buffer (50 mM, pH 7.5), samples were then eluted with high concentration of GSH (50 mM) and analysed on 12.5% SDS-PAGE followed by silver staining (Figure 5.3). Sepharose beads were used as a control to show if there is any nonspecific binding between proteins and Sepharose. GSTP1-A1 has been shown to interact with glutathione Sepharose beads, therefore a mixture of GSTP1-A1 and annexin was used as a positive control to make sure the approach is working. Annexin is a phospholipid and calcium binding protein and does not interact with GSH, thus only GSTP1-A1 should be present in the elute when incubated with glutathione Sepharose beads (Gerke and Moss, 2002). When run on SDS-PAGE, GST/annexin mix shows two strong bands (lane 5), the lower band, around 27 kDa, corresponds to GSTP1-A1, while upper band, around 30 kDa, corresponds to annexin. To make sure the proteins will interact with GSH attached to Sepharose beads GST/annexin mix was incubated with glutathione Sepharose beads and treated the same way as the microsome sample. When eluted with GSH (50 mM), only the band corresponding to GSTP1-A1 was present on the SDS-PAGE gel (lane 3). GST/annexin flow through was also analysed by SDS-PAGE (lane 4) and resulted in both GSTP1-A1 and annexin present on the gel, possibly due the oversaturation of the beads. The sample eluted with GSH following incubation of microsomes with glutathione Sepharose beads (lane 1) shows a distinct banding pattern with several strong bands present above 46 kDa and around 25 kDa. This is a very similar to the pattern seen previously in samples solubilised prior to incubation with beads. The sample incubated with Sepharose beads and eluted with GSH (lane 2) shows similar pattern. Most of the bands seen in lane 2 seem to correspond to the bands seen in sample incubated with glutathione Sepharose beads, however, some of the bands present in lane 1 above 46 kDa and around 25 kDa are not present. This suggest that these bands may be specific GSH binding proteins. Both flow through samples (lanes 6 and 7) look very alike and is hard to distinguish any specific differences between them.

The results strongly indicate that there is some specific binding between proteins and glutathione Sepharose beads, especially around 25 kDa and above 46 kDa, therefore bands present in these areas were cut from the gel and proteins were analysed by mass spectrometry.

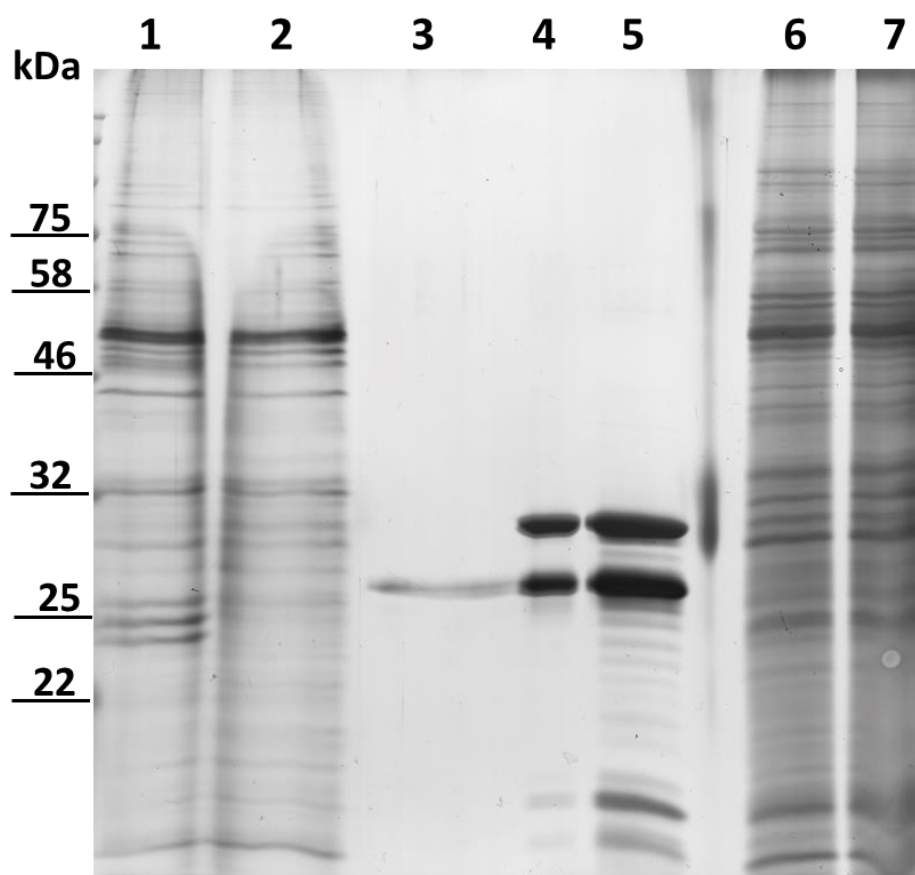


Figure 5.3 RLM proteins bound to glutathione Sepharose beads and Sepharose beads analysed on 12.5% SDS-PAGE followed by silver staining. RLM were incubated with glutathione Sepharose beads for 30 min at RT and solubilised with Triton X-100 (0.2%). Samples were gently washed three times with TrisHCl buffer (50 mM, pH 7.5), eluted with GSH (50 mM) and analysed on 12.5% SDS-PAGE. Lane 1 – RLM proteins bound to glutathione Sepharose beads eluted with GSH. Lane 2 - RLM proteins bound to Sepharose beads eluted with GSH. Lane 3 – GST/annexin eluted with GSH. Lane 4 – GST/annexin flow through. Lane 5 – GST/annexin mix. Lane 6 – Flow through glutathione Sepharose beads. Lane 7 – Flow through Sepharose beads.

5.2.2 Protein identification by mass spectrometry

The band pattern above 46 kDa and around 25 kDa showed the most differences between glutathione Sepharose beads and Sepharose beads therefore these areas were chosen for protein identification by mass spectrometry. The areas around 46 kDa and 25 kDa from both lanes were sent to the proteomics facility at the University of St Andrews and were prepared according to their recommendations.

In order to identify proteins bound specifically to GSH, proteins identified from glutathione Sepharose beads were compared to proteins obtained from Sepharose beads, this allowed us to eliminate the background proteins bound non-specifically to Sepharose. If the protein was present in both samples (glutathione Sepharose and Sepharose) it was considered to bind non-specifically to Sepharose beads and marked red in the table. However, if the protein was present only in glutathione Sepharose sample it was considered GSH binding protein and was marked green in the table. Any contaminations present in the samples were marked orange in the table. There were several proteins binding specifically to GSH in the area around 25 kDa (Table 5.1). All of the proteins around 25 – 26 kDa in size belonged to the GST family. The GST proteins had high number of matches and sequences, together with high emPAI number, thus confirming that identification of these proteins is not a coincidence and that these proteins bind to GSH (Table 5.1). There were only two positive matches in proteins isolated from 46 kDa gel fragment, elongation factor 1 gamma and alpha (Table 5.2). A fraction of the remaining eluted sample was also sent for protein identification by mass spectrometry to check if there any proteins present that were not detected by silver staining. All the proteins which were positively identified as binding to GSH, in the elute sample, belong to GST family (Table 5.3).

The results of the experiment have demonstrated that this approach works and can be used to isolate GSH binding proteins. However, it was not possible to identify a putative GSH transporter using this approach. There might be several reasons it was not possible to isolate GSH transporter. Perhaps the interaction between GSH and the GSH transporter was not strong enough, therefore we decided to improve the approach.

Table 5.1. Mass spectrometry identification of proteins in gel fragment around 25 kDa. Green – GSH binding proteins, Red – Background, Orange - contamination

Score	Mass	Matches	Sequences	emPAI	Description
1034	25857	33	18	57.54	glutathione S-transferase Mu 2 [Rattus norvegicus]
1019	25858	35	17	57.54	Chain A, Crystal Structures Of Class Mu Chimeric Gst Isoenzymes M1-2 And M2-1
976	26049	30	14	26.16	rCG29047, isoform CRA_b [Rattus norvegicus] Chain A, First-sphere And Second-sphere Electrostatic Effects In The Active Site Of A Class
941	25921	30	14	26.54	Mu Glutathione Transferase
571	25835	17	9	4.29	glutathione S-transferase Yb-3 [Rattus norvegicus]
276	25781	9	5	2.05	glutathione S-transferase Mu 6 [Rattus norvegicus]
480	25687	23	10	5.46	PREDICTED: glutathione S-transferase alpha-1 isoform X1 [Rattus norvegicus]
411	25360	18	10	5.62	glutathione S-transferase alpha-3 [Rattus norvegicus] RecName: Full=Glutathione S-transferase alpha-2; AltName: Full=GST 1b-1b; AltName:
394	25657	19	10	5.46	Full=GST A2-2; AltName: Full=Glutathione S-transferase Ya-2; Short=GST Ya2
105	26876	7	5	1.44	rCG25753, isoform CRA_b [Rattus norvegicus] RecName: Full=Membrane-associated progesterone receptor component 1; AltName:
344	21699	10	6	2.75	Full=25-DX; AltName: Full=Acidic 25 kDa protein; AltName: Full=Ventral midline antigen; Short=VEMA
65	17402	2	2	0.73	progesterone receptor membrane component 2, isoform CRA_c [Rattus norvegicus]
310	56699	11	10	1.34	keratin, type I cytoskeletal 10 [Rattus norvegicus]
304	52936	9	7	0.89	keratin, type I cytoskeletal 14 [Rattus norvegicus]
266	48378	9	7	1.01	keratin, type I cytoskeletal 17 [Rattus norvegicus]
223	37932	8	6	1.14	PREDICTED: keratin, type I cytoskeletal 42 isoform X1 [Rattus norvegicus]
145	51001	3	3	0.33	PREDICTED: keratin, type I cytoskeletal 16 isoform X1 [Rattus norvegicus] RecName: Full=Keratin, type II cytoskeletal 1; AltName: Full=Cytokeratin-1; Short=CK-1;
293	65190	8	6	0.56	AltName: Full=Keratin-1; Short=K1; AltName: Full=Type-II keratin Kb1

Table 5.2 Mass spectrometry identification of proteins in gel fragment around 46 kDa. Green – GSH binding proteins, Red – Background, Orange – contamination

Score	Mass	Matches	Sequences	emPAI	Description
1054	52719	44	25	11.54	epoxide hydrolase 1 precursor [Rattus norvegicus]
598	25516	28	14	22.33	epoxide hydrolase 1, microsomal, isoform CRA_a [Rattus norvegicus]
976	51171	23	14	3.43	ATP synthase beta subunit, partial [Rattus norvegicus]
971	50371	32	16	3.53	elongation factor 1-gamma [Rattus norvegicus]
737	49093	22	9	1.39	dolichyl-diphosphooligosaccharide--protein glycosyltransferase 48 kDa subunit precursor [Rattus norvegicus]
643	50460	20	10	1.57	elongation factor-1 alpha [Rattus norvegicus]
534	61055	21	11	1.36	UDP-glucuronosyltransferase 2B17 precursor [Rattus norvegicus]
459	61068	17	10	1.18	UDP-glucuronosyltransferase 2B37 precursor [Rattus norvegicus]
451	61032	18	10	1.18	PREDICTED: UDP-glucuronosyltransferase 2B17 isoform X1 [Rattus norvegicus]
449	61117	19	11	1.36	unnamed protein product [Rattus norvegicus]
362	61066	15	8	0.87	RecName: Full=UDP-glucuronosyltransferase 2B37; Short=UDPGT 2B37; AltName: Full=17-beta-hydroxysteroid-specific UDPGT; AltName: Full=UDP-glucuronosyltransferase R-21; Short=UDPGTr-21; AltName: Full=UDPGTr-5; Flags: Precursor
210	31802	9	7	1.83	PREDICTED: UDP-glucuronosyltransferase 2B17-like [Rattus norvegicus]
188	61459	9	8	0.86	RecName: Full=UDP-glucuronosyltransferase 2B2; Short=UDPGT 2B2; AltName: Full=3-hydroxyandrogen-specific UDPGT; AltName: Full=RLUG23; AltName: Full=UDPGTr-4; Flags: Precursor
167	61125	8	7	0.73	PREDICTED: UDP-glucuronosyltransferase 2B37 isoform X1 [Rattus norvegicus]
80	61455	5	5	0.47	UDP-glucuronosyltransferase [Rattus norvegicus]
34	60720	2	2	0.17	RecName: Full=UDP-glucuronosyltransferase 1-6; Short=UDPGT 1-6; Short=UGT1*6; Short=UGT1-06; Short=UGT1.6; AltName: Full=A1; AltName: Full=P-nitrophenol-specific UDPGT; AltName: Full=UDP-glucuronosyltransferase 1A6; Short=UGT1A6; Flags: Precursor

Table 5.3 Mass spectrometry identification of eluted proteins. Green – GSH binding proteins, Red – Background, Orange - contamination

Score	Mass	Matches	Sequences	emPAI	Description
1655	25686	50	12	8.38	glutathione S-transferase Mu 2 [Rattus norvegicus]
1482	25687	48	11	8.38	Chain A, Crystal Structures Of Class Mu Chimeric Gst Isoenzymes M1-2 And M2-1
1448	25669	45	10	6.79	glutathione S-transferase (EC 2.5.1.18) [Rattus norvegicus]
1435	25878	46	10	6.65	rCG29047, isoform CRA_b [Rattus norvegicus]
389	25234	11	4	1.14	glutathione S-transferase mu 3 [Rattus norvegicus]
449	11685	7	2	1.24	60S acidic ribosomal protein P2 [Rattus norvegicus]
361	56470	16	7	0.82	keratin, type I cytoskeletal 10 [Rattus norvegicus]
133	48840	6	3	0.34	keratin, type I cytoskeletal 15 [Rattus norvegicus] RecName: Full=Keratin, type II cytoskeletal 1; AltName: Full=Cytokeratin-1; Short=CK-1; AltName: Full=Keratin-1; Short=K1; AltName: Full=Type-II keratin Kb1
351	64791	11	4	0.35	Full=Keratin-1; Short=K1; AltName: Full=Type-II keratin Kb1
339	60272	10	3	0.27	PREDICTED: keratin, type II cytoskeletal 6A-like isoform X4 [Rattus norvegicus]
262	61889	8	4	0.37	keratin, type II cytoskeletal 5 [Rattus norvegicus]
136	74442	5	4	0.3	PREDICTED: keratin, type II cytoskeletal 2 epidermal isoform X1 [Rattus norvegicus] RecName: Full=Glutathione S-transferase alpha-2; AltName: Full=GST 1b-1b; AltName: Full=GST A2-2; AltName: Full=Glutathione S-transferase Ya-2; Short=GST Ya2
334	25543	18	6	2.08	AltName: Full=Glutathione S-transferase alpha-2; Short=GST Ya2
306	25573	18	6	2.08	PREDICTED: glutathione S-transferase alpha-1 isoform X1 [Rattus norvegicus]
223	25303	16	5	1.57	glutathione S-transferase alpha-3 [Rattus norvegicus]

5.3 Mts-Aft-Biotin photocrosslinking

One of the reasons why the previous attempts of isolating the ER GSH transporter, using glutathione Sepharose beads, were not able to isolate the transporter could be that the binding of GSH to the transporter is not strong enough and could be lost during washes. To strengthen the interaction between GSH and GSH transporter a photocrosslinking method was used. Mts-Aft-Biotin (2-[N2-(4-azido-2,3,5,6-tetrafluorobenzoyl)-N6-(6-biotinamidocaproyl)-Llysiny] ethyl methanethiosulfonate) was used as the crosslinking molecule. Mts-Aft-Biotin has three unique features making it a useful crosslinker for our studies, it contains a thiol reactive group (sulfhydryl reactive methanethiosulfonate (Mts)), photocrosslinking group (tetrafluorophenyl azide (Aft)) and biotin (Figure 5.4).

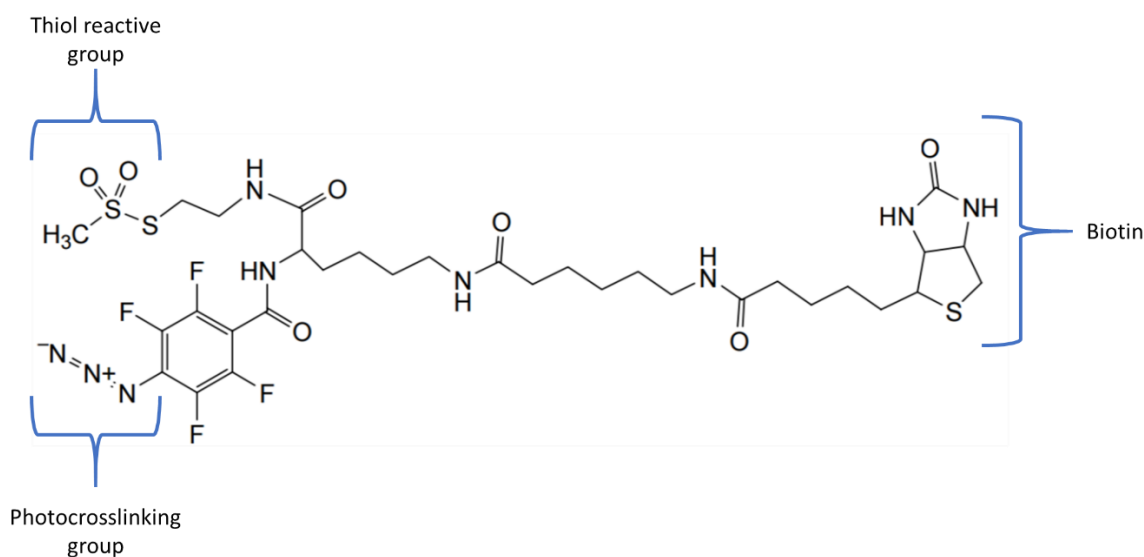


Figure 5.4 Chemical structure of (2-[N2-(4-azido-2,3,5,6-tetrafluorobenzoyl)-N6-(6-biotinamidocaproyl)-Llysiny]ethyl methanethiosulfonate) with 3 specific features marked: thiol reactive group, photocrosslinking group and biotin.

By attaching GSH to Mts-Aft-Biotin (GS-Mts-Aft-Biotin), through methanethiosulfonate group (Mts) (Figure 5.5a), it might be possible to create a covalent bond between GS-Mts-Aft-Biotin and GSH binding proteins, including the GSH transporter, allowing its isolation using streptavidin beads (Figure 5.5b). Once the Mts group reacts with a free thiol a disulfide bond forms that can be later broken with a reducing agent (Figure 5.5b).

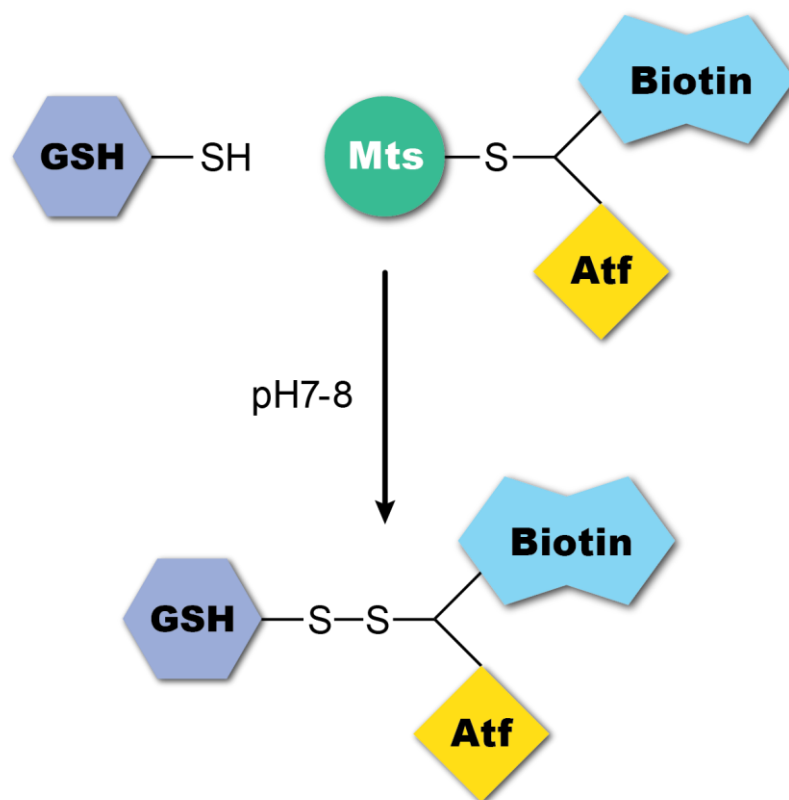


Figure 5.5a. Attachment of GSH to Mts-Aft-Biotin crosslinker. GSH can be attached to Mts-Aft-Biotin through methanethiosulfonate group (Mts).

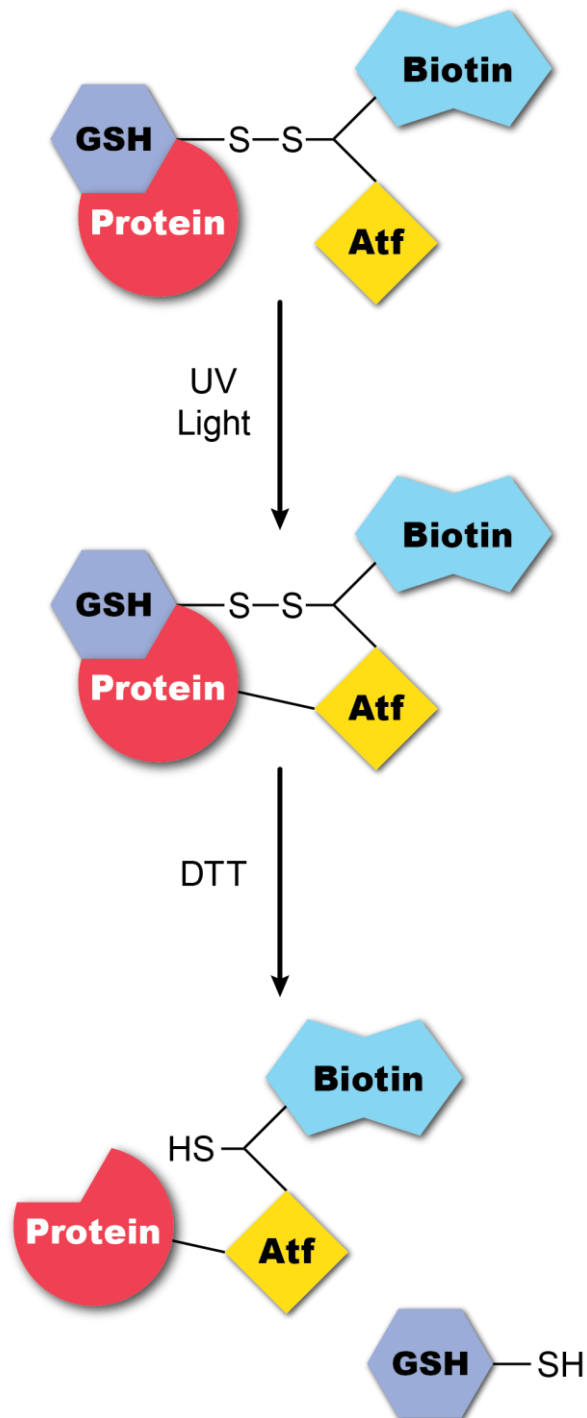


Figure 5.5b. The mechanism of action of GS-Mts-Aft-Biotin. Proteins are able to bind GSH attached to Mts-Aft-Biotin through SH- group of Mts motif. Upon exposing to the UV light, the GSH binding protein is crosslinked to Aft motif of the crosslinker. DTT is used to break down disulfide bond between GSH and the crosslinker. Proteins are then isolated using streptavidin beads.

Mts-Aft-Biotin was mixed with GSH in 1:2 ratio to make sure all Mts-Aft-Biotin will react with the excess of GSH. Next GS-Mts-Aft-Biotin was purified by HPLC and collected as fractions (Figure 5.6). GSH is eluted early in the gradient due to its polarity, the first two small peaks (a and b) seen in HPLC chromatograph corresponds to GSH and GSSG. It was assumed the last peak (e) in HPLC chromatograph corresponds to remaining Mts-Aft-Biotin, however the identity of 2 very sharp peaks (c and d) is unknown. To identify the two unknown peaks and to make sure the last peak corresponds to Mts-Aft-Biotin all the fractions containing mentioned peaks were analysed by mass spectrometry (Figure 5.7). Analysis of the first sharp peak (c) revealed molecular mass of 1041 g/mol (Figure 5.7a). After analysing what the mass can correspond to, it appeared that 1041 g/mol corresponds to GS-Mts-Aft-Biotin with the photocrosslinking group removed. This suggested that GS-Mts-Aft-Biotin is very light sensitive and should be kept in the dark all the time. The mass of the compound present in the second peak (d) equals to 1067 g/mol, this is the exact mass of GS-Mts-Aft-Biotin (Figure 5.7b). The analysis of the last peak (e) revealed a mass of 736 g/mol (Figure 5.7c). This was very surprising but the mass of 736 g/mol is most likely corresponding to Mts-Aft-Biotin with both thiol reactive group and photocrosslinking group removed. The fractions corresponded to second sharp peak (d) were combined, freeze dried and used in the next experiment.

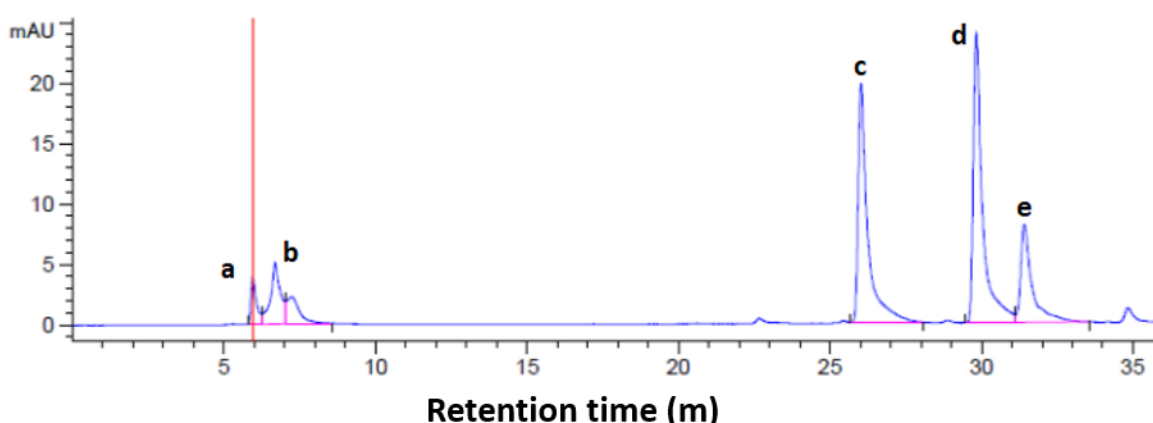
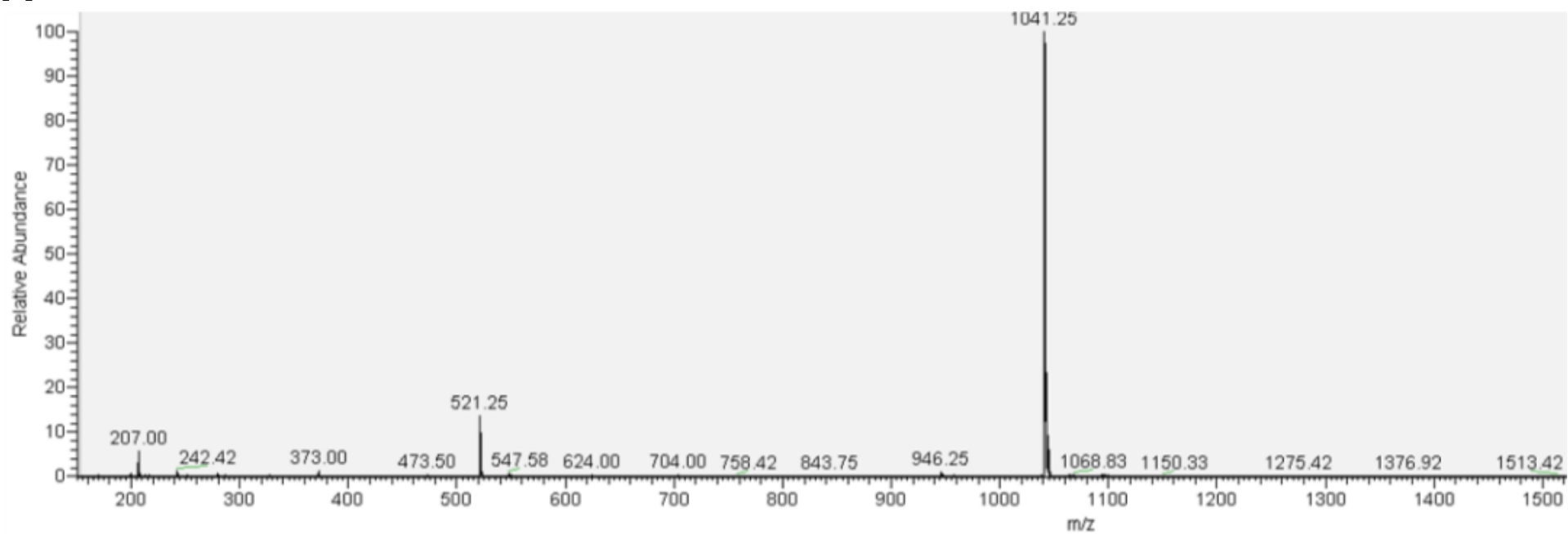
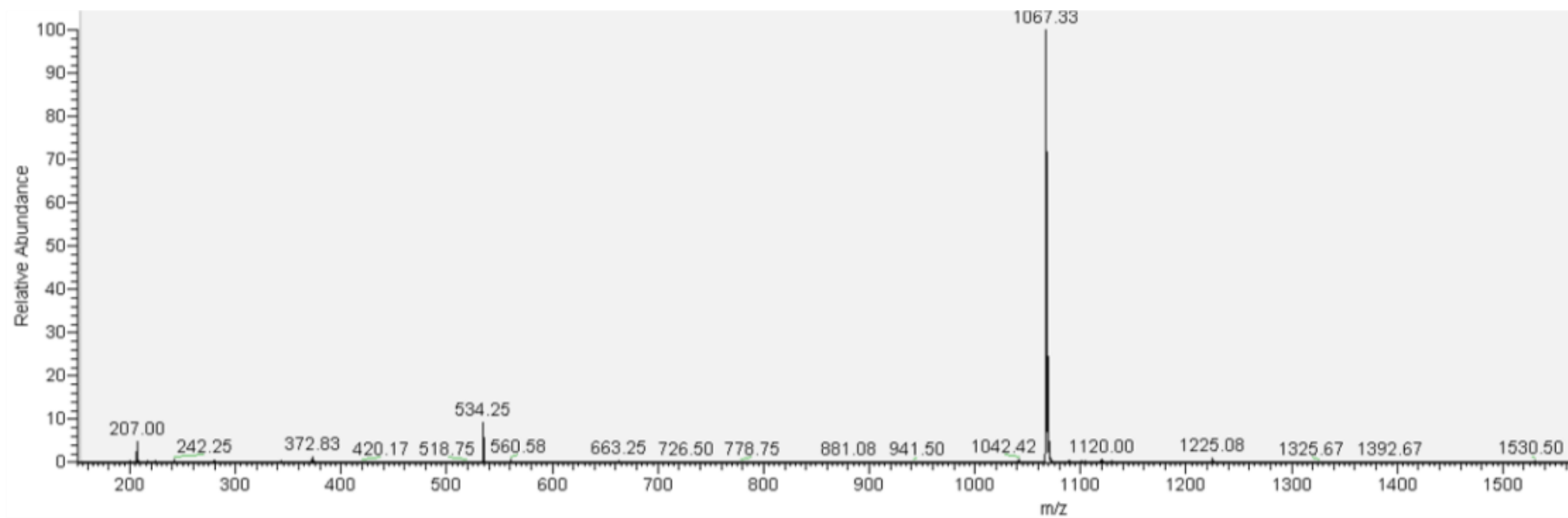


Figure 5.6 HPLC chromatogram of GSH conjugation to Mts-Aft-Biotin. GS-Mts-Aft-Biotin was analysed by high-pressure liquid chromatography (HPLC) carried out on a Shimadzu instrument with a Phenomenex Gemini C18 column (110 Å, 5 µm, 250×4.60 mm). Peaks: **a** – GSH, **b** – GSSG, **c** and **d** – unknown, **e** - Mts-Aft-Biotin.

A

B

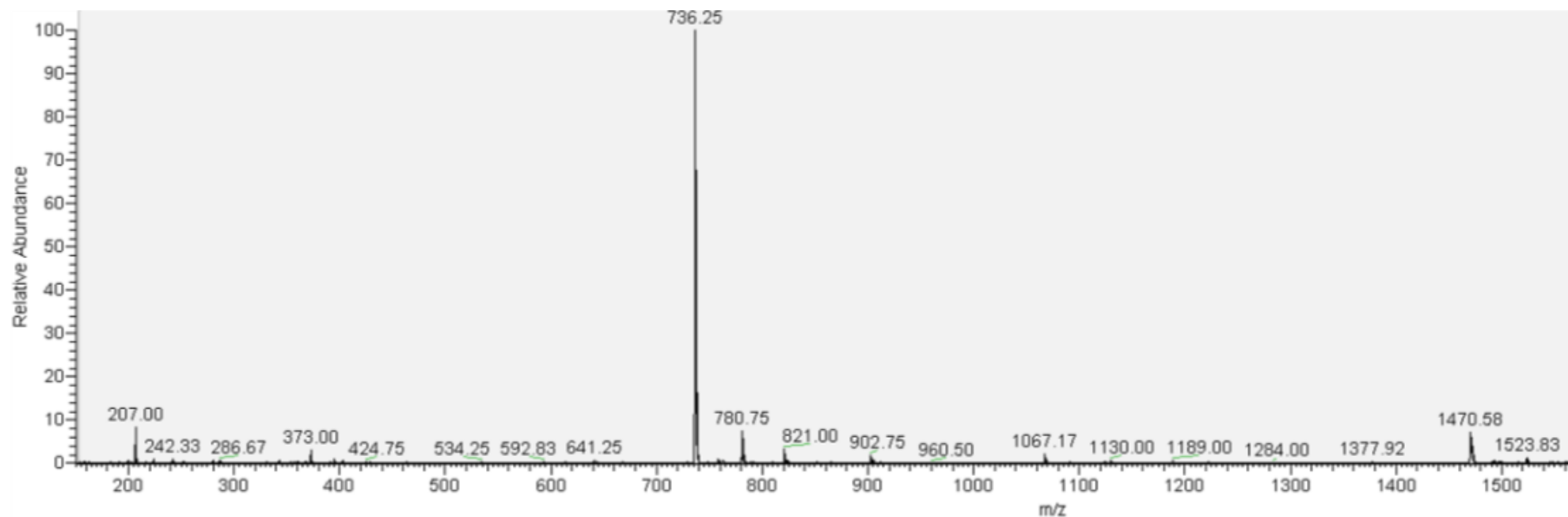
C

Figure 5.7 Mass spectrometry analysis of HPLC peaks from GSH to Mts-Aft-Biotin conjugation. The conjugated product was analysed using liquid chromatography mass spectrometry (LCMS) carried out on a Thermo Scientific LCQ Fleet quadrupole mass spectrometer. **A)** GS-Mts-Aft-Biotin with photocrosslinking group removed (1041 g/mol). **B)** GS-Mts-Aft-Biotin (1067 g/mol). **C)** Mts-Aft-Biotin with both thiol reactive group (Mts) and photocrosslinking group (Aft) removed (736 g/mol).

GS-Mts-Aft-Biotin was added to RLM and incubated for 30 min at room temperature and then exposed to UV for 5 min. Triton X-100 (0.2%) was added to the RLM prior to incubation with streptavidin beads for 30 min at RT. RLM were washed 3 times with Tris buffer (50 mM, pH 7.5), and eluted with biotin (20 mM) before the samples were analysed on 12.5% SDS-PAGE and silver stained (Figure 5.8, lane 1). Mts-Aft-Biotin was also incubated with cysteine in order to block the SH- group of the crosslinker and used as a control to monitor non-specific interactions to GSH (Figure 5.8, lane 2). Both samples displayed several bands indicating protein binding but there were no differences between microsomes incubated with GS-Mts-Aft-Biotin and microsomes incubated with blocked crosslinker. The reason for not seeing any difference between both samples could be explained by a high background of non-specific interactions with the beads.

The interaction between biotin and streptavidin is very strong therefore more washes could be used to reduce the background. To further reduce background 1 mM DTT was added to washes to break the disulfide bond between the crosslinker and free thiols. GS-Mts-Aft-Biotin was added to RLM and incubated for 30 min at RT and then exposed to UV for 5 minutes. Microsomes were centrifuged and washed 3 times with PBS in order to remove any residual crosslinker. Microsomes were solubilised in 500 µl of IP buffer and incubated with streptavidin beads for 30 minutes at RT. After incubation microsomes were washed 3 times with RIPA buffer containing 1 mM DTT and eluted with 20 mM biotin. In addition to cysteine blocked crosslinker two more controls were used. One control included UV inactivated Mts-Aft-Biotin, the crosslinker was exposed to UV for 15 minutes in order to inactivate photoreactive crosslinking group. The second control included Mts-Aft-Biotin without any modifications. All the samples were analysed on 12.5% SDS-PAGE followed by silver staining (Figure 5.9). The sample containing GS-Mts-Aft-Biotin (lane 1) contained only a few proteins that bound to the beads. There are more proteins present in the cysteine blocked Mts-Aft-Biotin sample (lane 2), all the proteins present are also more abundant when compared to the GS-Mts-Aft-Biotin sample. All the proteins present in GS-Mts-Aft-Biotin sample are also present in cysteine blocked sample, indicating there are no GSH specific proteins present. It was expected that microsomes incubated with UV treated Mts-Aft-Biotin would not result in any proteins present on the gel, however, there are no differences in the banding pattern between UV treated Mts-Aft-Biotin (lane 3) and Mts-Aft-Biotin (lane 4).

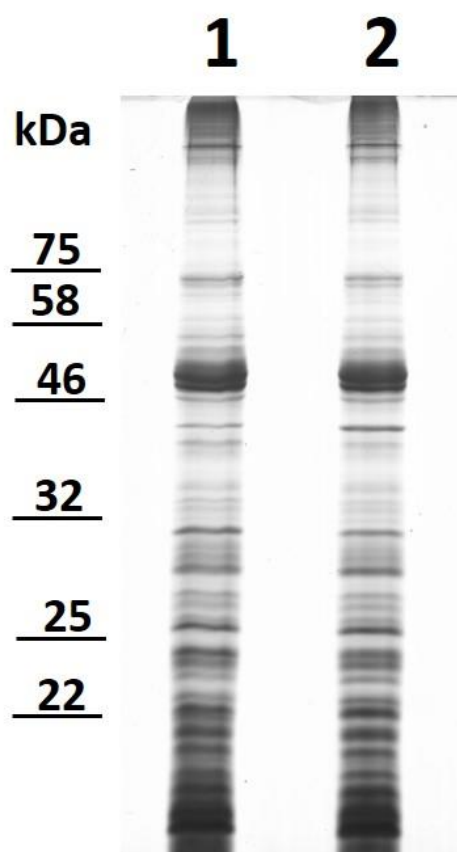


Figure 5.8 Silver stain analysis of proteins crosslinked and biotinylated by GS-Mts-Aft-Biotin. RLM were incubated with GS-Mts-Aft-Biotin, exposed to UV for 5 min, solubilised by Triton X-100 (0.2%) and incubated with streptavidin beads. Samples were eluted with biotin, separated on 12.5% SDS-PAGE and silver stained. Lane 1 – RLM proteins crosslinked using GS-Mts-Aft-Biotin. Lane 2 – RLM proteins crosslinked using Mts-Aft-Biotin with SH- group blocked by cysteine.

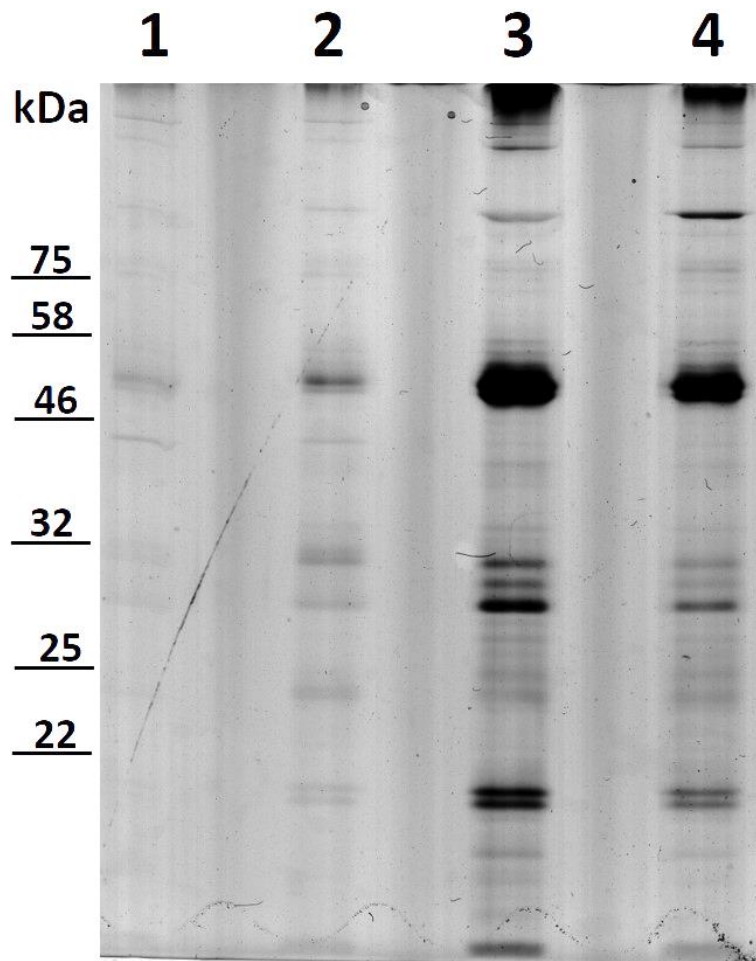


Figure 5.9 Silver staining analysis of proteins crosslinked and biotinylated by GS-Mts-Aft-Biotin. RLM were incubated with GS-Mts-Aft-Biotin, exposed to UV for 5 min. Microsomes were centrifuged and washed 3 times with PBS, prior to solubilisation in 500 μ l of IP buffer and incubation with streptavidin beads for 30 min at RT. After incubation microsomes were washed 3 times with RIPA buffer containing 1 mM DTT. Samples were eluted with Biotin, separated on 12.5% SDS-PAGE and stained using silver staining method. Lane 1 – RLM proteins crosslinked using GS-Mts-Aft-Biotin. Lane 2 – RLM proteins crosslinked using Mts-Aft-Biotin with SH- group blocked by cysteine. Lane 3 - RLM proteins crosslinked using UV inactivated Mts-Aft-Biotin. Lane 4 - RLM proteins crosslinked using Mts-Aft-Biotin.

It is possible that silver staining is not sensitive enough to detect all the proteins isolated using GS-Mts-Aft-Biotin therefore analysing biotinylated proteins by Western blot using fluorescent streptavidin may allow for detection of proteins that have not been seen by silver staining. The remaining eluted samples were analysed on 12.5% SDS-PAGE and subjected to Western blotting (Figure 5.10). Western blotting confirmed the results seen by silver staining. Sample containing GS-Mts-Aft-Biotin (lane 1) displayed even fewer proteins than in silver staining analysis. Sample treated with cysteine blocked Mts-Aft-Biotin sample (lane 2), contained more proteins than the GS-Mts-Aft-Biotin treated sample. There are no differences between UV treated Mts-Aft-Biotin sample (lane 3) and Mts-Aft-Biotin sample (lane 4). The results indicating that there are no GSH specific proteins isolated using GS-Mts-Aft-Biotin.

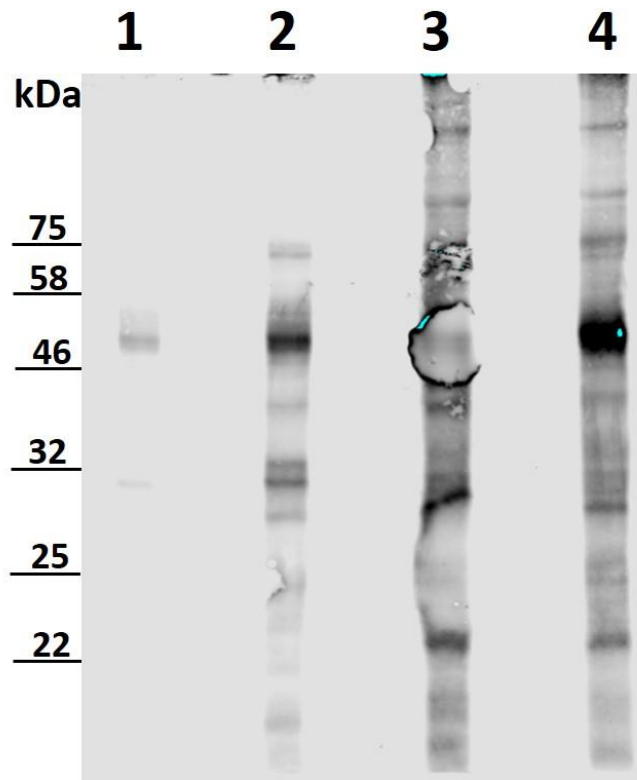


Figure 5.10 Western blot analysis of biotinylated protein. RLM were incubated with GS-Mts-Aft-Biotin, exposed to UV for 5 min. Microsomes were centrifuged and washed 3 times with PBS, prior to solubilisation in 500 μ l of IP buffer and incubation with streptavidin beads for 30 minutes at RT. After incubation microsomes were washed 3 times with RIPA buffer containing 1 mM DTT. Samples were eluted with Biotin, separated on 12.5% SDS-PAGE and subjected to Western blotting. Streptavidin 800 (1:10000) for 40 min. Lane 1 – RLM proteins crosslinked using GS-Mts-Aft-Biotin. Lane 2 – RLM proteins crosslinked using Mts-Aft-Biotin with SH-group blocked by cysteine. Lane 3 - RLM proteins crosslinked using UV inactivated Mts-Aft-Biotin. Lane 4 - RLM proteins crosslinked using Mts-Aft-Biotin.

5.4 Discussion

Mammalian glutathione transporters are still not fully understood and some of the research regarding GSH transporters remain unclear. Finding the mammalian GSH transporter(s) is important to gain a better understanding, and possibly control, of redox balance within the cell. We focused on identifying the mammalian ER GSH transporter(s) using microsomes to mimic the ER environment separated from the rest of the cell. We were able to selectively separate proteins interacting with GSH. This might be the initial step in identifying the mammalian ER GSH transporter(s) in the future.

Our first approach relied on affinity purification with glutathione Sepharose beads and further identification of proteins interacting specifically with GSH. All of the proteins identified belong to the GST family. As glutathione Sepharose beads are commonly used to purify GST-tagged proteins (Frangioni and Neel, 1993) these results were not surprising. Members of GSTs are well characterised (Sheehan et al., 2001) and it is unlikely that any of these proteins are involved in GSH transport. Initially elongation factor 1 appeared to be a surprising match, however, elongation factor 1 gamma also displays GST activity, therefore this explains why it binds to GSH (Koonin et al., 1994, Tshabalala et al., 2016) and possibly excludes its role in GSH transport. It is intriguing that except GSTs no other proteins were identified as binding specifically to GSH. It is very likely that the amount of various GSTs present in microsomes is higher than the amount of other proteins that could potentially bind to GSH (including GSH transporters), maybe there are not enough of them to be detected by mass spectrometry, therefore other proteins cannot compete for GSH binding and only GSTs are isolated using this method.

The other approach using Mts-Aft-Biotin, a photoactivated crosslinker, seemed to offer an improvement over glutathione Sepharose beads because it can form a covalent bond with substrate proteins, making it easier to isolate them. By attaching GSH to Mts-Aft-Biotin, and creating GS-Mts-Aft-Biotin, we expected to be able to isolate more GSH binding proteins than using the previous glutathione Sepharose approach, thanks to the crosslinking properties of the compound. However, when compared to the control, Mts-Aft-Biotin incubated with cysteine, in order to block a sulfhydryl reactive methanethiosulfonate group, no GSH specific proteins were present on both SDS-PAGE and Western blot. This raises the questions why there

was a distinct banding pattern present using glutathione Sepharose beads but not when using GS-Mts-Aft-Biotin. This can possibly be explained by the differences in how GSH is attached to Sepharose and Mts-Aft-Biotin. In the case of glutathione Sepharose beads, GSH is linked to Sepharose by 12-atom spacer arm, this give proteins a lot of space to interact with GSH. In the case of GS-Mts-Aft-Biotin, GSH is in close proximity to a bulky tetrafluorophenyl azide group (Aft), this may not allow enough space for proteins to interact with GSH. The fact that previously seen GSTs were not present while using GS-Mts-Aft-Biotin seems to confirm this hypothesis. UV inactivated Mts-Aft-Biotin was also an important control in determining if there are any strong interactions between Mts-Aft-Biotin and proteins that are not related to crosslinking. However, there were a lot of interactions between proteins and UV inactivated Mts-Aft-Biotin, possibly because Mts-Aft-Biotin was not fully inactivated. Perhaps longer exposure to UV will be needed to completely inactivate Mts-Aft-Biotin.

Both approaches did not succeed in isolating and identifying the ER GSH transporter, however, they may give an important clue on how to tackle the problem of identifying the ER GSH transporter in the future. In both approaches, glutathione Sepharose beads and GS-Mts-Aft-Biotin, GSH is immobilised by central SH group, this may impair GSH binding to some proteins as SH group may be involved. The binding mechanism of GSTs to GSH involves carboxylate group of the γ -glutamyl side chain and it does not require an active SH group, that is why it was possible to isolate GSTs proteins (Adang et al., 1990), however, the binding mechanism of GSH transporter might be different than the mechanism seen in GSTs and may require an active SH group. Therefore, in the future another method might be used, one that does not involve inactivation of SH group, and this may produce different results. However, compared to other methods of alteration of GSH structure, attaching GSH to other molecules via its SH group is the easiest and fastest way to modify GSH, thus it is often the first approach to try in many GSH related research. GSH is a small molecule so it is challenging and difficult to modify GSH in any way without substantially changing its structure.

Chapter 6

Discussion

6.1 Discussion

Glutathione (GSH) is the most abundant non-protein thiol compound present in mammalian/eukaryotic cells. GSH is essential in many cellular processes including protection against reactive oxygen species (ROS), detoxification of xenobiotics, disulfide bond formation, immune function, apoptosis, modulation of cell proliferation, and is also a key determinant of redox signalling (Sies, 1999). The synthesis of GSH takes place in the cytoplasm, from where GSH is transported to other parts of the cell, however this process is poorly understood. All of the currently used methods to assess/investigate GSH transport including, filtration, radiolabelled GSH and light scattering methods, have their limitations (Banhegyi et al., 1999, Csala et al., 2001, Csala et al., 2003). In our research we developed two novel assays able to monitor GSH transport into the ER.

Both assays rely on the same principle of selective permeability of biological membranes but use different reporting proteins/molecules. Biological membranes allow some molecules to pass freely, through diffusion, while other molecules need to be transported in order to cross the membrane. Microsomes used in both assays mimic the ER membrane and the ER environment. The first assay developed uses roGFP as a reporter protein allowing the transport of GSH across the ER membrane to be monitored, as well as the transport of other reducing agents, or any compounds able to alter the redox status of roGFP. Because roGFP responds to changes in the redox status of the environment the transport of GSH, and other reducing agents, can be measured over time, revealing the kinetics of transport for each reducing agent. By using solubilised microsomes as a control this approach allowed us to demonstrate that the ER membrane is indeed a barrier for GSH transport. It was also shown that GSH requires a transporter to cross the ER membrane and is not able to simply diffuse across the lipid bilayer.

The other assay also monitors the transport of GSH across the ER membrane but uses the properties of GSTs to conjugate GSH to variety of different substrates. GSTP1-1A present inside the microsomes has a high specificity for GSH however, the specificity for substrates vary, and therefore the selection of an appropriate substrate for this assay is crucial. In the experiment CDNB and Cl-BODIPY were used as substrates. As GSH was transported across the ER membrane, more conjugated product was formed. By measuring the increase in the absorbance

or/and fluorescence it was possible to estimate the rate of GSH transport. Because the conjugated product is very stable it is possible to use it for further analysis. In our case the conjugated product was analysed by HPLC and mass spectrometry to prove the transport of GSH across the ER membrane.

These two assays can greatly contribute to redox biology research and help us understand the redox control in the ER, therefore researchers are the main group of people who will benefit from our findings. Both assays can be used to investigate how GSH transport into the ER can be inhibited, or stimulated, perhaps by different GSH analogues as showed in the case of GOH and N-ethylsuccinimido-S-glutathione (ESG). Moreover, roGFP based transport assay can also be used to investigate transport of other reducing agents into the ER and how they affect the redox status of the ER.

The assays developed could also find an application in medical research. The inability of proteins to fold correctly may results in cell death and the accumulation of misfolded proteins, which could potentially lead to diseases like Alzheimer's disease or Parkinson's disease. The oxidative protein folding taking place in the ER is an essential process required for proper folding of secretory proteins, for example insulin. The inability of insulin to fold correctly and make native disulfide bonds results in a loss of secretion of insulin. By controlling GSH transport into the ER it might be possible to regulate redox status of the ER, for example making it more oxidative by inhibit GSH transport or more reduced by increasing GSH transport. This could possibly maintain an optimised redox balance in the ER and consequently lead to milder manifestation of the diseases caused by misfolded proteins. Our assays can be used to monitor this process, therefore, pharmaceutical companies could also be interested in our assays.

Despite relying on similar principles, both assays are quite different, with their own pros and cons, providing different information about GSH transport and redox state of the ER. The roGFP based assay is more dynamic than GST based assay and informs about the overall redox state in the ER. It is important to remember that reduction of roGFP may not be caused directly by GSH, the addition of GSH into the microsomes may reduce other proteins which in turn reduce roGFP. Because roGFP can easily be reduced or oxidised it is possible to perform more complex experiments related to the redox state of the ER. In the roGFP assay we used oxidised roGFP to measure the transport of GSH, however, reduced roGFP can be

used to monitor the transport of GSSG, or other reducing/oxidising agents. The roGFP assay requires fluorescence measurement, therefore, roGFP based assay requires a more advanced equipment that may not be accessible, for example fluorometer or in our case plate reader with fluorescence modules adjusted for the roGFP fluorescence wavelengths.

GST based assay is more direct than roGFP assay because there is direct interaction between GSTP1-A1 and GSH. GST based assays result in stable product formation therefore the conjugated product might be analysed by many different methods/techniques, depending on the substrate used. However, the choice of substrate is crucial for GST based assay. Different substrates for GST may offer different advantages but may also have limitations, for example GSTP1-A1 reacted very fast with CDNB and GSH however it required TCA precipitation as an additional step. Cl-BODIPY offered no background but the rate of reaction with GSH was very slow. Some substrates for GST based assays may be membrane impermeable or may cross membrane slower than GSH, making them inappropriate for the assay. Compared to roGFP assay, GST based assay can only be used to monitor the transport of GSH but not GSSG.

Some research suggested that GSSG is also transported into the ER and is important to maintain reduced environment of the cytosol, however, there is very little known about this process (Hwang et al., 1992, Banhegyi et al., 1999). This project focused exclusively on GSH transport into the ER, however, as mentioned previously the roGFP assay can easily be used to monitor transport of GSSG into the ER.

One of the very interesting results came from GOH and ESG, a glutathione analogue and alkylated GSH, inhibition of GSH transport. Because of the structural similarities GOH was synthesised to act as an inhibitor for GSH transport but the results obtained were opposite to what was expected. It was expected that GOH and ESG will act as competitive inhibitors and slow down GSH transport, instead both seemed to accelerate GSH transport. It is not known how GOH and ESG accelerate GSH transport and if GSH transporter is involved in the process, however, it led us to suggest that the GSH transport can be regulated using GSH analogues. Unfortunately, the effect of GOH and ESG on GSH transport could not be assessed using GST based transport assay as they both inhibit GST.

There have been few assays described previously to study GSH transport into the ER. G. Bánhegyi et al. (Banhegyi et al., 1999) used light scattering and rapid sedimentation to assess GSH transport into microsomes, M. Csala et al. (Csala et al., 2001) attempted to measure GSH transport into microsomes using rapid filtration. Although all of these techniques can provide information about GSH transport, however, they are not GSH specific nor GSH sensitive. Comparing to the methods mentioned above our assays show more versatility also more specificity and sensitivity for GSH, especially in GST based assay.

The main goal of the project was to identify the mammalian ER GSH transporter, we tried to achieve this by isolating a GSH transporter using GSH as affinity ligand. The first approach used glutathione Sepharose beads was successful in separation of several proteins interacting specifically with GSH. However, after mass spectrometry identification of isolated proteins we found that all of them belong to GST family. Despite not being able to identify the GSH transporter using glutathione Sepharose beads this approach proved to be capable of isolating other GSH binding proteins, therefore, we believed that the approach of using GSH as affinity ligand has a potential of helping us identify GSH transporter but needs to be improved. Using Mts-Aft-Biotin with GSH attached to its thiol reactive group (Mts motif) seemed to be a good way of improving glutathione Sepharose beads, mostly because of the ability of Mts-Aft-Biotin to create a strong covalent bond upon exposure to the UV light. However, Mts-Aft-Biotin did not bring us any closer in identifying the GSH transporter. It is possible that proteins are not able to bind GSH attached to Mts-Aft-Biotin due to GSH being in very close proximity to bulky photocrosslinking group (Aft motif).

In the future the problem with Mts-Aft-Biotin could be solved by synthesising our own Mts-Aft-Biotin with a spacer introduced between Mts and Aft motifs. However, the attachment of GSH to Mts-Aft-Biotin and glutathione Sepharose beads may also be considered to be important. We do not know the interaction between GSH and the transporter, but it is possible that SH- group is involved in the transport process. GSH is attached to both glutathione Sepharose beads and Mts-Aft-Biotin by its SH- group, this type of attachment makes GSH lose one of its most important properties. The loss of SH- group may make GSH transporter unable to recognise and bind GSH. Therefore, attaching GSH to Mts-Aft-Biotin without involving SH- group may result in more protein binding to GSH.

In the future we are planning to continue searching for the mammalian GSH ER transporter using modified version of Mts-Aft-Biotin (or possibly another crosslinker) with longer linker. Upon successful identification of GSH transporter both transport assays can be used to validate the results. Because microsomes for the assays are prepared from stable cell lines it might possible to remove the transporter, using siRNA knockdown or CRISPR knockout, from the cells before preparation of microsomes and then perform the transport assays. Once the transporter will be identified we will try to gain knowledge about its mechanism of action, which consequently will allow us to design an inhibitor for GSH transport. We are also planning to investigate the transport of GSSG in more detail. At some point we want to validate the finding of other research groups including M. Csala claim of ryanodine receptor type 1 (RyR1) being involved in the ER GSH transport of sarcoplasmic reticulum (Csala et al., 2001) and the recent claim of AJ Ponsoero about GSH transport into the ER by Sec61 (Ponsoero et al., 2017).

In the project we developed two assays able to monitor GSH transport across the ER membrane. Both assays rely on the same principle of selective membrane permeability however provide slightly different information about GSH transport and can complement each other. We also attempted to identify the mammalian GSH ER transporter by isolating GSH binding proteins using GSH as an affinity ligand. We were able to isolate several GSH binding proteins using glutathione Sepharose beads, however, they all belong to the GST family. We tried to improve this approach using Mts-Aft-Biotin, a photo crosslinking agent, however we were not able to isolate any specific GSH binding proteins. We plan to improve and continue this approach in the future.

References

- Adang, A. E. P., Brussee, J., Vandergen, A. & Mulder, G. J. 1990. The glutathione-binding site in glutathione s-transferases - investigation of the cysteinyl, glycy and gamma-glutamyl domains. *Biochemical Journal*, 269, 47-54.
- Aliosman, F., Akande, O., Antoun, G., Mao, J. X. & Buolamwini, J. 1997. Molecular cloning, characterization, and expression in *Escherichia coli* of full-length cDNAs of three human glutathione S-transferase Pi gene variants - Evidence for differential catalytic activity of the encoded proteins. *Journal of Biological Chemistry*, 272, 10004-10012.
- Anfinsen, C. B., Haber, E., Sela, M. & White, F. H. 1961. Kinetics of formation of native ribonuclease during oxidation of reduced polypeptide chain. *Proceedings of the National Academy of Sciences of the United States of America*, 47, 1309-1314.
- Appenzeller-Herzog, C. 2011. Glutathione- and non-glutathione-based oxidant control in the endoplasmic reticulum. *Journal of Cell Science*, 124, 847-855.
- Appenzeller-Herzog, C., Riemer, J., Christensen, B., Sorensen, E. S. & Ellgaard, L. 2008. A novel disulphide switch mechanism in Ero1 alpha balances ER oxidation in human cells. *Embo Journal*, 27, 2977-2987.
- Appenzeller-Herzog, C., Riemer, J., Zito, E., Chin, K.-T., Ron, D., Spiess, M. & Ellgaard, L. 2010. Disulphide production by Ero1 alpha-PDI relay is rapid and effectively regulated. *Embo Journal*, 29, 3318-3329.
- Auchere, F., Santos, R., Planamente, S., Lesuisse, E. & Camadro, J.-M. 2008. Glutathione-dependent redox status of frataxin-deficient cells in a yeast model of Friedreich's ataxia. *Human Molecular Genetics*, 17, 2790-2802.
- Bachhawat, A. K., Thakur, A., Kaur, J. & Zulkifli, M. 2013. Glutathione transporters. *Biochimica Et Biophysica Acta-General Subjects*, 1830, 3154-3164.
- Ballatori, N., Hammond, C. L., Cunningham, J. B., Krance, S. M. & Marchan, R. 2005. Molecular mechanisms of reduced glutathione transport: role of the MRP/CFTR/ABCC and OATP/SLC21A families of membrane proteins. *Toxicology and Applied Pharmacology*, 204, 238-255.
- Ballatori, N., Krance, S. M., Notenboom, S., Shi, S., Tieu, K. & Hammond, C. L. 2009. Glutathione dysregulation and the etiology and progression of human diseases. *Biological Chemistry*, 390, 191-214.
- Banhegyi, G., Lusini, L., Puskas, F., Rossi, R., Fulceri, R., Braun, L., Mile, V., Di Simplicio, P., Mandl, J. & Benedetti, A. 1999. Preferential transport of glutathione versus glutathione disulfide in rat liver microsomal vesicles. *Journal of Biological Chemistry*, 274, 12213-12216.
- Birk, J., Meyer, M., Aller, I., Hansen, H. G., Odermatt, A., Dick, T. P., Meyer, A. J. & Appenzeller-Herzog, C. 2013. Endoplasmic reticulum: reduced and oxidized glutathione revisited. *Journal of Cell Science*, 126, 1604-1617.
- Borst, P. & Elferink, R. O. 2002. Mammalian ABC transporters in health and disease. *Annual Review of Biochemistry*, 71, 537-592.

- Bourbouloux, A., Shahi, P., Chakladar, A., Delrot, S. & Bachhawat, A. H. 2000. Hgt1p, a high affinity glutathione transporter from the yeast *Saccharomyces cerevisiae*. *Journal of Biological Chemistry*, 275, 13259-13265.
- Braakman, I. & Bulleid, N. J. 2011. Protein Folding and Modification in the Mammalian Endoplasmic Reticulum. *Annual Review of Biochemistry*, Vol 80, 80, 71-99.
- Brechbuhl, H. M., Gould, N., Kachadourian, R., Riekhof, W. R., Voelker, D. R. & Day, B. J. 2010. Glutathione Transport Is a Unique Function of the ATP-binding Cassette Protein ABCG2. *Journal of Biological Chemistry*, 285, 16582-16587.
- Bresell, A., Weinander, R., Lundqvist, G., Raza, H., Shimoji, M., Sun, T. H., Balk, L., Wiklund, R., Eriksson, J., Jansson, C., Persson, B., Jakobsson, P. J. & Morgenstern, R. 2005. Bioinformatic and enzymatic characterization of the MAPEG superfamily. *Febs Journal*, 272, 1688-1703.
- Bulleid, N. J. & Ellgaard, L. 2011. Multiple ways to make disulfides. *Trends in Biochemical Sciences*, 36, 485-492.
- Burchell, A., Hume, R. & Burchell, B. 1988. A new microtechnique for the analysis of the human hepatic-microsomal glucose-6-phosphatase system. *Clinica Chimica Acta*, 173, 183-192.
- Cabibbo, A., Pagani, M., Fabbri, M., Rocchi, M., Farmery, M. R., Bulleid, N. J. & Sitia, R. 2000. ERO1-L, a human protein that favors disulfide bond formation in the endoplasmic reticulum. *Journal of Biological Chemistry*, 275, 4827-4833.
- Chakravarthi, S., Jessop, C. E. & Bulleid, N. J. 2006. The role of glutathione in disulphide bond formation and endoplasmic-reticulum-generated oxidative stress. *Embo Reports*, 7, 271-275.
- Chen, Z. F., Putt, D. A. & Lash, L. H. 2000. Enrichment and functional reconstitution of glutathione transport activity from rabbit kidney mitochondria: Further evidence for the role of the dicarboxylate and 2-oxoglutarate carriers in mitochondrial glutathione transport. *Archives of Biochemistry and Biophysics*, 373, 193-202.
- Claude, A. 1941. Particulate components of cytoplasm. *Cold Spring Harbor Symposia on Quantitative Biology*, 9, 263-271.
- Cleland, W. W. 1964. Dithiothreitol new protective reagent for sh groups. *Biochemistry*, 3, 480.
- Cline, D. J., Redding, S. E., Brohawn, S. G., Psathas, J. N., Schneider, J. P. & Thorpe, C. 2004. New water-soluble phosphines as reductants of peptide and protein disulfide bonds: Reactivity and membrane permeability. *Biochemistry*, 43, 15195-15203.
- Coin, I., Beyermann, M. & Bienert, M. 2007. Solid-phase peptide synthesis: from standard procedures to the synthesis of difficult sequences. *Nature Protocols*, 2, 3247-3256.
- Collet, J. F. & Bardwell, J. C. 2005. Oxidative protein folding in bacteria. *Endoplasmic Reticulum: A Metabolic Compartment*, 363, 75-80.
- Cooper, G. M. 2000. *The Cell, A Molecular Approach*, Sinauer Associates.
- Csala, M., Fulceri, R., Mandl, J., Benedetti, A. & Banhegyi, G. 2001. Ryanodine receptor channel-dependent glutathione transport in the sarcoplasmic reticulum of skeletal muscle. *Biochemical and Biophysical Research Communications*, 287, 696-700.

- Csala, M., Fulceri, R., Mandl, J., Benedetti, A. & Banhegyi, G. 2003. Glutathione transport in the endo/sarcoplasmic reticulum (Reprinted from Thiol Metabolism and Redox Regulation of Cellular Functions). *Biofactors*, 17, 27-35.
- Cummings, B. S., Angeles, R., Mccauley, R. B. & Lash, L. H. 2000. Role of voltage-dependent anion channels in glutathione transport into yeast mitochondria. *Biochemical and Biophysical Research Communications*, 276, 940-944.
- Cuozzo, J. W. & Kaiser, C. A. 1999. Competition between glutathione and protein thiols for disulphide-bond formation. *Nature Cell Biology*, 1, 130-135.
- Dalle-Donne, I., Rossi, R., Colombo, G., Giustarini, D. & Milzani, A. 2009. Protein S-glutathionylation: a regulatory device from bacteria to humans. *Trends in Biochemical Sciences*, 34, 85-96.
- Delic, M., Mattanovich, D. & Gasser, B. 2010. Monitoring intracellular redox conditions in the endoplasmic reticulum of living yeasts (vol 306, pg 61, 2010). *Fems Microbiology Letters*, 309, 114-114.
- Dickinson, D. A. & Forman, H. J. 2002. Glutathione in defense and signaling - Lessons from a small thiol. *Cell Signaling, Transcription, and Translation as Therapeutic Targets*, 973, 488-504.
- Dobson, C. M. 2003. Protein folding and misfolding. *Nature*, 426, 884-890.
- Dooley, C. T., Dore, T. M., Hanson, G. T., Jackson, W. C., Remington, S. J. & Tsien, R. Y. 2004. Imaging dynamic redox changes in mammalian cells with green fluorescent protein indicators. *Journal of Biological Chemistry*, 279, 22284-22293.
- Eaton, W. A., Munoz, V., Thompson, P. A., Henry, E. R. & Hofrichter, J. 1998. Kinetics and dynamics of loops, alpha-helices, beta-hairpins, and fast-folding proteins. *Accounts of Chemical Research*, 31, 745-753.
- Ebeling, W., Hennrich, N., Klockow, M., Metz, H., Orth, H. D. & Lang, H. 1974. Proteinase k from tritirachium-album limber. *European Journal of Biochemistry*, 47, 91-97.
- Ellis, R. J. 2001. Macromolecular crowding: an important but neglected aspect of the intracellular environment. *Current Opinion in Structural Biology*, 11, 114-119.
- Fang, Y. Z., Yang, S. & Wu, G. Y. 2002. Free radicals, antioxidants, and nutrition. *Nutrition*, 18, 872-879.
- Fernandes, A. P. & Holmgren, A. 2004. Glutaredoxins: Glutathione-dependent redox enzymes with functions far beyond a simple thioredoxin backup system. *Antioxidants & Redox Signaling*, 6, 63-74.
- Forman, H. J., Zhang, H. & Rinna, A. 2009. Glutathione: Overview of its protective roles, measurement, and biosynthesis. *Molecular Aspects of Medicine*, 30, 1-12.
- Frand, A. R. & Kaiser, C. A. 1998. The ERO1 gene of yeast is required for oxidation of protein dithiols in the endoplasmic reticulum. *Molecular Cell*, 1, 161-170.
- Frangioni, J. V. & Neel, B. G. 1993. Solubilization and purification of enzymatically active glutathione-s-transferase (PGEX) fusion proteins. *Analytical Biochemistry*, 210, 179-187.

- Garcia-Ruiz, C. & Fernandez-Checa, J. C. 2006. Mitochondrial glutathione: Hepatocellular survival-death switch. *Journal of Gastroenterology and Hepatology*, 21, S3-S6.
- Gavin, A. C., Bosche, M., Krause, R., Grandi, P., Marzioch, M., Bauer, A., Schultz, J., Rick, J. M., Michon, A. M., Cruciat, C. M., Remor, M., Hofert, C., Schelder, M., Brajenovic, M., Ruffner, H., Merino, A., Klein, K., Hudak, M., Dickson, D., Rudi, T., Gnau, V., Bauch, A., Bastuck, S., Huhse, B., Leutwein, C., Heurtier, M. A., Copley, R. R., Edlmann, A., Querfurth, E., Rybin, V., Drewes, G., Raida, M., Bouwmeester, T., Bork, P., Seraphin, B., Kuster, B., Neubauer, G. & Superti-Furga, G. 2002. Functional organization of the yeast proteome by systematic analysis of protein complexes. *Nature*, 415, 141-147.
- Gerke, V. & Moss, S. E. 2002. Annexins: From structure to function. *Physiological Reviews*, 82, 331-371.
- Goldberger, R. F., Epstein, C. J. & Anfinsen, C. B. 1963. Acceleration of reactivation of reduced bovine pancreatic ribonuclease by a microsomal system from rat liver. *Journal of Biological Chemistry*, 238, 628.
- Goodrich, J. M. & Basu, N. 2012. Variants of glutathione s-transferase pi 1 exhibit differential enzymatic activity and inhibition by heavy metals. *Toxicology in Vitro*, 26, 630-635.
- Griffith, O. W. & Meister, A. 1979. Translocation of intracellular glutathione to membrane-bound gamma-glutamyl transpeptidase as a discrete step in the gamma-glutamyl cycle - glutathionuria after inhibition of transpeptidase. *Proceedings of the National Academy of Sciences of the United States of America*, 76, 268-272.
- Gross, E., Sevier, C. S., Heldman, N., Vitu, E., Bentzur, M., Kaiser, C. A., Thorpe, C. & Fass, D. 2006. Generating disulfides enzymatically: Reaction products and electron acceptors of the endoplasmic reticulum thiol oxidase Ero1p. *Proceedings of the National Academy of Sciences of the United States of America*, 103, 299-304.
- Habig, W. H., Pabst, M. J. & Jakoby, W. B. 1974. Glutathione s-transferases - first enzymatic step in mercapturic acid formation. *Journal of Biological Chemistry*, 249, 7130-7139.
- Hagenbuch, B. & Meier, P. J. 2003. The superfamily of organic anion transporting polypeptides. *Biochimica Et Biophysica Acta-Biomembranes*, 1609, 1-18.
- Han, G., Tamaki, M. & Hruby, V. 2001. Fast, efficient and selective deprotection of the tert-butoxycarbonyl (Boc) group using HCl/dioxane (4 M). *Journal of Peptide Research*, 58, 338-341.
- Hansen, R. E., Roth, D. & Winther, J. R. 2009. Quantifying the global cellular thiol-disulfide status. *Proceedings of the National Academy of Sciences of the United States of America*, 106, 422-427.
- Hanson, G. T., Aggeler, R., Oglesbee, D., Cannon, M., Capaldi, R. A., Tsien, R. Y. & Remington, S. J. 2004. Investigating mitochondrial redox potential with redox-sensitive green fluorescent protein indicators. *Journal of Biological Chemistry*, 279, 13044-13053.
- Hardesty, B. & Kramer, G. 2001. Folding of a nascent peptide on the ribosome. *Progress in Nucleic Acid Research and Molecular Biology*, Vol 66, 66, 41-66.
- Hatahet, F. & Ruddock, L. W. 2009. Protein Disulfide Isomerase: A Critical Evaluation of Its Function in Disulfide Bond Formation. *Antioxidants & Redox Signaling*, 11, 2807-2850.

- Hatzoglou, M., Fernandez, J., Yaman, I. & Closs, E. 2004. Regulation of cationic amino acid transport: The story of the CAT-1 transporter. *Annual Review of Nutrition*, 24, 377-399.
- Hauser, M., Donhardt, A. M., Barnes, D., Naider, F. & Becker, J. M. 2000. Enkephalins are transported by a novel eukaryotic peptide uptake system. *Journal of Biological Chemistry*, 275, 3037-3041.
- Hayes, J. D., Flanagan, J. U. & Jowsey, I. R. 2005. Glutathione transferases. *Annual Review of Pharmacology and Toxicology*, 45, 51-88.
- Hebert, D. N. & Carruthers, A. 1992. Glucose transporter oligomeric structure determines transporter function - reversible redox-dependent interconversions of tetrameric and dimeric GLUT1. *Journal of Biological Chemistry*, 267, 23829-23838.
- Hedstrom, L., Szilagy, L. & Rutter, W. J. 1992. Converting trypsin to chymotrypsin - the role of surface loops. *Science*, 255, 1249-1253.
- Hilz, H., Wieggers, U. & Adamietz, P. 1975. Stimulation of proteinase-k action by denaturing agents - application to isolation of nucleic-acids and degradation of masked proteins. *European Journal of Biochemistry*, 56, 103-108.
- Ho, Y., Gruhler, A., Heilbut, A., Bader, G. D., Moore, L., Adams, S. L., Millar, A., Taylor, P., Bennett, K., Boutilier, K., Yang, L. Y., Wolting, C., Donaldson, I., Schandorff, S., Shewnarane, J., Vo, M., Taggart, J., Goudreault, M., Muskat, B., Alfarano, C., Dewar, D., Lin, Z., Michalickova, K., Willems, A. R., Sassi, H., Nielsen, P. A., Rasmussen, K. J., Andersen, J. R., Johansen, L. E., Hansen, L. H., Jespersen, H., Podtelejnikov, A., Nielsen, E., Crawford, J., Poulsen, V., Sorensen, B. D., Matthiesen, J., Hendrickson, R. C., Gleeson, F., Pawson, T., Moran, M. F., Durocher, D., Mann, M., Hogue, C. W. V., Figgeys, D. & Tyers, M. 2002. Systematic identification of protein complexes in *Saccharomyces cerevisiae* by mass spectrometry. *Nature*, 415, 180-183.
- Holm, P. J., Morgenstern, R. & Hebert, H. 2002. The 3-D structure of microsomal glutathione transferase 1 at 6 angstrom resolution as determined by electron crystallography of p22(1)2(1) crystals. *Biochimica Et Biophysica Acta-Protein Structure and Molecular Enzymology*, 1594, 276-285.
- Hopkins, F. G. 1929. On glutathione : A reinvestigation. *Journal of Biological Chemistry*, 84, 269-320.
- Hopp, T. P., Prickett, K. S., Price, V. L., Libby, R. T., March, C. J., Cerretti, D. P., Urdal, D. L. & Conlon, P. J. 1988. A short polypeptide marker sequence useful for recombinant protein identification and purification. *Bio-Technology*, 6, 1204-1210.
- Hoseki, J., Oishi, A., Fujimura, T. & Sakai, Y. 2016. Development of a stable ERroGFP variant suitable for monitoring redox dynamics in the ER. *Bioscience Reports*, 36.
- Huang, Z. Z., Chen, C. J., Zeng, Z. H., Yang, H. P., Oh, J., Chen, L. X. & Lu, S. C. 2001. Mechanism and significance of increased glutathione level in human hepatocellular carcinoma and liver regeneration. *Faseb Journal*, 15, 19-21.
- Hwang, C., Sinskey, A. J. & Lodish, H. F. 1992. Oxidized redox state of glutathione in the endoplasmic-reticulum. *Science*, 257, 1496-1502.
- Iantomasi, T., Favilli, F., Marraccini, P., Magaldi, T., Bruni, P. & Vincenzini, M. T. 1997. Glutathione transport system in human small intestine epithelial cells. *Biochimica Et Biophysica Acta-Biomembranes*, 1330, 274-283.

- Inoue, M., Kinne, R., Tran, T. & Arias, I. M. 1984. Glutathione transport across hepatocyte plasma-membranes - analysis using isolated rat-liver sinusoidal-membrane vesicles. *European Journal of Biochemistry*, 138, 491-495.
- Jao, S. C., Chen, J., Yang, K. & Li, W. S. 2006. Design of potent inhibitors for *Schistosoma japonica* glutathione S-transferase. *Bioorganic & Medicinal Chemistry*, 14, 304-318.
- Jessop, C. E. & Bulleid, N. J. 2004. Glutathione directly reduces an oxidoreductase in the endoplasmic reticulum of mammalian cells. *Journal of Biological Chemistry*, 279, 55341-55347.
- Johnston, R. B. & Bloch, K. 1951. Enzymatic synthesis of glutathione. *Journal of Biological Chemistry*, 188, 221-240.
- Kannan, R., Mittur, A., Bao, Y. Z., Tsuruo, T. & Kaplowitz, N. 1999. GSH transport in immortalized mouse brain endothelial cells: Evidence for apical localization of a sodium-dependent GSH transporter. *Journal of Neurochemistry*, 73, 390-399.
- Kanzok, S. M., Schirmer, R. H., Turbachova, I., Iozef, R. & Becker, K. 2000. The thioredoxin system of the malaria parasite *Plasmodium falciparum* - Glutathione reduction revisited. *Journal of Biological Chemistry*, 275, 40180-40186.
- Karala, A.-R., Lappi, A.-K., Saaranen, M. J. & Ruddock, L. W. 2009a. Efficient Peroxide-Mediated Oxidative Refolding of a Protein at Physiological pH and Implications for Oxidative Folding in the Endoplasmic Reticulum. *Antioxidants & Redox Signaling*, 11, 963-970.
- Keen, J. H. & Jakoby, W. B. 1978. Glutathione transferases - catalysis of nucleophilic reactions of glutathione. *Journal of Biological Chemistry*, 253, 5654-5657.
- Kispal, G., Csere, P., Guiard, B. & Lill, R. 1997. The ABC transporter Atm1p is required for mitochondrial iron homeostasis. *Febs Letters*, 418, 346-350.
- Kodali, V. K. & Thorpe, C. 2010. Oxidative Protein Folding and the Quiescin-Sulfhydryl Oxidase Family of Flavoproteins. *Antioxidants & Redox Signaling*, 13, 1217-1230.
- Koonin, E. V., Mushegian, A. R., Tatusov, R. L., Altschul, S. F., Bryant, S. H., Bork, P. & Valencia, A. 1994. Eukaryotic translation elongation-factor 1-gamma contains a glutathione transferase domain - study of a diverse, ancient protein superfamily using motif search and structural modeling. *Protein Science*, 3, 2045-2054.
- Kumar, C., Igarria, A., D'autreaux, B., Planson, A.-G., Junot, C., Godat, E., Bachhawat, A. K., Delaunay-Moisan, A. & Toledano, M. B. 2011. Glutathione revisited: a vital function in iron metabolism and ancillary role in thiol-redox control. *Embo Journal*, 30, 2044-2056.
- Ladner, J. E., Parsons, J. F., Rife, C. L., Gilliland, G. L. & Armstrong, R. N. 2004. Parallel evolutionary pathways for glutathione transferases: Structure and mechanism of the mitochondrial class kappa enzyme rGSTK1-1. *Biochemistry*, 43, 352-361.
- Lappi, A.-K. & Ruddock, L. W. 2011. Reexamination of the Role of Interplay between Glutathione and Protein Disulfide Isomerase. *Journal of Molecular Biology*, 409, 238-249.
- Lash, L. H. 2005. Role of glutathione transport processes in kidney function. *Toxicology and Applied Pharmacology*, 204, 329-342.

- Lash, L. H. & Jones, D. P. 1983. Transport of glutathione by renal basal-lateral membrane-vesicles. *Biochemical and Biophysical Research Communications*, 112, 55-60.
- Lash, L. H. & Jones, D. P. 1984. Renal glutathione transport - characteristics of the sodium-dependent system in the basal-lateral membrane. *Journal of Biological Chemistry*, 259, 4508-4514.
- Lash, L. H. & Putt, D. A. 1999. Renal cellular transport of exogenous glutathione: Heterogeneity at physiological and pharmacological concentrations. *Biochemical Pharmacology*, 58, 897-907.
- Lautier, D., Canitrot, Y., Deeley, R. G. & Cole, S. P. C. 1996. Multidrug resistance mediated by the multidrug resistance protein (MRP) gene. *Biochemical Pharmacology*, 52, 967-977.
- Le Gall, S., Neuhof, A. & Rapoport, T. 2004. The endoplasmic reticulum membrane is permeable to small molecules. *Molecular Biology of the Cell*, 15, 447-455.
- Le Moan, N., Clement, G., Le Maout, S., Tacnet, F. & Toledano, M. B. 2006. The *Saccharomyces cerevisiae* proteome of oxidized protein thiols - Contrasted functions for the thioredoxin and glutathione pathways. *Journal of Biological Chemistry*, 281, 10420-10430.
- Lemasters, J. J. 2005. Dying a thousand deaths: Redundant pathways from different organelles to apoptosis and necrosis. *Gastroenterology*, 129, 351-360.
- Li, L. Q., Lee, T. K., Meier, P. J. & Ballatori, N. 1998. Identification of glutathione as a driving force and leukotriene C-4 as a substrate for oatp1, the hepatic sinusoidal organic solute transporter. *Journal of Biological Chemistry*, 273, 16184-16191.
- Lillig, C. H. & Berndt, C. 2013. Cellular functions of glutathione Preface. *Biochimica Et Biophysica Acta-General Subjects*, 1830, 3137-3138.
- Limor-Waisberg, K., Ben-Dor, S. & Fass, D. 2013. Diversification of Quiescin sulfhydryl oxidase in a preserved framework for redox relay. *Bmc Evolutionary Biology*, 13.
- Lindwall, G. & Boyer, T. D. 1987. Excretion of glutathione conjugates by primary cultured rat hepatocytes. *Journal of Biological Chemistry*, 262, 5151-5158.
- Liu, R. M. & Pravia, K. A. G. 2010. Oxidative stress and glutathione in TGF-beta-mediated fibrogenesis. *Free Radical Biology and Medicine*, 48, 1-15.
- Lohman, J. R. & Remington, S. J. 2008. Development of a family of redox-sensitive green fluorescent protein indicators for use in relatively oxidizing subcellular environments. *Biochemistry*, 47, 8678-8688.
- Lopez-Mirabal, H. R. & Winther, J. R. 2008. Redox characteristics of the eukaryotic cytosol. *Biochimica Et Biophysica Acta-Molecular Cell Research*, 1783, 629-640.
- Loudet, A. & Burgess, K. 2007. BODIPY dyes and their derivatives: Syntheses and spectroscopic properties. *Chemical Reviews*, 107, 4891-4932.
- Lu, S. & Ge, J. L. 1992. Loss of suppression of gsh synthesis under low cell density in primary cultures of rat hepatocytes. *Gastroenterology*, 102, A845-A845.
- Lu, S. C. 2009. Regulation of glutathione synthesis. *Molecular Aspects of Medicine*, 30, 42-59.

- Lu, S. C. 2013. Glutathione synthesis. *Biochimica Et Biophysica Acta-General Subjects*, 1830, 3143-3153.
- Lushchak, V. I. 2012. Glutathione homeostasis and functions: potential targets for medical interventions. *Journal of amino acids*, 2012, 736837-736837.
- Lyles, M. M. & Gilbert, H. F. 1991. Catalysis of the oxidative folding of ribonuclease-a by protein disulfide isomerase - dependence of the rate on the composition of the redox buffer. *Biochemistry*, 30, 613-619.
- Mahagita, C., Grassl, S. M., Piyachaturawat, P. & Ballatori, N. 2007. Human organic anion transporter 1B1 and 1B3 function as bidirectional carriers and do not mediate GSH-bile acid cotransport. *American Journal of Physiology-Gastrointestinal and Liver Physiology*, 293, G271-G278.
- Mao, Q. C., Deeley, R. G. & Cole, S. P. C. 2000. Functional reconstitution of substrate transport by purified multidrug resistance protein MRP1 (ABCC1) in phospholipid vesicles. *Journal of Biological Chemistry*, 275, 34166-34172.
- Markovic, J., Borrás, C., Ortega, A., Sastre, J., Vina, J. & Pallardo, F. V. 2007. Glutathione is recruited into the nucleus in early phases of cell proliferation. *Journal of Biological Chemistry*, 282, 20416-20424.
- Massey, V. & Williams, C. H. 1965. On reaction mechanism of yeastglutathione reductase. *Journal of Biological Chemistry*, 240, 4470.
- Mayor, U., Guydosh, N. R., Johnson, C. M., Grossmann, J. G., Sato, S., Jas, G. S., Freund, S. M. V., Alonso, D. O. V., Daggett, V. & Fersht, A. R. 2003. The complete folding pathway of a protein from nanoseconds to microseconds. *Nature*, 421, 863-867.
- Meyer, A. J. & Dick, T. P. 2010. Fluorescent Protein-Based Redox Probes. *Antioxidants & Redox Signaling*, 13, 621-650.
- Meyer, Y., Buchanan, B. B., Vignols, F. & Reichheld, J.-P. 2009. Thioredoxins and Glutaredoxins: Unifying Elements in Redox Biology. *Annual Review of Genetics*, 43, 335-367.
- Miyake, T., Hazu, T., Yoshida, S., Kanayama, M., Tomochika, K., Shinoda, S. & Ono, B. 1998. Glutathione transport systems of the budding yeast *Saccharomyces cerevisiae*. *Bioscience Biotechnology and Biochemistry*, 62, 1858-1864.
- Miyake, T., Kanayama, M., Sammoto, H. & Ono, B. 2002. A novel cis-acting cysteine-responsive regulatory element of the gene for the high-affinity glutathione transporter of *Saccharomyces cerevisiae*. *Molecular Genetics and Genomics*, 266, 1004-1011.
- Mojica, E.-R. E., Kim, S. & Aga, D. S. 2008. Formation of N-ethylmaleimide (NEM)-Glutathione conjugate and N-ethylmaleamic acid revealed by mass spectral characterization of intracellular and extracellular microbial metabolites of NEM. *Applied and Environmental Microbiology*, 74, 323-326.
- Molteni, S. N., Fassio, A., Ciriolo, M. R., Filomeni, G., Pasqualetto, E., Fagioli, C. & Sitia, R. 2004. Glutathione limits Ero1-dependent oxidation in the endoplasmic reticulum. *Journal of Biological Chemistry*, 279, 32667-32673.

- Morgan, B., Ezerina, D., Amoako, T. N. E., Riemer, J., Seedorf, M. & Dick, T. P. 2013. Multiple glutathione disulfide removal pathways mediate cytosolic redox homeostasis. *Nature Chemical Biology*, 9, 119-125.
- Muller, A., Hinrichs, W., Wolf, W. M. & Saenger, W. 1994. Crystal-structure of calcium-free proteinase-k at 1.5-angstrom resolution. *Journal of Biological Chemistry*, 269, 23108-23111.
- Nguyen, V. D., Saaranen, M. J., Karala, A.-R., Lappi, A.-K., Wang, L., Raykhel, I. B., Alanen, H. I., Salo, K. E. H., Wang, C.-C. & Ruddock, L. W. 2011. Two Endoplasmic Reticulum PDI Peroxidases Increase the Efficiency of the Use of Peroxide during Disulfide Bond Formation. *Journal of Molecular Biology*, 406, 503-515.
- Niu, L.-Y., Guan, Y.-S., Chen, Y.-Z., Wu, L.-Z., Tung, C.-H. & Yang, Q.-Z. 2012. BODIPY-Based Ratiometric Fluorescent Sensor for Highly Selective Detection of Glutathione over Cysteine and Homocysteine. *Journal of the American Chemical Society*, 134, 18928-18931.
- Njalsson, R. & Norgren, S. 2005. Physiological and pathological aspects of GSH metabolism. *Acta Paediatrica*, 94, 132-137.
- Oakley, A. 2011. Glutathione transferases: a structural perspective. *Drug Metabolism Reviews*, 43, 138-151.
- Oka, Y., Asano, T., Shibasaki, Y., Lin, J. L., Tsukuda, K., Katagiri, H., Akanuma, Y. & Takaku, F. 1990. C-Terminal truncated glucose transporter is locked into an inward-facing form without transport activity. *Nature*, 345, 550-553.
- Oppenheimer, L., Wellner, V. P., Griffith, O. W. & Meister, A. 1979. Glutathione synthetase - purification from rat-kidney and mapping of the substrate binding-sites. *Journal of Biological Chemistry*, 254, 5184-5190.
- Osawa, H., Stacey, G. & Gassmann, W. 2006. ScOPT1 and AtOPT4 function as proton-coupled oligopeptide transporters with broad but distinct substrate specificities. *Biochemical Journal*, 393, 267-275.
- Ostergaard, H., Henriksen, A., Hansen, F. G. & Winther, J. R. 2001. Shedding light on disulfide bond formation: engineering a redox switch in green fluorescent protein. *Embo Journal*, 20, 5853-5862.
- Ostergaard, H., Tachibana, C. & Winther, J. R. 2004. Monitoring disulfide bond formation in the eukaryotic cytosol. *Journal of Cell Biology*, 166, 337-345.
- Pagani, M., Fabbri, M., Benedetti, C., Fassio, A., Pilati, S., Bulleid, N. J., Cabibbo, A. & Sitia, R. 2000. Endoplasmic reticulum oxidoreductin 1-L beta (ERO1-L beta), a human gene induced in the course of the unfolded protein response. *Journal of Biological Chemistry*, 275, 23685-23692.
- Ponsero, A. J., Igarria, A., Darch, M. A., Miled, S., Outten, C. E., Winther, J. R., Palais, G., D'autreaux, B., Delaunay-Moisan, A. & Toledano, M. B. 2017. Endoplasmic Reticulum Transport of Glutathione by Sec61 Is Regulated by Ero1 and Bip. *Molecular Cell*, 67, 962-+.
- Ranat, S. & Dringen, R. 2007. Gap junction hemichannel-mediated release of glutathione from cultured rat astrocytes. *Neuroscience Letters*, 415, 45-48.
- Rancy, P. C. & Thorpe, C. 2008. Oxidative Protein Folding in Vitro: A Study of the Cooperation between Quiescin-Sulfhydryl Oxidase and Protein Disulfide Isomerase. *Biochemistry*, 47, 12047-12056.

- Rawlings, N. D. & Barrett, A. J. 1994. Families of serine peptidases. *Proteolytic Enzymes: Serine and Cysteine Peptidases*, 244, 19-61.
- Rebbeor, J. F., Connolly, G. C. & Ballatori, N. 2002. Inhibition of Mrp2-and Ycf1p-mediated transport by reducing agents: evidence for GSH transport on rat Mrp2. *Biochimica Et Biophysica Acta-Biomembranes*, 1559, 171-178.
- Rebbeor, J. F., Connolly, G. C., Dumont, M. E. & Ballatori, N. 1998a. ATP-dependent transport of reduced glutathione in yeast secretory vesicles. *Biochemical Journal*, 334, 723-729.
- Rebbeor, J. F., Connolly, G. C., Dumont, M. E. & Ballatori, N. 1998b. ATP-dependent transport of reduced glutathione on YCF1, the yeast orthologue of mammalian multidrug resistance associated proteins. *Journal of Biological Chemistry*, 273, 33449-33454.
- Reinemer, P., Dirr, H. W., Ladenstein, R., Schaffer, J., Gallay, O. & Huber, R. 1991. The 3-dimensional structure of class-pi glutathione-s-transferase in complex with glutathione sulfonate at 2.3 a resolution. *Embo Journal*, 10, 1997-2005.
- Roos, D., Weening, R. S., Voetman, A. A., Vanschaik, M. L. J., Bot, A. A. M., Meerhof, L. J. & Loos, J. A. 1979. Protection of phagocytic leukocytes by endogenous glutathione - studies in a family with glutathione-reductase deficiency. *Blood*, 53, 851-866.
- Rubio-Aliaga, I. & Daniel, H. 2008. Peptide transporters and their roles in physiological processes and drug disposition. *Xenobiotica*, 38, 1022-1042.
- Rutkevich, L. A. & Williams, D. B. 2012. Vitamin K epoxide reductase contributes to protein disulfide formation and redox homeostasis within the endoplasmic reticulum. *Molecular Biology of the Cell*, 23, 2017-2027.
- Schafer, F. Q. & Buettner, G. R. 2001. Redox environment of the cell as viewed through the redox state of the glutathione disulfide/glutathione couple. *Free Radical Biology and Medicine*, 30, 1191-1212.
- Schulman, S., Wang, B., Li, W. & Rapoport, T. A. 2010. Vitamin K epoxide reductase prefers ER membrane-anchored thioredoxin-like redox partners. *Proceedings of the National Academy of Sciences of the United States of America*, 107, 15027-15032.
- Seeley, S. K., Poposki, J. A., Maksimchuk, J., Tebbe, J., Gaudreau, J., Mannervik, B. & Bull, A. W. 2006. Metabolism of oxidized linoleic acid by glutathione transferases: Peroxidase activity toward 13-hydroperoxyoctadecadienoic acid. *Biochimica Et Biophysica Acta-General Subjects*, 1760, 1064-1070.
- Seelig, G. F., Simonsen, R. P. & Meister, A. 1984. Reversible dissociation of gamma-glutamylcysteine synthetase into 2 subunits. *Journal of Biological Chemistry*, 259, 9345-9347.
- Sengupta, R. & Holmgren, A. 2014. Thioredoxin and glutaredoxin-mediated redox regulation of ribonucleotide reductase. *World journal of biological chemistry*, 5, 68-74.
- Sevier, C. S., Cuozzo, J. W., Vala, A., Aslund, F. & Kaiser, C. A. 2001. A flavoprotein oxidase defines a new endoplasmic reticulum pathway for biosynthetic disulphide bond formation. *Nature Cell Biology*, 3, 874-882.

- Sevier, C. S. & Kaiser, C. A. 2006. Disulfide transfer between two conserved cysteine pairs imparts selectivity to protein oxidation by Ero1. *Molecular Biology of the Cell*, 17, 2256-2266.
- Shao, S. & Hegde, R. S. 2011. Membrane Protein Insertion at the Endoplasmic Reticulum. *Annual Review of Cell and Developmental Biology*, Vol 27, 27, 25-56.
- Sheehan, D., Meade, G., Foley, V. M. & Dowd, C. A. 2001. Structure, function and evolution of glutathione transferases: implications for classification of non-mammalian members of an ancient enzyme superfamily. *Biochemical Journal*, 360, 1-16.
- Shi, Y. 2013. Common Folds and Transport Mechanisms of Secondary Active Transporters. *Annual Review of Biophysics*, Vol 42, 42, 51-72.
- Si, K. 2015. Prions: What Are They Good For? *Annual Review of Cell and Developmental Biology*, Vol 31, 31, 149-169.
- Sies, H. 1999. Glutathione and its role in cellular functions. *Free Radical Biology and Medicine*, 27, 916-921.
- Sipos, K., Lange, H., Fekete, Z., Ullmann, P., Lill, R. & Kispal, G. 2002. Maturation of cytosolic iron-sulfur proteins requires glutathione. *Journal of Biological Chemistry*, 277, 26944-26949.
- Snoke, J. E. & Bloch, K. 1952. Formation and utilization of gamma-glutamylcysteine in glutathione synthesis. *Journal of Biological Chemistry*, 199, 407-414.
- Snoke, J. E., Yanari, S. & Bloch, K. 1953. Synthesis of glutathione from gamma-glutamylcysteine. *Journal of Biological Chemistry*, 201, 573-586.
- Srikanth, C. V., Vats, P., Bourbonloux, A., Delrot, S. & Bachhawat, A. K. 2005. Multiple cis-regulatory elements and the yeast sulphur regulatory network are required for the regulation of the yeast glutathione transporter, Hgt1p. *Current Genetics*, 47, 345-358.
- Stornaiuolo, M., Lotti, L. V., Borgese, N., Torrisi, M. R., Mottola, G., Martire, G. & Bonatti, S. 2003. KDEL and KKXX retrieval signals appended to the same reporter protein determine different trafficking between endoplasmic reticulum, intermediate compartment, and Golgi complex. *Molecular Biology of the Cell*, 14, 889-902.
- Stout, C. E., Costantin, J. L., Naus, C. C. G. & Charles, A. C. 2002. Intercellular calcium signaling in astrocytes via ATP release through connexin hemichannels. *Journal of Biological Chemistry*, 277, 10482-10488.
- Suzuki, T., Coggan, M., Shaw, D. C. & Board, P. G. 1987. Electrophoretic and immunological analysis of human glutathione-s-transferase isozymes. *Annals of Human Genetics*, 51, 95-106.
- Tavender, T. J., Springate, J. J. & Bulleid, N. J. 2010. Recycling of peroxiredoxin IV provides a novel pathway for disulphide formation in the endoplasmic reticulum. *Embo Journal*, 29, 4185-4197.
- Toppo, S., Vanin, S., Bosello, V. & Tosatto, S. C. E. 2008. Evolutionary and structural insights into the multifaceted glutathione peroxidase (Gpx) superfamily. *Antioxidants & Redox Signaling*, 10, 1501-1513.
- Tsay, Y.-F., Chiu, C.-C., Tsai, C.-B., Ho, C.-H. & Hsu, P.-K. 2007. Nitrate transporters and peptide transporters. *Febs Letters*, 581, 2290-2300.

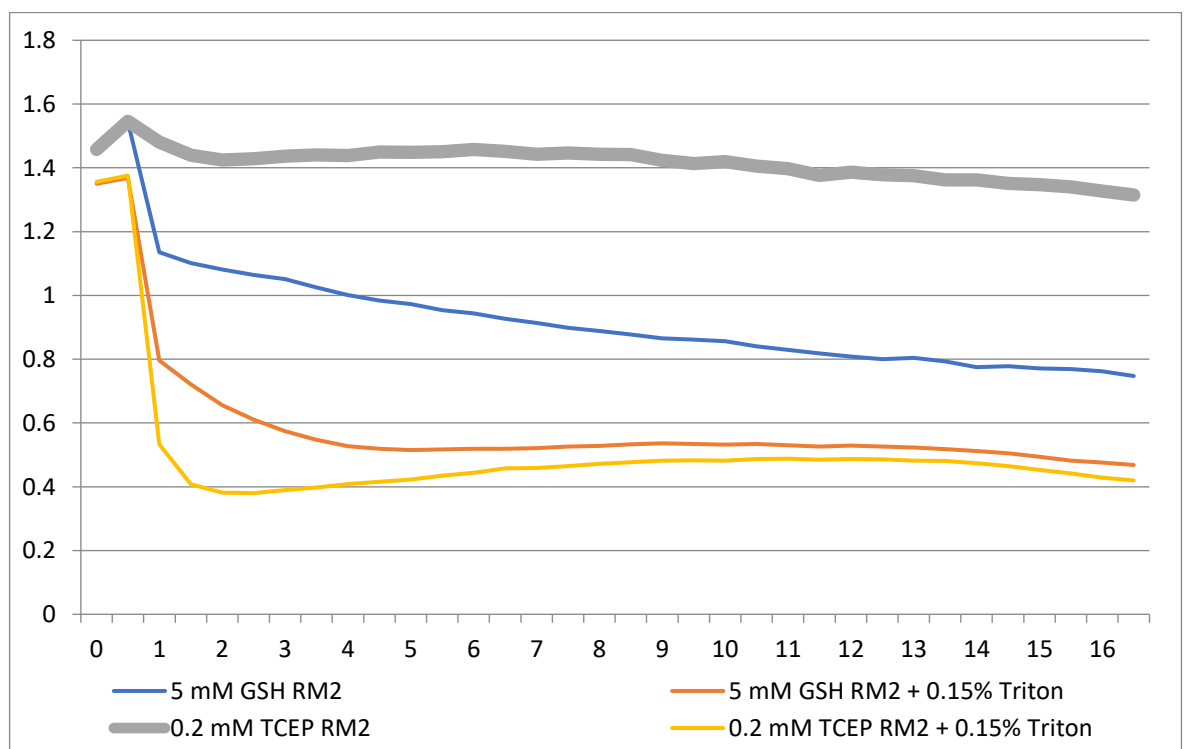
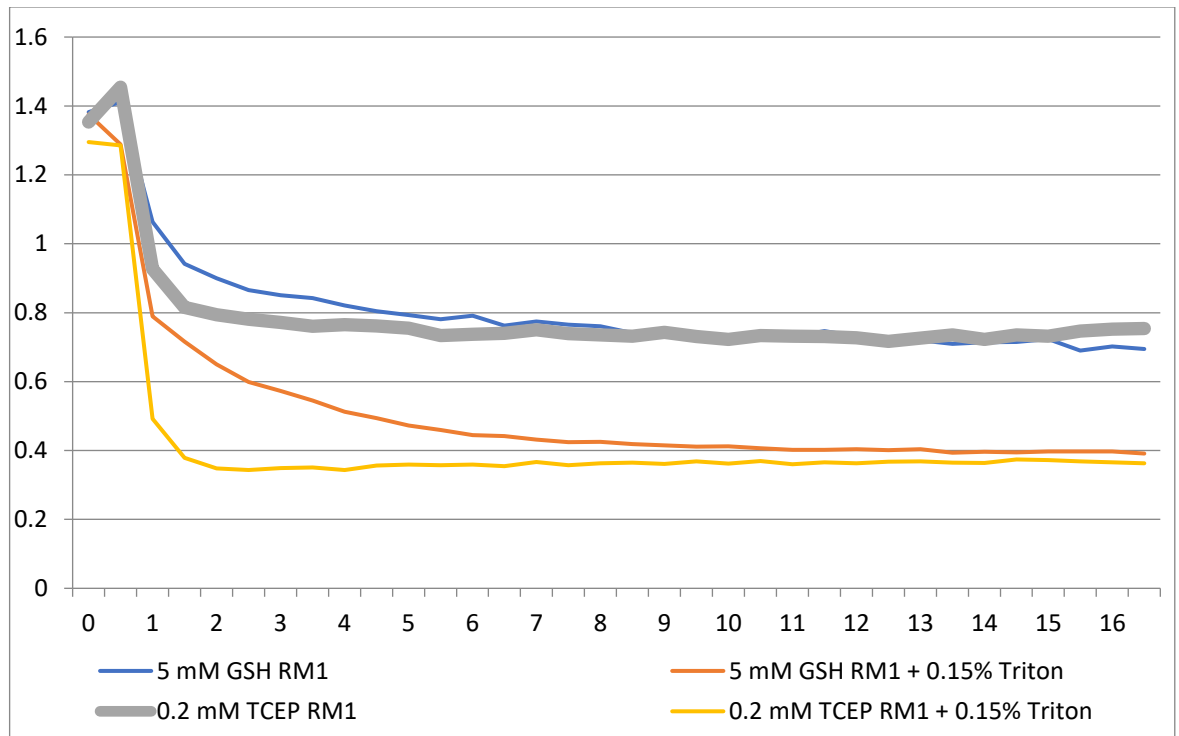
- Tshabalala, T. N., Tomescu, M.-S., Prior, A., Balakrishnan, V., Sayed, Y., Dirr, H. W. & Achilonu, I. 2016. Energetics of Glutathione Binding to Human Eukaryotic Elongation Factor 1 Gamma: Isothermal Titration Calorimetry and Molecular Dynamics Studies. *Protein Journal*, 35, 448-458.
- Tu, B. P. & Weissman, J. S. 2002. The FAD- and O₂-dependent reaction cycle of Ero1-mediated oxidative protein folding in the endoplasmic reticulum. *Molecular Cell*, 10, 983-994.
- Tu, B. P. & Weissman, J. S. 2004. Oxidative protein folding in eukaryotes: mechanisms and consequences. *Journal of Cell Biology*, 164, 341-346.
- Valsta, L. M., Hendricks, J. D. & Bailey, G. S. 1988. The significance of glutathione conjugation for aflatoxin-b1 metabolism in rainbow-trout and coho salmon. *Food and Chemical Toxicology*, 26, 129-135.
- Van Lith, M., Tiwari, S., Pediani, J., Milligan, G. & Bulleid, N. J. 2011. Real-time monitoring of redox changes in the mammalian endoplasmic reticulum. *Journal of Cell Science*, 124, 2349-2356.
- Van Meer, G., Voelker, D. R. & Feigenson, G. W. 2008. Membrane lipids: where they are and how they behave. *Nature Reviews Molecular Cell Biology*, 9, 112-124.
- Voehringer, D. W., Mcconkey, D. J., McDonnell, T. J., Brisbay, S. & Meyn, R. E. 1998. Bcl-2 expression causes redistribution of glutathione to the nucleus. *Proceedings of the National Academy of Sciences of the United States of America*, 95, 2956-2960.
- Wajih, N., Hutson, S. M. & Wallin, R. 2007. Disulfide-dependent protein folding is linked to operation of the vitamin K cycle in the endoplasmic reticulum - A protein disulfide isomerase-VKORC1 redox enzyme complex appears to be responsible for vitamin K-1 2,3-epoxide reduction. *Journal of Biological Chemistry*, 282, 2626-2635.
- Walter, P. & Blobel, G. 1981. Translocation of proteins across the endoplasmic-reticulum signal recognition protein (SRP) mediates the selective binding to microsomal-membranes of invitro-assembled polysomes synthesizing secretory protein. *Journal of Cell Biology*, 91, 551-556.
- Wang, F., An, J., Zhang, L. & Zhao, C. 2014. Construction of a fluorescence turn-on probe for highly discriminating detection of cysteine. *Rsc Advances*, 4, 53437-53441.
- Wu, G. Y., Fang, Y. Z., Yang, S., Lupton, J. R. & Turner, N. D. 2004. Glutathione metabolism and its implications for health. *Journal of Nutrition*, 134, 489-492.
- Yen, M. R., Tseng, Y. H. & Saier, M. H. 2001. Maize Yellow Stripe1, an iron-phytosiderophore uptake transporter, is a member of the oligopeptide transporter (OPT) family. *Microbiology-Sgm*, 147, 2881-2883.
- Zaman, G. J. R., Lankelma, J., Vantellingen, O., Beijnen, J., Dekker, H., Paulusma, C., Oudeelferink, R. P. J., Baas, F. & Borst, P. 1995. Role of glutathione in the export of compounds from cells by the multidrug-resistance-associated protein. *Proceedings of the National Academy of Sciences of the United States of America*, 92, 7690-7694.
- Zimmermann, R., Eyrisch, S., Ahmad, M. & Helms, V. 2011. Protein translocation across the ER membrane. *Biochimica Et Biophysica Acta-Biomembranes*, 1808, 912-924.
- Zito, E., Chin, K.-T., Blais, J., Harding, H. P. & Ron, D. 2010a. ERO1-beta, a pancreas-specific disulfide oxidase, promotes insulin biogenesis and glucose homeostasis (vol 188, pg 821, 2010). *Journal of Cell Biology*, 189, 769-769.

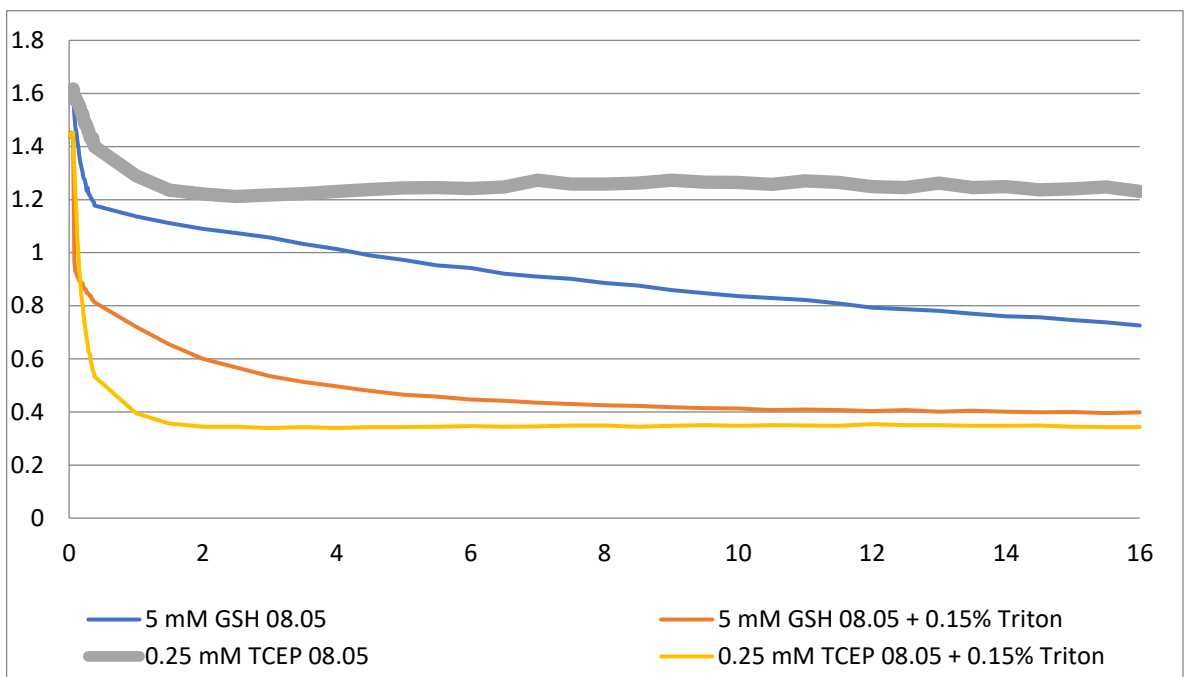
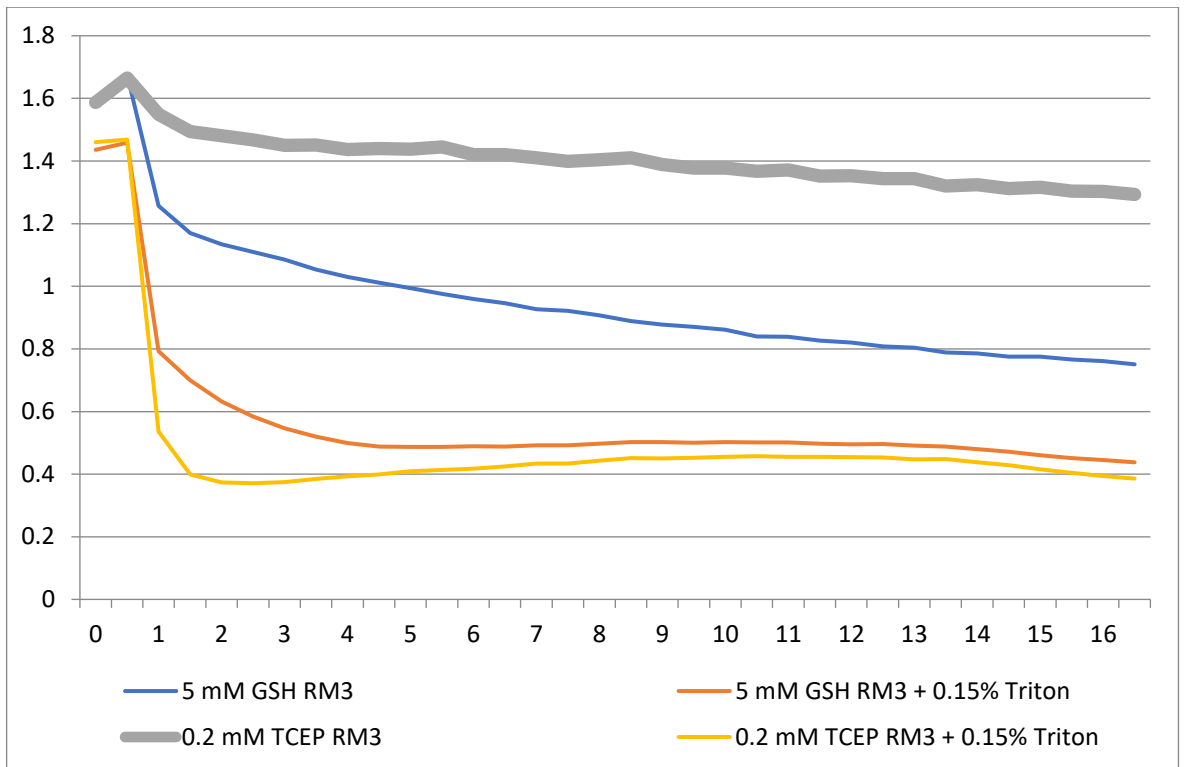
Zito, E., Melo, E. P., Yang, Y., Wahlander, A., Neubert, T. A. & Ron, D. 2010b. Oxidative Protein Folding by an Endoplasmic Reticulum-Localized Peroxiredoxin. *Molecular Cell*, 40, 787-797.

Zou, C. G., Agar, N. S. & Jones, G. L. 2002. Chlorodinitrobenzene-mediated damage in the human erythrocyte membrane leads to haemolysis. *Life Sciences*, 71, 735-746.

Appendix

TCEP can be used to determine intactness of microsomes. 4 different batches of microsomes were tested below. If microsomes were very leaky TCEP was able to reduce roGFP more, however if microsomes are intact the degree of roGFP reduction by TCEP was not be significant when compared to GSH.





The presence of GSH to CI-BODIPY conjugate was confirmed by HPCL and mass spectrometry. The retention time for GS-BODIPY was equal to 12.63 and the mass was confirmed to be 525 g/mol

